A Study of the Falcon Concentrator

by Mark Buonvino

A thesis submitted to the

Faculty of Graduate Studies and Research

in partial fulfilment of the requirements

for the degree of Master of Engineering

Department of Mining and Metallurgical Engineering

McGill University, Montreal

Abstract

A Falcon model B6 was tested on a massive gold-copper sulphide ore (Agnico-Eagle LaRonde Division, AELR), to assess its ability to produce a smeltable concentrate (200000 to 300000 g/t); a fine gold-pyrite-silica flotation tail (Meston Resources, MR) to assess the Falcon's ability to recover gold from a low density and very fine material; and a synthetic magnetite-silica ore to obtain more fundamental information on its mode of operation.

For 20 kg of AELR's flotation concentrate fed at 20 to 30% solids at 20-30 l/min, the Falcon recovered $22 \pm 3\%$ of the gold at a grade of 900 g/t. It overloaded when more than 20 kg of material was processed and recovery dropped sharply.

Samples of MR's flotation tails were processed with the Falcon. Three different bowls (8, 10, 14 degree) were tested at two flowrates (10, 20 L/min), and three densities (10, 20, 30 % w/w). None of the parameters were found significant for pyrite, but bowl angle and flowrate were found to be significant for gold. On average, the Falcon recovered 50% of the gold and 20% of the pyrite at a concentrate grade of 4.0 g/t gold in a weight yield of 10%.

Three 3-level nested factorial experiments were performed with an artificial feed consisting of silica and magnetite to study the effect of gangue particle size, bowl type, % solids, and flowrate. A typical loading cycle includes (i) the initial unselective creation of a first concentrate bed; (ii) more selective recovery as bed growth stops and (iii) saturation of the bed surface leading to a zero incremental recovery.

i

A sythetic feed (5% magnetite, p5% silica) was used to characterize the Falcon's loading cycle, its overload, and the effect of operating variables. Overload with the synthetic feed was virtually complete upon feeding 30 kg, either at 20 or 30 L/min. Three 3-level nested factorial experiments showed that for a constant mass of the synthetic feed, magnetite recovery increased with decreasing particle size and bowl angle. These effects masked the impact of feed flowrate and density. Magnetite recovery was found maximum for the finest sizes (< 50 μm), intermediate for the coarsest sizes (+200 μm), and lowest at intermediate sizes.

Résumé

Le séparateur Falcon est un nouvel appareil centrifuge qui a été conçu pour récupérer de l'or fin ($< 53\mu$m). Cette étude visait à mieux comprendre son fonctionnement.

Un concentré de flottation de la mine Agnico-Eagle, Division LaRonde (75% de pyrite, 200 g/t d'or) a été traité avec un séparateur Falcon afin de produire un concentré fusionable (200000 à 300000 g/t). Pour une masse traitée de 20 kg, le meilleur rendement (récuperation d'or: 22 ± 3%; teneur du concentré: 900 g/t) a été atteint à une densité de 20 à 30 l/min, et un débit de 20 à 30 l/min à l'alimentation. On a noté qu'en augmentant la masse de 20 à 80 kilogrammes, la récupération d'or a diminué de façon très marquée.

On a effectué une deuxième série d'essais avec un rejet de flottation très fin de la mine Meston (60% de silice, 1% de pyrite, 1 g/t d'or) afin de réduire les pertes d'or du circuit de flottation. En moyenne, le Falcon a pu récupérer 50% de l'or des rejets, dans un concentré de 4 g/t qui pourrait être cyanuré.

Une dernière serie d'essai a été complétée avec une alimentation synthétique (95% de silice et 5% de magnétite) afin de préciser le fonctionnement du Falcon et d'identifier le lien entre la récupération et les conditions d'opération. Le bol à l'angle le plus aigu, 8°, en présence de la gangue fine, -75 μm, a permis de maximiser la récuperation de magnétite. Plus précisément, la récupération de magnétite était plus élevée pour les tailles granulométrique très fines ($< 50 \mu$m), moyenne pour les tailles

grossières (+ 200 μm), et faible pour le reste.

On a identifié 3 étapes qui caractérisent le cycle de fonctionnement du séparateur: i) au début du cyle, l'accumulation de solides contre la paroi du bol, et la formation d'une couche de concentré; ii) une phase de récupération sélective à la surface de la première couche du concentré; iii) et la saturation à la surface vers la fin du cycle.

Acknowledgements

Table of Contents

Chapter 1 Introduction

Chapter 2 Fine Particle Recovery by Gravity Separation

Chapter 3 Gold Recovery from Agnico-Eagle Division Laronde

Chapter 4 Gold Recovery from Meston's Flotation Tails

Chapter 5 Fundamental Investigation of Falcon Concentrator

Chapter 6 Conclusions

Appendices

List of Figures

List of Tables

Chapter 1

Introduction

1.1 Introduction

The concentration of gold by gravity dates from prehistoric times. In fact, it was nature's way of preconcentration in some of the best known gold producing areas, such as the Witwatersrand (Splaine et al., 1982). Such deposits can become consolidated (e.g. the Hemlo area), and are mined as hard-rock operations. Others remain unconsolidated; such are the gold placer deposits of the former Soviet Union, Yukon, Brasil, Bolivia, and much of Africa (Laplante, 1988). In all cases gravity concentration can be used. For placer deposits it is the principal and often sole recovery method. For example, Douglas and Moir (1961) reviewed South African gold recovery practice and pointed out that 2/3 of the major plants incorporated gravity concentration followed by cyanidation of the bulk ore; up to 73% of the gold being recovered by gravity concentration when gold was relatively coarse ($> 150 \mu$m). For hard rock operations, gravity concentration plays a lesser, but still important function by reducing gold losses from the cyanidation and flotation circuits. These losses can be significant. For example, Noranda's base metal mills loose about 4.7 tonnes of gold per year (Ounpuu, 1992), which represents roughly $57 MM/ year. The most common causes for these losses are high levels of refractory gold, gold that has not been adequately liberated, and/or gold that is too coarse for flotation. Traditional gravity concentration could decrease the losses in certain cases, but because the gold associated with base-metal mines usually tends to be fine ($< 150 \mu$m), complicated labour intensive circuits are required. The practice has, however, evolved slightly with the arrival of two Canadian-designed centrifugal concentrators-the Knelson (KC) and the Falcon (FC) which can recover fines.

1

While the KC has undergone considerable testing by several researchers (eg. Liu, 1989, Banisi, 1990, Laplante, 1992, Ounpuu, 1992)- some of these will be reviewed in later sections- little data are yet available to quantify the FC's performance. In particular, what applications are most suitable for the FC? McAlister (1992) has already has presented several case studies. It is useful, at this point, to present the results of these case studies since they serve as a starting point for the investigation of the FC :

1) At Placer Dome-Cambell Red Lake, free gold was recovered from a calcine using a gravity circuit consisting of a Reichert Spiral, James Table and FC prior to cyanidation. The FC treated the spiral tails and the shaking table treated the spiral concentrate. The FC and table concentrates were cast into bullion on-site in a bullion furnace.

2) At the Skyline Johnny Mountain concentrator, free gold was recovered from a jig/table gravity circuit tailing by installing a FC on a primary cyclone overflow, the flotation feed. McAlister reported that the gold recovery from the gravity circuit increased from 20 to 30%.

3) At the Meston Resources mill significant gold recovery was reported from the flotation feed (gravity circuit tail), copper concentrate, and flotation tailings in tests with a FC model B6. Details of the Meston circuit will be given later. The objective of the research was to determine if the FC could be used to produce a smeltable concentrate from the final flotation concentrate, which could lead to the eventual additional bullion production on site. Direct casting of bullion has the advantage of a higher and quicker pay-back for gold- where smelters typically pay 96.5% in 90 days, refiners pay 99.5% in 60 days.

2

A two-stage rougher-cleaner FC test was performed on a sample of this material; no mention is given of the sample weight. McAlister reported that the final cleaner concentrate assayed 7709 g/t Au at a gold recovery of 37.1%.

A sample of flotation tailings was processed with a FC model B6. The objective was to determine if the FC could effectively scavenge gold from the overflow of the desliming cyclone. The material assayed 1.4 g/t Au and was mostly composed of ferrosilicates with trace amounts of pyrite and gold. A final concentrate was produced which assayed 15 g/t at a 33% gold recovery. Because of its low grade, the best alternative for reprocessing of this concentrate is cyanidation. This would of course depend on the mineralogical characteristics of the recovered gold and the capacity of the already existing cyanidation circuit. In this case, since most of the gold is cyanidable and the cyanidation circuit has extra capacity, the installation of a FC would be warranted, provided the above results can be validated.

4) At Echo Bay's Lupin operations, a FC Model B6 was installed to treat the final tailings from a cyanidation leach operation. Gold in the final tailings at Lupin occurs as occlusions in sulphides which are amenable to gravity concentration. A two-stage rougher-cleaner FC operation was used; no mention is given of sample weight. McAlister reported that the final cleaner concentrate assayed 5.4 g/t at a gold recovery of 21.5%. As a result of this work considerable testing of a continuous FC was initiated, and is still in progress.

Muir (1989) described the development of a gravity process flowsheet at Blackdome Mining corporation which included a FC. Overall gold recovery improved

from 90% to 95% with the addition of a secondary gravity separation circuit. The flowsheet included a primary grinding stage where the ball mill discharge was treated by jigging to remove the coarse gold. The jig tail was hydrosized to produce a fine fraction which reported to flotation, and a coarse fraction which was recirculated to the primary mill for further grinding. Approximately 35% of the gold was recovered from the flotation circuit, and the remaining was recovered from the gravity circuit. The jig concentrate was processed through two stages of gravity separation made up of two Deister tables and two FC's. A regrind step was included in between the stages to liberate more gold. No complete metallurgical balance or size-by-size analysis is given.

The above information strongly suggests that a more comprehensive study of the FC is warranted; one that considers a variety of feeds tested sytematically over a wide experimental range.

Although the FC was designed to recover fine gold, it may be suitable for the recovery of other minerals as well. For example, Morley (1992) reported on the use of the FC to recover fine cassiterite from the Rio Kemptville concentrator. Several tests were performed with a FC model B6 on different streams to recover additional tin values from the circuit- cyclone overflow, flotation scavenger tail and a flotation concentrate. The performance of the unit was gauged on the basis of four criteria: 1) Performance versus existing plant spirals; 2) Desliming capability; 3) Feed sizing capability; 4) Capacity of the unit. The results will now be summarized and discussed since they do reveal useful information on the nature of the separator.

The East Kemptville Tin Concentrator used a combined gravity/flotation process

for the recovery of tin, copper, and zinc. The gravity circuit consists Reichert cones, spirals and shaking tables. The ore contains 0.2% Sn and is first ground fairly coarse to 80% passing 600 μm prior to being classified in three stages of cyclones. The primary stage underflow is fed to the cones, while the secondary and tertiary stage cyclone underflows are sent to individual spiral banks. The spirals therefore have to treat fine, difficult to recover material (98% passing 100 μm). The overall unit recovery for the two spiral banks is about 18% at a grade of 0.3-0.4% Sn.

A considerable portion of the fine tin is lost in the overflow in order to establish a suitable feed for the downstream gravity circuit. A 10 kg sample of the primary cyclone overflow was thus processed with the FC to determine the feasibility of recovering the fine tin from the cycone overflow. Preliminary results showed that the FC was able to recover 57% of the tin and produce a concentrate at a grade of close to 15% Sn.

Different masses of primary cyclone overflow (5.4 kg and 9.6 kg at 10% solids) were fed to the FC, and the recovery of Sn, Cu, and Zn were calculated. The recovery of tin was comparable for both tests, 59% for the first test, and 57% for the second, but the grade increased from 0.5% to 1% from test 1 to test 2. Morley attributed the lower grade in the first test to incomplete recovery of the heavy mineral. He claimed that the unit was retaining too much of the tails because "the tails was a necessary component in making up the volume of the solids bed." If not enough feed is introduced to the FC, little upgrading will occur.

The tin flotation circuit at Rio Kemptville had a feed which consisted of about 6%

5

-5 μm material. With the nature of the froth and the circuit configuration, it was not unusual to have about 30-50% -5 μm material in certain streams, such as the first cleaner tails. This hampered the cleaning process by rendering the froth sticky. A reduction in the amount of low grade slimes would allow proper drainage of the froth and thus prevent a portion of the gangue from being entrained into the concentrate. This would improve collection efficiency by freeing up more collector, and lead to a conservation of the reagent, thus lowering operating costs.

The FC appeared to operate well as a desliming unit as consequently, several tests were performed on the flotation circuit upgrade the first cleaner tails and the flotation concentrate by removal of the slime component. For the cleaner tails, the FC was able to recover 81% of the tin and produce a 6% Sn concentrate from a 4% Sn feed. For the final concentrate, the FC was able to recover 99% of the tin, at a grade of 47% Sn from a 41% Sn feed. Both these results show that the FC was able to remove the slimes effectively without incurring any significant tin losses.

With regards to particle size effects, it was reported by Morley that coarse grains above 150 μm reported to the concentrate regardless of the particle specific gravity. In streams with locked tin, such as the scavenger tails from the flotation process, the FC recovered the coarse waste particles at about the same frequency as the locked tin, and thus little upgrading or recovery was realized.

The behavior of the sulphide minerals, chalcopyrite and sphalerite, as found to be similar to that of the cassiterite. These minerals, because they are denser than silica, and less dense than cassiterite, will be the last gangue particles to be rejected. The

recovery of the sulphides thus depends largely on the grade of the cassiterite required in the concentrate. Since a high grade tin concentrate is required, then the unit must be run long enough to reject the sulphides, obviously at the expense of tin recovery. Perhaps a better strategy would be to produce a bulk cassiterite/sulphide gravity concentrate that could then be upgraded in the flotation circuit.

The above results suggest that investigating the FC in a system of heavy (5 g/cm^3) and light (2.7 g/cm^3) minerals is warranted.

In conclusion, then, the main factors affecting the performance of the FC are the size, liberation characteristics and particle specific gravities of the material being fed. The FC was able to outperform the spirals in recovering fine tin below 150 μm from the primary cyclone overflow. Coarse particles greater than 150 μm seemed to be recovered by the FC quite readily, irrespective of their specific gravity, and little or no upgrading could be realized in those sizes, as was shown with the scavenger tails tests. Morley, however, did not test the effect of rotor pitch in his work. Perhaps a steeper pitched rotor may have produced better grades with the scavenger tails. Unfortunately, the mine closed down and no follow-up test work could be performed.

The capacity of the FC appears to be limited to the amount of available surface area on the bed. The thicker the bed, the less surface area will be available and thus the less amount of tin will be recovered. A compromise must thus be reached between the amount of tin recovered and the concentrate grade required.

1.2 Outline of Thesis

Before addressing the research work performed with the FC, a literature search was conducted on gravity separation with particular emphasis on fine particle recovery. Chapter 2 will present this summary.

Several 1 t/h, batch-type FCs model B6 have been leased out to different mines wanting to install gravity circuits in their mills, mostly gold producers. One of these units has been leased to Agnico-Eagle, division LaRonde (AELR), a small gold producer located 40 km west of Val d'Or, P.Q. Since a portion of the funding supporting this research came from AELR, the initial test work with the FC had to address their needs- decreasing the amount of gold locked-up in their circuit and reporting to the flotation concentrate by producing a smeltable gold concentrate. The thesis will first present the results of this investigation in Chapter 3.

A second support group involved in the investigation of the FC is Meston Resources, a gold producer located in Chibougamau, Quebec. While their economic interests are similar to those of AELR, ie. an increase in revenue, their technical requirements were slightly different. The objective here was to use the FC to recover additional gold values from the flotation tails' deslimer cyclone. Chapter 4 of the thesis will present the results of this study.

Since little data were available about the FC at the onset of this study, a basic understanding was first required prior to developing a detailed scientific test scheme. Chapters 3 and 4 present a great deal of basic information which generated a large amount of questions such as "How does the FC work, and "How is it affected by the

operating conditions?" Chapter 5, then, will present the experimental results of test work designed to answer some of these more fundamental questions. A novel testing approach using an artificially prepared feed consisting of silica and magnetite will be described as well.

Finally, in Chapter 6, general conclusions with regards to the FC will be presented and suggestions for future test work will be indicated.

The appendices at the end of the thesis contain all the detailed results of the test work. These data will be referred to in different sections of the work as deemed necessary.

Chapter 2

Fine Particle Recovery by Gravity Separation

2.1 Fine Particle Recovery by Gravity Separation

This section will describe the mechanisms of gravity separation, first in general terms and then as they apply to fine particle recovery. The purpose is not to focus on their mathematical analysis, but to present the basic concepts so as to get a "working knowledge" of gravity separation. The most common separators, jigs, spirals, and tables, will be used to illustrate how the different mechanisms operate. Several excellent references are available, and most of the material in this section is taken from Burt (1984) and Kelly and Spotiswood (1982).

Gravity concentration is the separation of one mineral from another based on the difference in their density. In general terms, the larger the density differential, the higher is the recovery of the valuable component, if all other factors being equal. The efficiency of gravity separators is sensitive to particle size and shape. In short, as particle size decreases to below 37 μm, gravity separation becomes more difficult. Sivamohan (1985) attributes these difficulties to the low mass and hence low momentum of the fine particles, colloidal coatings, heteroaggregation, high surface area, increased surface energy (increased electrostatic interactions), and increased pulp viscosity. It is not surprising, then, that traditional gravity based methods such as spirals and jigs perform poorly in the recovery of fines.

The various mechanisms which govern gravity concentration can be classified into two broad categories (Burt, 1989): first, those mechanisms relating to movement in a vertical plane, or stratification; second, movement on an inclined plane, or film concentration.

Stratification mechanisms relate mostly to jigging. Burt (1984) claims that four mechanisms have been identified as being important in jigging: differential acceleration at the beginning of the fall, hindered settling, minimization of potential energy and interstitial trickling. Differential acceleration at the beginning of the fall is density-dependent, size independent:

$$\frac{dv}{dt} = (1 - \frac{\rho}{\rho'}) * g \qquad \qquad 2.1$$

where v is the particle velocity (cm/s), ρ is the fluid specific gravity, and ρ' is the particle specific gravity.

Fine dense particles will generally be recovered more effectively when this mechanism predominates. Unfortunately drag forces rapidly become significant and the terminal velocity, which is size dependent, is rapidly reached. This may partially explain why jigs are generally inefficient in recovering particles below 150μm.

The terminal velocity of particles is size dependent. For particles finer than 75μm, Stokes' equation applies and a general equation for the terminal velocity is

$$v_t = K * (\rho' - \rho) * d^2 \qquad \qquad 2.2$$

where v_t is the terminal settling velocity (cm/s), d is the particle diameter (cm), ρ' and ρ are the particle and fluid specific density respectively, and K is a constant term.

Thus the effect of particle size rapidly becomes important, and fine particles will increasingly become difficult to recover.

As the solids concentration of a suspension increases, particles get closer and closer such that they will begin to crowd or interfere with each other (Svarovsky, 1990).

12

The settling rate will steadily decline with increasing concentration. This is referred to as **hindered settling** and can described by the following empirical relationship:

$$\frac{v_p}{v_g} = \epsilon^2 * f(\epsilon) \qquad\qquad 2.3$$

where v_p is the hindered settling velocity, v_g is the settling velocity of a single particle as calculated from Stokes' law, ϵ is the volume voidage fraction of the fluid, and $f(\epsilon)$ is a 'voidage function' which, for Newtonian fluids, is $\epsilon^{2.5}$.

Strictly speaking, the above relationships apply only to the cases when flocculation is absent, such as with coarse mineral suspensions. Suspensions of fine particles, due to the high specific surface area of the particles, will often flocculate and therefore show different behavior. Svarovsky (1990) comments that with increasing concentration, an interface can be observed which becomes sharper as the concentration is increased. The particles below the interface settle "en masse" or all at the same velocity irrespective of their size, which is obviously not conducive to selective separation.

At the end of each settling cycle in a jig, coarse particles will bridge together and come to rest. The finer particles will then trickle through the interstices of the larger ones. This is known as interstitial trickling.

Flaky particles are generally not well recovered by jigs. First, their terminal velocity is much lower than that of spherical particles of equal mass. Second, their shape restricts their motion during the trickling phase. Laplante (1988) comments that although jigs are often used in gold concentration, their effectiveness rapidly decreases below 100 μm.

13

A different approach to the conventional analysis of gravity separation has been used by Mayer (as quoted by Burt) who proposed that the stratification process is linked to the potential energy of the bed of particles. Loosening of the bed will enable particles to move to a lower potential energy state. Laplante (1988) considers the approach of limited use because it does not help understand the size/density relationship, nor the kinetics of separation. It is more of a "black box" approach to modelling the jigging process.

2.2 Film Concentration

Film concentration covers two very distinct cases. The first, thin film concentration, is when film thickness and particle diameter are of the same order of magnitude. This case is of limited pratical application, because it corresponds to extremely low capacities per surface area. The second is for thicker films, and is refered to as flowing film concentration.

As a fluid film flows across an inclined plane surface, its velocity increases with the distance from the surface, and a velocity gradient results which increases from zero at the deck surface or bed to a maximum just below the fluid surface. If a range of particles of different size and density are introduced into this flowing film they will arrange themselves with the denser phase settling to the bottom of the film and remaining closer to the feed end of the plane. The light phase will remain closer to the surface of the film where it will be dragged by the fluid further down the plane to the discharge. This is the basic mechanism of flowing film concentration. This approach to gravity

14

concentration is rather limited since it considers only very few layers of coarse particles, hence very low capacities. As well, as particle size decreases, larger concentration areas are required which renders this approach impractical. By artificially imparting a continuous shear to the mineral particles, such as in the case of the Mozley shaking table, however, the surface area required for concentration may be reduced.

Bagnold (1954) showed that a dispersive force is set up between the particles when a suspension of mineral particles is subjected to a continuous shear. Pressure develops across the plane of shear perpendicular to the surface and proportional to the square of the particle diameter. This dispersive force causes the bed of particles to dilate which leads to a vertical stratification with coarse lights on top followed by fine lights and coarse heavies and lights on the bottom. Burt (1984) mentions that in order to maintain sufficient shear by fluid motion alone, the flowrates must be fast and forward down an inclined surface. Addition of a mechanism to move the deck relative to the flowing film allows sufficient shear to be achieved at much lower slopes and fluid velocities, which enhances the recovery of very fine material. Table 2.1 presents a range of gravity concentration devices that use this principle (Burt, 1980).

The major machine variables are, first, the shear forces imparted to the particles in the pulp by the action of the shaking mechanism, if any; second, the forward velocity of the pulp stream, and finally the time the concentrate remains on the table surface or in the separator.

Feed characteristics, such as density, flowrate, and size distribution, are important because they may affect the flow velocities of the particles. For example, Douglas and

15

Stationary Decks	Stirred Beds	Centrifugal Device
-Buddle -Round Table -Round Frame -Strake -Corduroy Table -McKelvey Device -D/B Tilting Frame -Spiral Sluice	-Vanners -Shaking Table -Kieve -Rock/Shake Vanner -GEC Duplex	-Ferrara's Tube -DTsS Centrifugal -YT Separator -Knelson -TsBS Separator -Kelsey Jig -Falcon
	Unidirectional Shear	
	-Endless Belt -Johnson Barrel -Hodgson Separator -Rotating Cone	
	Orbital Shear	
	-Shaken Helicoid -Bartles-Mozley -Bartles Crossbelt	

Table 2.1: Range of Fine Gravity Concentration Equipment (Burt, 1980)

Bailey (1960) found that for a fine wolframite (74% passing 53 μm) ore processed with a shaken helicoid concentrator, the maximum fines recovery was obtained when the slurry density was between 10 and 15% solids. Mills (1979) explained this as being due to fines entrainment in the wake of the rising coarse particles. As the percent solids increases, particle/particle interference becomes more frequent, and thus entrainment becomes more significant.

Burt and Ottley (1979), in their studies with the Bartles/Mozley concentrator, found that high flowrates resulted in a decrease in recovery. Below the optimum flowrate, lower flowrates did not have a considerable influence, and in fact, the recovery remained constant. Sivamohan (1985) mentions that this phenomenon is common in all film-type concentrators. The faster the flowing film, the higher the fines losses. An

optimum flowrate can be expected under any given set of experimental conditions.

Most gravity concentration devices function more efficiently on prepared feeds; that is, removal of oversize material and slimes. Chaston (1962), for example, obtained a significant increase in recovery and enrichment after desliming a fine tin ore with hydrocyclones, prior to tabling on a fully riffled sand table.

There is a wide body of literature available which discusses the various gravity separators presented in the previous sections. Since this thesis will be dealing with a centrifugal type separator, nothing further will be said about these.

2.3 Centrifugal Separation

The use of centrifugal force to increase the settling rate of particles in classification has been recognized for many decades. The simplest case of centrifugal separation applies to a solid/liquid separating centrifuge, or sedimentation centrifuge. The particle terminal settling velocity under centrifugal acceleration can be approximated by Stokes' law[1] by replacing g, the gravitational acceleration, with $R\omega^2$ (where R is the radius of particle position, and ω is the angular speed). Particle motion, however, is now no longer at constant velocity but as the particles move radially outwards they are continuously accelerated. From equation 2.1, the net effect is an increase in the initial settling velocity, which will enhance the separation. As well, from equation 2.2, there will be an increase in the terminal settling velocity of the individual particles through an

---

[1]Stokes' Law yields only an approximation of terminal velicity as (i) the flow regime is unlikely to be laminar at high 'g and (ii) settling is hindered rather than free.

increase in the value of the constant K which is proportional to the acceleration. Also, the hindered settling ratio will now become v_p/v_c which is lower than the settling ratio under gravity forces, hence the particle velocity will be greater.

Only in the late 1950's, however, did the principle of centrifugal separation become recognized as a way of enhancing gravity concentration (Burt,1984). The centrifugal force can be applied to rotating tubes, cones, or drums. In simplest terms, the constant unidirectional rotation enhances the Bagnold shear force which dilates the bed and promotes separation by interstitial trickling. The reasoning is analogous to the case of centrifugal sedimentation. The equations of motion described previously may not necessarily apply since gravity centrifuges deal with films as opposed to a continuous solid phase dispersed in a continuous liquid phase.

The following sections will briefly describe some of the existing centrifugal separators. The first of these, the Ferrara tube, is not an industrial unit but an experimental device used to understand the principle. The analysis is similar to Gaudin's (1939) who analysed the forces acting on a single particle rolling or sliding in a two dimensional laminar film along a smooth bed.

2.3.1 Ferrara's Tube

A major attempt to develop the principle of a rotating tube separator was carried out by Ferrara (1960). His batch device consisted of a long, small diameter perspex tube (1100 mm by 20 mm) which could be rotated on its own axis up to speeds of 2200 rpm. The separation in the tube was based on two principles:

1) As slurry is fed into the tube the particles move through fluid layers. They are acted upon by a centrifugal force which pushes them towards the wall and a dragging effect, due to the water flow, which pushes them towards the discharge. As a result, the particles move along a spiral path. The heavier particles reach the tube wall sooner and spiral less than the lights, hence the separation.

2) At the wall, the particles are film-sized by the axial flow of slurry and wash water, such that coarse lights are discharged from the tube first. Thus separation is achieved by suitable relative adjustment of the axial flow and the rotational velocity.

Ferrara derived the equation for the motion of a particle in a cylindrical tube by assuming laminar flow conditions. There are three forces said to act on each particle: the centrifugal force, the frictional force between the particle and the tube wall, and the thrust of the fluid.

The equation of motion under this condition is then defined as follows:

$$\frac{4}{3}\pi(\frac{d}{2})^3\rho'\frac{dv}{dt} = -\frac{4}{3}\pi(\frac{d}{2})^3(\rho'-\rho)\psi\omega^2(r_1-\frac{d}{2}) - 18k\mu\frac{1}{r_1^4}Q(\frac{d}{2})^3 - 6\pi k\mu v(\frac{d}{2}) \quad 2.4$$

The variables in equation (2.4) are defined as follows: r_1 is the inside radius of the tube; ω is the angular velocity of the tube; d is the diameter of the particle; ρ' and ρ are the densities of the particle and the fluid; ψ is the coefficient of friction between the particle and the tube wall; k is the coefficient of the non-sphericity of the particle; μ is the viscosity of the fluid; Q is the flow of the fluid through the tube; v is the velocity of the particle along the tube wall.

An interesting feature of Ferrara's equation is that it takes into account the shape of the particles. The author admits himself, however, that the equation has limited use. Perhaps the biggest objection to his type of analysis is that it is overly simplistic since it ignores the effect of particle concentration. A further objection is that it is experimentally quite difficult to study the trajectory of a single particle, except at very low concentrations. Leeder, as quoted by Holtham (1991), recognized that the division of particle transport between suspended load and bed load is better defined in terms of whether the particles are operated on by fluid momentum transfer alone or by a combination of solid and fluid momentum transfer. His analysis uses sediment transport theory and is beyond the scope of this discussion. It is recognized, however, that six modes of particle motion were described in his paper; these are summarized as follows:

1) rolling.

2) uninterrupted saltation.

3) uninterrupted partly suspensive saltation in which normal ballistic saltation trajectory is modified by fluid turbulence.

4) interrupted partly suspensive saltation as 3) above, but with the addition of upward acceleration due to inter-particle collision.

5) interrupted suspension, in which the particle is maintained in suspension by both fluid turbulence and inter-particle collisions. .

6) uninterrupted suspension, in which there is true suspension of the particle by fluid turbulence.

Holtham defines "suspended load' as those particles held in true suspension

against gravity, or a centrifugal force, by random eddy currents of turbulence having velocity components normal to the bed greater than the terminal settling velocity of the particles relative to the fluid surrounding them, ie. particles in mode 6 only. Modes 1 to 5 are all modes of bed load transport.

In a gravity concentrating device, where a load of heterogeneous particles (in terms of size and density) is being transported, all six modes can co-exist. The preferred mode of transport is dependent on the critical shear velocity for the initiation of motion. Holtham refers to Bagnold's work (1966) to show that a particle should become liable to suspension at a transport stage of $0.8v_t/v_o^*$, where v_t is the particle terminal velocity in water and v_o^* is the critical shear velocity for the initiation of transport. It can be seen that as particle size decreases, the aforementioned ratio decreases quite rapidly, since the terminal settling velocity also decreases rapidly. For example, for quartz particles finer than 100 μm some suspension should occur at the threshold of bed movement, and these particles should be transported entirely by mode 6, turbulent suspension. However, turbulence is considerably dampened by the presence of solids, resulting in a delay in its onset until a much higher transport stage is reached.

2.3.2 Knelson Concentrator

The Knelson Concentrator (KC) consists of a double walled, conical shaped, riffled concentrator vessel. The unit is essentially a high speed, ribbed, rotary cone with a drive unit. The KC uses the principles of hindered settling, and interstitial trickling enhances by centrifugal force (Knelson, 1988). The latter force causes the feed to fill the

ribs from bottom to top. Heavy particles are forced out against the walls and are trapped between the ribs. Because of the centrifugal force generated by the rotation of the bowl, the denser particles will be concentrated very close to the bowl surface, deep within each riffle (Laplante, 1992). Lighter particles will be carried by water to the top of the unit, ejected against its outer wall, and then evacuated through an opening at its bottom.

The cone is surrounded by a pressurized water jacket that forces water through the holes in the cone to keep the bed of heavy particles fluidized and thus prevent compaction. The water addition is the key to the performance of the KC. The degree of fluidization essentially controls the concentrate bed bulk SG and porosity and hence which minerals will or will not report to the bed (Ounpuu,1992). Lower pressures are used for low SG gangue material and higher pressures for high SG gangue material.

Banisi (1990) showed that a laboratory KC yielded gold recoveries comparable to those achieved by amalgamation, although the test work was limited to two samples. Nevertheless, he concluded that the laboratory KC is a legitimate tool which can be used to estimate the amount of 'gravity recoverable', or free gold in a stream. For example, this technique was used to study the behavior of gold in the grinding circuit of Hemlo Mines. He found that in the first loop of the grinding circuit, gold grades were in good agreement (when considering mass balance constraints) and the behavior of gold to grinding and classification could readily be estimated. Gold's behavior in grinding circuits is of particular interest because it is so different from that of other minerals, both in terms of malleability and density, that it accumulates in grinding circuits, which can result in losses due to overgrinding, difficulties in estimating head grade or gold

22

inventory, and a security risk.

2.3.3 Kelsey Jig

The Kelsey Centrifugal Jig design is based on a conventional jig operating within a centrifuge. It consists of a rotating bowl, with a series of individual hutches wrapped around it. The pulsation is provided by a diaphragm whose stroke is controlled by a cam-motor assembly independent of the main drive. This allows better control of the pulse rate and stroke length.

The feed enters from the top and the centrifugal force imparted by the bowl rotation forces the slurry to make contact with the ragging material. High frequency pulsations imparted by the diaphragm create an inward water pulse which causes the ragging to dilate and contract at the same frequency. This, in turn, results in differential acceleration of the feed and ragging particles according to their specific gravity. Particles then settle under centrifugal force causing the heavy particles to separate from the lighter particles. Those of higher specific gravity move through the ragging and the retention screen into the hutches where they are discharged through spigots into the concentrate launder. Particles with specific gravities less than the ragging are displaced from the surface of the ragging layer by incoming feed. The Kelsey is capable of recovering cassiterite as fine as 8 to 10 μm. It suffers from a high maintenance cost and frequent breakdowns because the unit is mechanically complex (Burt, 1984). A mechanically improved Kelsey jig has been sent to the Iron Ore Company of Canada and is presently undergoing testing.

Perhaps one of the more clearer descriptions of the Kelsey Jig is given by Wyslouzil (1990) who evaluated this unit at the Rio Kemptville Tin operations in Nova Scotia, Canada. Unlike a conventional jig, the hutch is oriented on a vertical plane. The jigging portion of the separator operates as a conventional jig with the exception of having an increased 'settling force'; namely the centrifugal force generated by the rotation of the bowl.

The major variables affecting the performance of the Kelsey Jig are: 1) ragging material; 2) jig rotational speed; 3) pulse action; 4) pulse water.

The ragging material must be selected to suit the nature of the feed in terms of specific gravity and size distribution. Its specific gravity must be between that of the waste and that of the material being recovered. The size distribution of the ragging must be suitable for the material being processed. If the ragging is too coarse, poor concentrate grades will result. If the ragging is too fine, passage of concentrate will be restricted and poor recoveries will result. The recovery of fines is dependent on the magnitude of the centrifugal force generated by the rotation of the bowl. Jig rotational speeds can range from 200 to 800 RPMs. At these speeds, the apparent gravitational force ranges from 20 to 160 times the normal gravitational force (Wyslouzil, 1990). Recovery is increased initially with increasing gravitational force but drops off at higher levels, which is due to compaction of the ragging material.

The force required to compact the ragging and stop the flow of concentrate is a function of both ragging weight and the stroke amplitude; thus, the performance characteristics of the jig with respect to centrifugal force can be altered by varying the

amplitude of the pulse stroke. At lower rotational speeds, a shorter stroke results in better control of the concentrate grades due to smaller dilations (Wyslouzil, 1990). At higher rotational speeds, a more powerful stroke is required to counter-act the compaction of the ragging.

The water pulse controls the rate and magnitude of dilation of the ragging layer. Increasing the pulse frequency increases the number of dilations and therefore increases the probability of trapping heavies in the ragging bed. It appears that the concentrate grade decreases as the pulse rate increased. The effect of pulse rate on recovery is less significant.

Proper screen selection is also important since it must allow the desired mineral to pass through with recovering excessive amounts of large, heavy middlings.

In terms of grade/recovery relationships the Kelsey Jig was able consistently produce better results than tables. At East Kemptville, recoveries of more than 90% tin were attained at final concentrate grades of 96% (Wyslouzil, 1990).

2.3.4 Falcon Concentrator Model B6

The FC consists of a linatexed, single walled, almost-conically shaped basket. Figure 2.1 illustrates the FC and its basket. The feed is introduced near the base of the bowl where it impacts on a rubber impellor rotating with the bowl. The centrifugal force generated by the rotation of the bowl forces the material to settle out to the wall of the bowl where it will migrate up the slightly inclined wall. The light material flows upwards and out of the bowl into a collection launder. The heavy material remains in

the bowl and is eventually removed by water flushing once the operating cycle is complete.

Selective recovery begins after a layer of feed (1-2 cm thick) has deposited on the wall of the bowl (Morley, 1989). At the wall the particles continue to separate not unlike in the Ferrara tube which has been described previously. The main forces acting on the particles are the centrifugal force due to the rotation of the bowl, the frictional force between the particles and the solids bed and the fluid drag force. Denser particles experience a larger frictional force than the less dense particles and will remain in the bowl.

The major variables which can be directly manipulated are feed flowrate, % solids, and rotor geometry. The rotor is a patented designed truncated cone, similar in shape to a hydrocyclone. The rotor assembly can be removed which allows for the installation of a several bowl types, 8, 10, and 14 degree bowls; the angle refers to the wall slope relative to the vertical center line.

Concentrate discharge in the FC model B6[2], is not continuous. It can be operated semi-continuously by installing a programmable variable speed motor drive. At the end of the operating cycle, the feed is stopped, the rotor speed is reduced to 5% of operating speed, and the concentrate bed is washed out using spray nozzles installed along the periphery of the bowl (McAlister, 1989). Rinsing time is typically 30 to 40

---

[2]B6 refers to the type and capacity of unit: "B" refers to a batch-type unit and 6 to the diameter of the rotor (measured at the the rim of the bowl), in inches. The rated capacity of the B6, the smallest model, is 0.5 tph.

seconds. Both the operating and the rinsing times can be controlled with digital timers. A continuous FC (C20), 20 tph in capacity, has been developed, and is presently undergoing plant testing at the Carol Lake plant, Iron Ore Company of Canada, and the Lupin Mine, Echo Bay Ltd.

Fresh Feed

Tail Discharge

Concentrate Removal
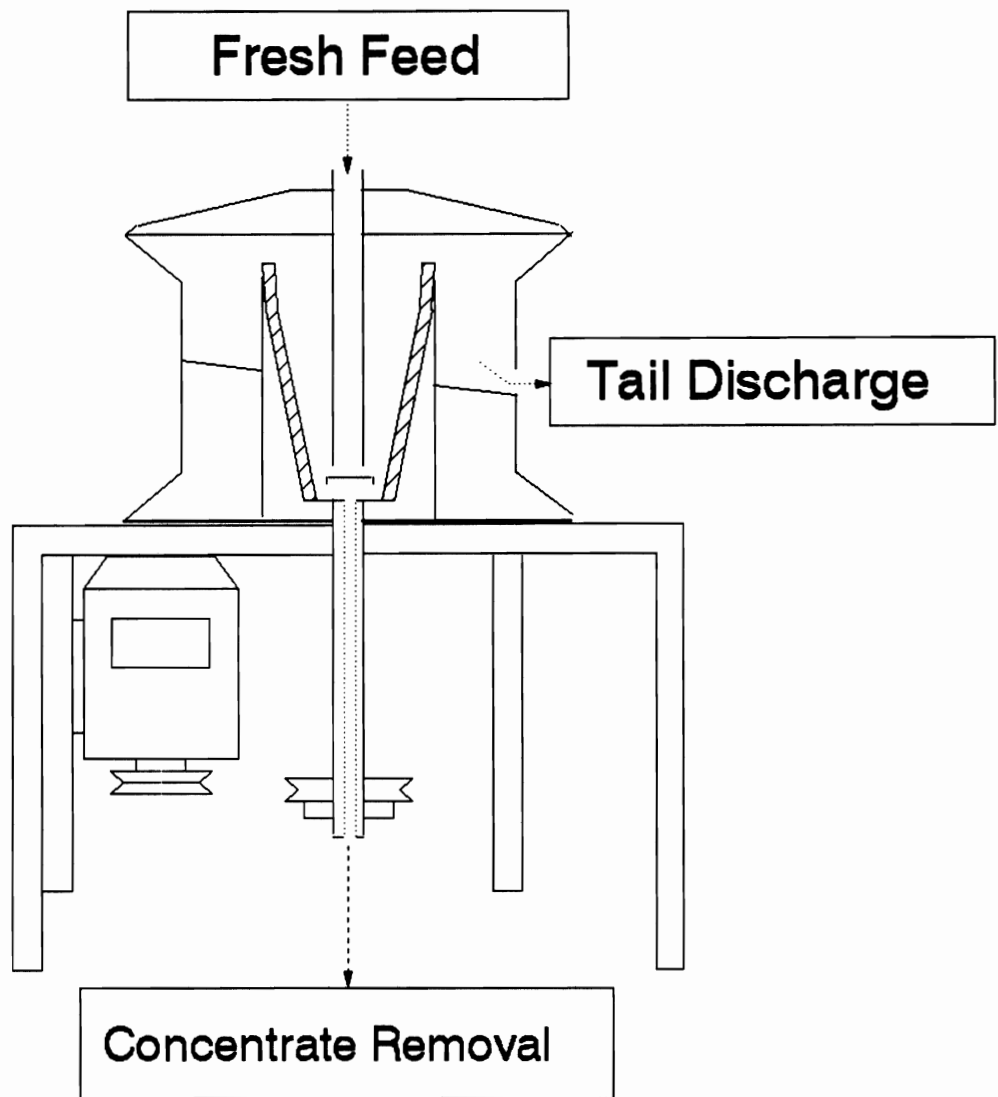
Figure 2.1: Falcon Concentrator Model B6

Chapter 3

Gold Recovery from Agnico-Eagle Division Laronde

3.1 Introduction

The Agnico-Eagle LaRonde Division (AELR) mill located near Val d'Or, Québec, treats 1700 metric tonnes of a pyrite-chalcopyrite ore containing roughly 3 g/t of gold by flotation and cyanidation. The flotation concentrate accounts for roughly 60% of the total gold and assays 200 g/t. If some of this gold can be recovered by gravity, then a better economic return on gold recovered can be expected because where smelters will only pay for 95-97% contained gold, usually after a 3 month delay, gold recovered by gravity is smelted directly and close to 100% payment can be achieved upon delivery of the bullion to the refinery. Thus, a 50% recovery by gravity increases total payment by 2-4%, even if the total recovery remains unchanged (Laplante, 1988).

The investigation of the AELR circuit was divided into five phases:

Phase 1- Sampling of the grinding circuit to determine the gold inventory.

Phase 2- Investigating gold's grinding and classification behavior.

Phase 3- Processing all samples with a 7.5 cm Knelson Concentrator (KC) to determine their amenability to gravity recovery- primary ball mill discharge (BMD1 and 2), sluice concentrates (SC1 and SC2), sluice tails (ST1 and 2), secondary cyclone overflow (SCOF1 and 2), primary cyclone feed (PCF1 and 2), primary cyclone underflow (PCUF 1 and 2), primary cyclone overflow (PCOF), regrind mill discharge (RMDS) and secondary cyclone underflow (SCUF).

Phase 4- Processing samples of selected streams with the FC to predict the amount

of recoverable gold, whether or not at smelting grade (20-30% Au). AELR's break-even estimate is 22% gold recovery (Robitaille, 1991), and the unit must be tested to determine if it can achieve this target. In the circuit, the obvious streams from which to recover gold by gravity are the regrind mill discharge, the secondary cyclone underflow and overflow, and the flotation concentrate.

Phase 5- Optimizing FC operation for maximum recovery and grade.

3.2 Phase 1: Sampling Survey of the AELR Grinding Circuit

The AELR grinding circuit was sampled January, 1991 to determine the gold inventory in the circuit. The circuit is divided into two separate lines and, at the time of sampling, line one was treating lower grade material (2 g/t Au) than line two (10 g/t). All the stream samples collected were subsequently processed with a 7.5 cm KC and assayed size-by-size to determine gold's amenability to gravity recovery, as well as its grinding and classification behavior.

3.2.1 AELR Grinding Circuit

The AELR grinding circuit flowsheet is shown in Figure 3.1. After three stages of crushing, the ore is fed to two separate primary grinding lines at a rate of approximately 37 tph, each. Two 3.5 x 5.2 m ball mills grind the ore to a P_{80} of 300 μm (48 mesh). A portion of each mill discharge is bled from the circuit via pinched sluices and redirected to a secondary grinding stage. The secondary grinding circuit
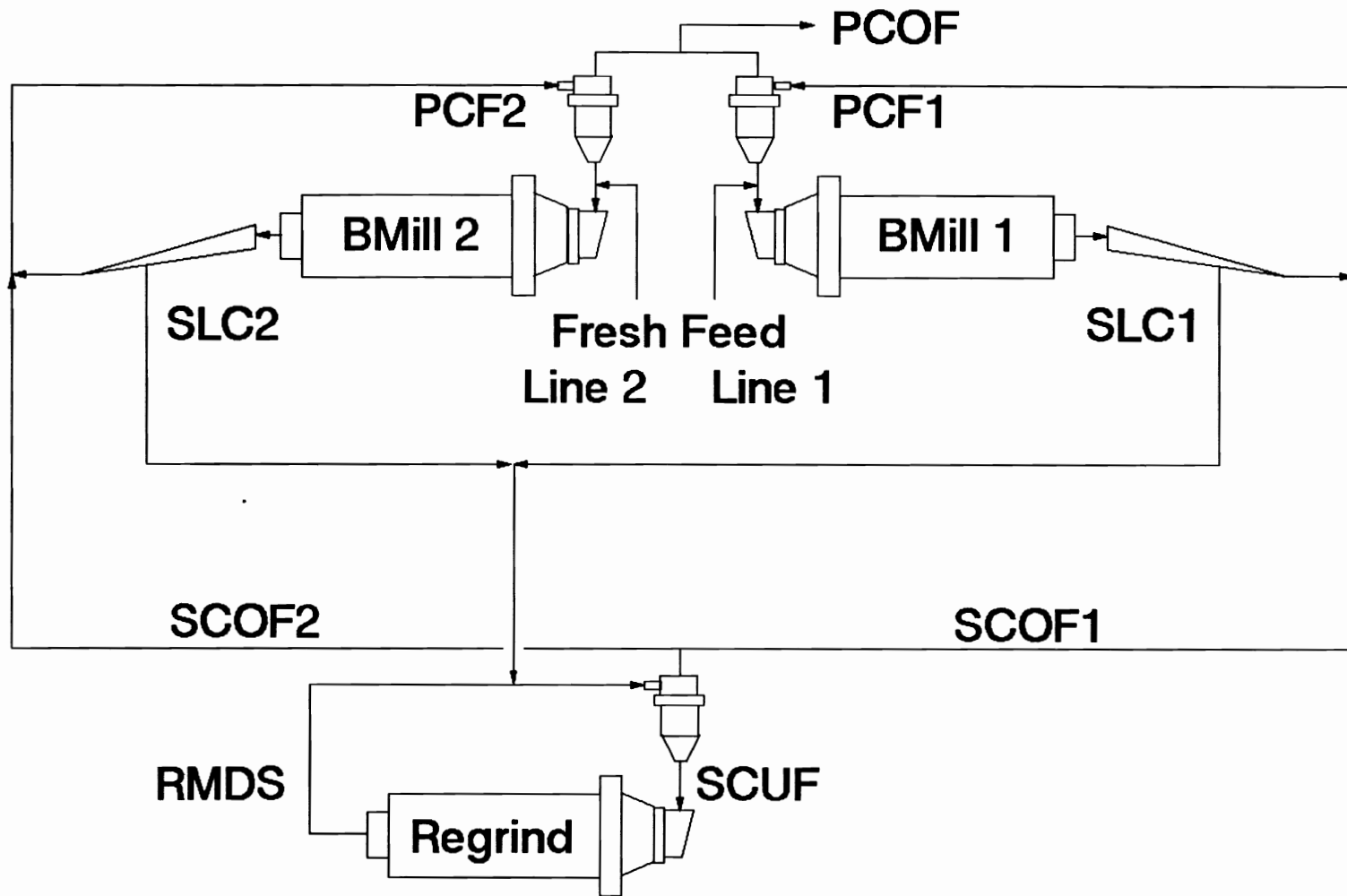
Note: BMD, PCUF, and SLT not labelled.

Figure 3.1: Schematic of AELR Grinding Circuit

can be operated either as a regrind section for the flotation concentrate when chalcopyrite liberation is more difficult to achieve, or as a secondary grinding circuit for the mill when extra grinding capacity is required. Otherwise, it is not used. At the time of sampling, it was operating in mode 2- the pinched sluice concentrates, which make up roughly 10% of the mill discharge flow, were directed to the secondary grinding stage where the ore was ground to a P_{80} of 150 μm (100 mesh) in a closed circuit cyclone/ ball mill circuit. The sluice tails were combined with the secondary cylone overflows and recirculated to the primary cyclones. The primary cyclone overflows are always combined and then pumped to the flotation circuit for further treatment.

3.2.2 Sampling of Gold Ores

Slurry sampling is an essential tool for the evaluation of plant performance but it is error-prone. It is important to understand the sources of errors if reliable results are desired. The total error is a combination of systematic, bias and random errors. It can never be truly reduced to zero. Even in the case of perfect sample preparation, the random sampling error is always present (Pitard, 1989). When the composition of the desired constituent is low, for example gold, then the random, or fundamental, error will be considerable. This is particularly true in the coarser size classes (Nigel,1990; Hallbauer and Joughin, 1972).

By extracting and then preconcentrating large slurry samples (10-20 kg),

33

sampling and assaying accuracy can be improved. Further, it can also reveal information on the nature of the gold particles present in the sample. For example, in step 1 of Figure 3.2, the easily recoverable coarse gold is removed with a laboratory KC. Treatment of the KC tails by flotation and then cyanidation can reveal quantitative information on the harder to recover gold.

Banisi (1990) has demonstrated that the occasional thick gold flake appearing in a coarse size class may cause a significant assaying bias. Consider Table 3.1 which shows the change in sample grade versus gold particle size (Bacon et al, 1989). The data show that this effect is most significant in the coarser sizes. For example, a 300 μm (48 mesh) gold flake may change the grade by as much as 17 g/t (0.5 tr.oz./st), which is significant. In fact, virtually no accurate information about free gold can be obtained above 600 μm because of the error (Laplante, 1990).

Size, μm	Mesh Size	Mass mg	1/2 A/T	1 AT	2 AT
600	28	4.000	8.00	4.00	2.00
300	48	0.500	1.00	0.50	0.25
212	65	0.170	0.34	0.17	0.18
150	100	0.060	0.12	0.06	0.03
106	150	0.020	0.04	0.02	0.01
75	200	0.008	0.02	0.01	0.002
53	325	0.002	0.004	0.002	0.001
38	400	0.001	0.002	0.001	<0.001

* AT= Assay Ton, tr.oz./st.

Table 3.1: Nugget Effect Showing Change in Gold Assay per Particle of Gold
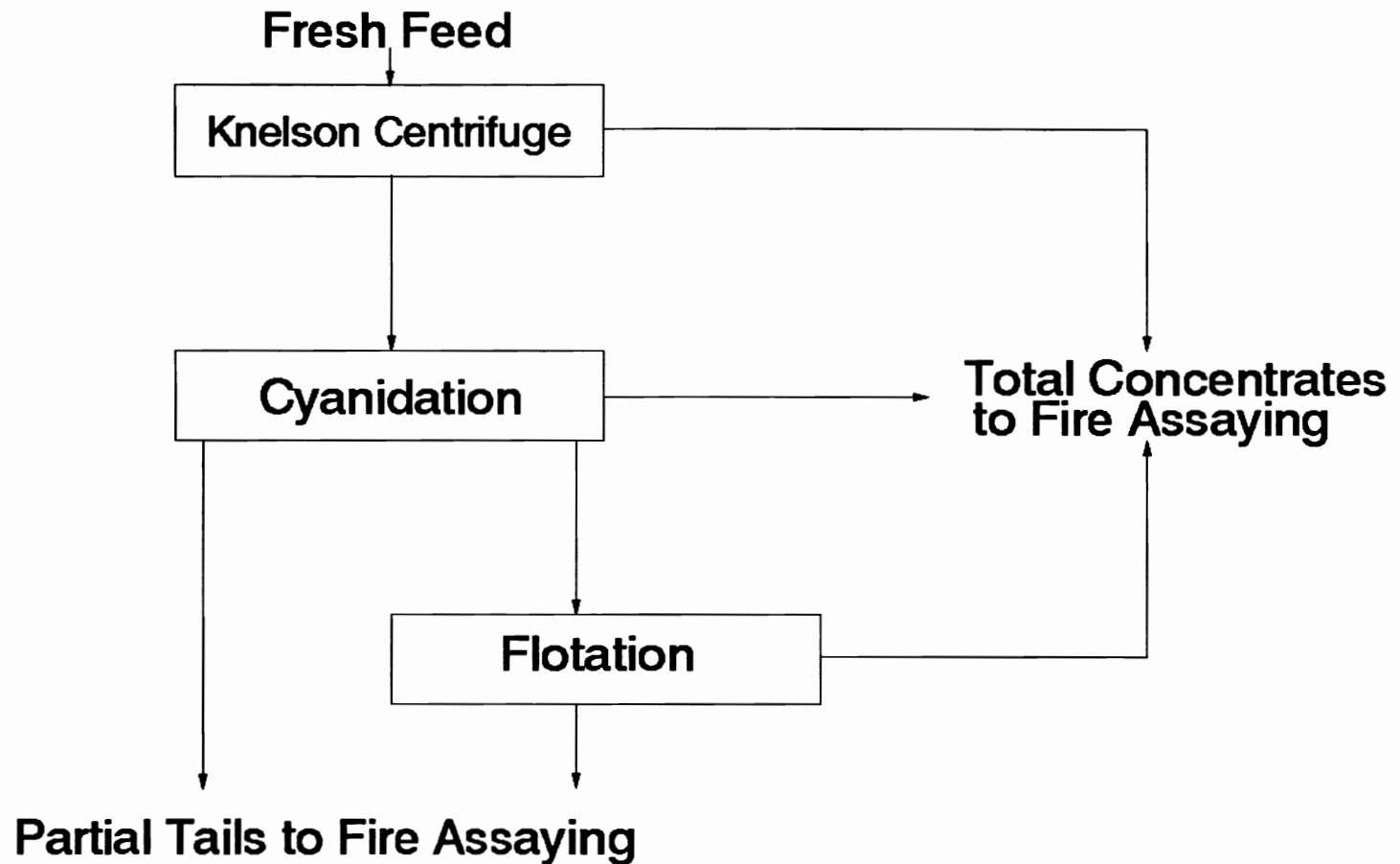
Figure 3.2: Extension of Preconcentration Scheme
to Determine Nature of Gold in Ore

3.2.3 Test Procedure

The AELR grinding circuit was sampled on January 4, 1991 under relatively high mill feed grade conditions. Each sample consisted of 8 increments taken at 15 minute intervals over a 2 hour period. Table 3.2 identifies each sample.

Six of the circuit streams could not be satisfactorily sampled. The individual primary cyclone overflows and the secondary cyclone feed were not sampled as the streams were unaccessible; the joint overflow (PCOF), however, was easily sampled. The full cross section of the sluice tail streams (SLT1 and 2) could not be sampled because of the high flowrate, and the bottom part of the sluice tail was left unsampled. As it contains a higher proportion of coarse and dense particles, these tail samples were biased.

The mass flowrate measurements presented in the table (SLC1 and 2, SCOF1 and 2) were calculated from timed and weighed samples. The overflow dry sample masses were lower because of their lower percent solids. Also, the results show a significant difference between the SCOF1 and the SCOF2 flowrates (13.9 vs. 6.6 tph). This difference stems from surging in the cyclones which was observed at a frequency of about 1 per minute during the 2 hour sampling campaign. Although both secondary cyclones surged, the problem was much more severe for the second.

The samples were dried and then screened at 1.7 mm (10 mesh). The undersize was then fed at a rate of 500 g/min to a 7.6 cm (3 inch) KC. The back-water pressure was maintained at 33 kPa (5 psi) for all samples except the cyclone

Sample Description	Mass of Sample (kg)	% Solids	Measured Flowrate (tph)
Ball mill Discharge 1 (BMD1)	13.5	73.9	
BMD2	16.4	77.5	
Sluice Conc 1 (SLC1)	6.8	50.2	9.9
SLC2	3.0	30.2	10.6
Sluice Tail 1 (SLT1)	12.7	67.1	
SLT2	7.5	51.4	
Secondary Cyclone O/F 1 (SCOF1)	3.0	28.5	13.9
SCOF2	2.5	27.5	6.6
Primary Cyclone Feed 1 (PCF1)	6.8	66.3	
PCF2	9.6	81.8	
Primary Cyclone U/F 1 (PCUF1)	15.6	76.6	
PUF2	18.8	80.2	
Primary Cyclone O/F (PCOF)	3.0	27.6	
Secondary Cyclone U/F (SCUF)	13.5	76.9	
Regrind Mill Discharge (RMDS)	12.9	76.7	

Table 3.2: Sample Description

overflows where the pressure was reduced by half to reduce fine losses. The KC tails and concentrate samples were weighed separately, dried and screened from 150 μm (100 mesh) down to 38 μm (400 mesh). The secondary cyclone overflows were wet screened at 30 μm (500 mesh) and then processed as above. Each of the size fractions was fire assayed for gold content at AELR. The gold grade of the original

KC feed was then back calculated from the assays of the concentrates and tails.

3.2.4 Mass Balance Results

Appendix I presents the individual metallurgical balances for the KC tests. These data were adjusted with the Norbal2 software package (Spring,1985), and the results are presented in Appendix II.

An overall balance of the circuit was first made using only the back calculated head assays from the KC tests and the estimated flowrates. Next, these results were combined with the assays of the size fractions ($+150$ μm down to -38 μm) to complete the balance. The standard deviations were estimated from the accuracy of the samples and the assays.

Table 3.3 compares the original and adjusted flowrates and head assays. As expected, there are some rather severe adjustments that have been made to the measured flows. Again, this can be traced to unsteady conditions in the mill at the time of sampling. The table also presents the original and adjusted head assays. Here as well are some rather severe adjustments; particularly the PCOF. As expected, the sluice tails were also largely adjusted. Because of the sampling bias their gold grades had been assigned a high standard deviation. Unsteady conditions in the plant and the fundamental sampling errors may account for the severe discrepencies. Given the careful treatment and size of the samples, the first is expected to be more significant. This is further confirmed when size-by-size data are

Stream	Flowrate		Au Assay, g/t		% Au Distribution
	Measured	Calculated	Measured	Calculated	
BMD1		216.4	17.3	19.5	1063
BMD2		221.0	26.4	25.7	1430
SLC1	9.9	6.8	30.5	30.4	52
SLC2	10.6	8.5	40.1	39.7	85
SLT1		209.6	14.1	19.1	1011
SLT2		212.5	36.7	25.1	1345
SCOF1	13.9	9.3	41.6	42.1	101
SCOF2	6.6	6.0	25.0	25.4	260
PCF1		218.9	28.1	20.1	1110
PCF2		218.5	19.0	25.1	1384
PUF1		179.4	25.0	23.2	1047
PUF2		184.0	28.7	29.0	1347
PCOF		74.0	21.9	5.4	100
SCUF		105.0	155.7	140.5	3720
RMDS		105.0	129.1	140.5	3720

Table 3.3: Comparison of Original and Adjusted Flowrates and Assays

examined, as corrections are systematic rather than random.

To use Norbal2 required seven independent flowrate estimates, not including the fresh feed rates to the primary ball mills which were given by the grinding control system at AELR. Four of these flowates, SCOF 1 and 2 and the SLC 1 and 2, were measured. The other three estimates were assumed, and correspondingly assigned high standard deviations. Several different estimates were tried; those shown gave

the best fit.

As expected, the assays of the size fractions did show some severe adjustments, because of the low mass and fineness of material in some of the size fractions.

The measured gold assays of the PCF show that higher grade material is being fed to the circuit 1 cyclone, which is incorrect because mill 2 was being fed higher grade ore at the time of sampling. Norbal2 did adjust the results to make them more consistent, however. The two streams making up the PCF is the SCOF and the SLT. Because the SLT accounts for most of the material in the stream, and because the SLT1 grade is lower than the sluice tail grade of circuit 2, then the PCF1 grade should be lower than of the primary cyclone feed of circuit 2. In addition, they should be close to the grade of the SLT's, which is reflected in the mass balanced data, but not in the measured data.

The high circulating load, 3720% and the high gold assays of the RMDS and SCUF clearly indicate that gold is building up in the regrind circuit. This is not unusual and can be accounted for by gold's high density and grinding behavior (ie. its classification and malleability as will be presented next).

3.3 Phase 2: Gold's Grinding and Classification Behavior

To determine why gold was accumulating in the regrind circuit required the investigation of its grinding and classification behavior which shall now be discussed.

The grinding behavior will be described in terms of the selection function, a first order rate of breakage constant, and the classification behavior will be described in terms of separation efficiency in the secondary grinding loop's hydrocyclone.

3.3.1 Grinding Behavior of Gold- The Selection Function

The selection functions of the ore and gold were determined and compared to assess gold's grinding behavior (Banisi, 1990). The ore breakage function was estimated from grinding of a single size class (420-600 μm) of the actual ore for very short periods of time and using the analytical procedure of Herbst and Fuerstenau (1968). The gold breakage function was taken from Banisi (1990). BALLDATA and BALLMILL, two software programs developed at McGill, were used for the determination of the selection functions. Details of the calculation procedures and software codes may be found elsewhere (Laplante, 1989). The simulation results are presented in Appendix III and summarized in Figure 3.3 and Table 3.4. Figure 3.3 shows that the selection function of gold is considerably lower than the ore's. Gold's SF is also noisier, which is expected, given the cumulative effect of assay errors. The gap between the two SF's increases with increasing particle size, which is confirmed from their ratio shown in Table 3.4.

In his study of the Hemlo Gold grinding circuit, Banisi (1990) also measured the selection function ratios and reported values as high as 20. Decreasing ratios with decreasing particle size were also observed.

41
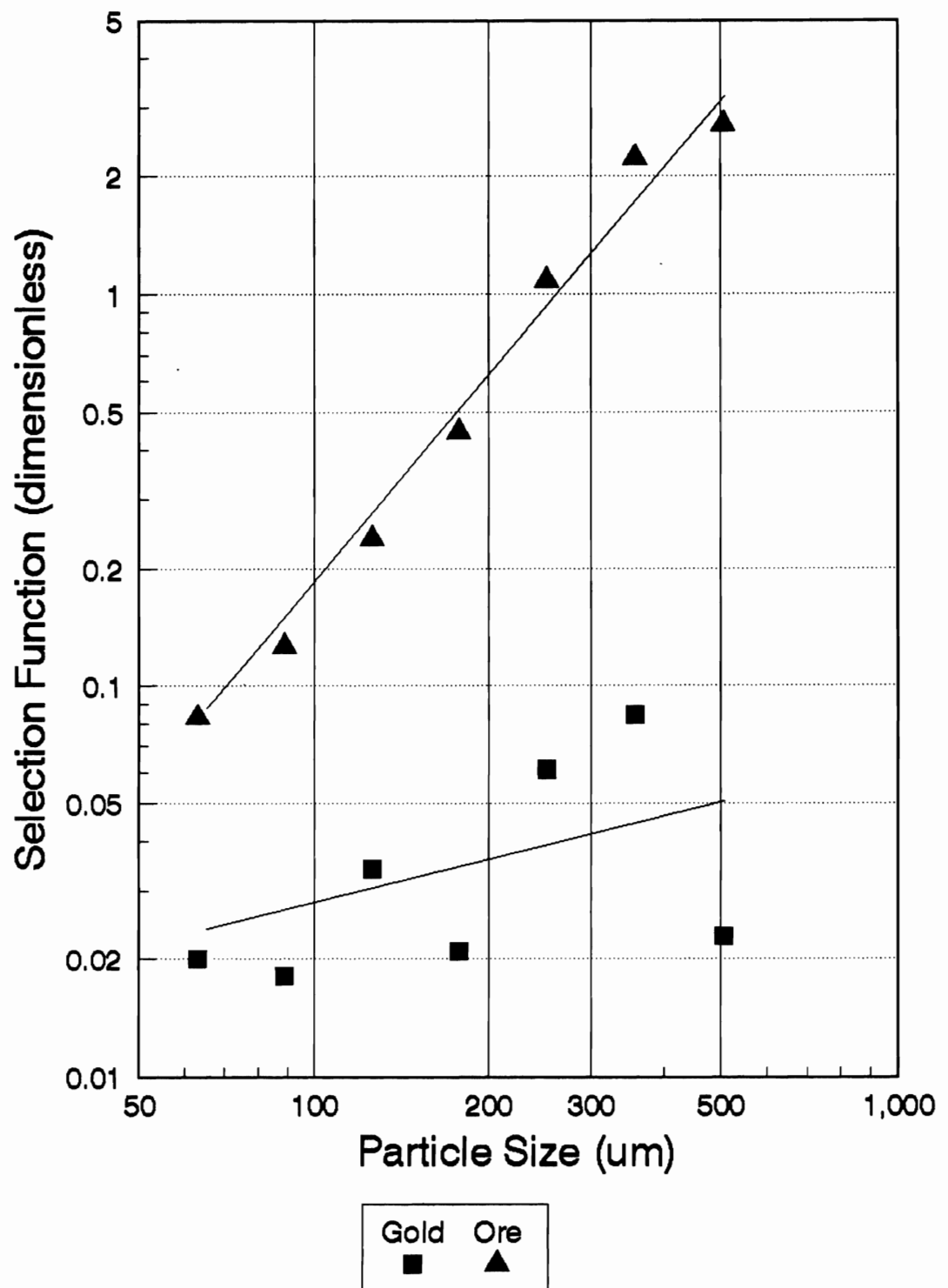
Figure 3.3: Selection Function for
Gold and the Overall Ore

Size	Gold	Ore	Ratio
+425-600	0.023	2.703	116
+300-425	0.084	2.219	27
+212-300	0.061	1.084	18
+150-212	0.021	0.444	21
+106-150	0.034	0.238	7
+75-106	0.018	0.127	7
+53-75	0.020	0.083	4
+38-53	0.040	0.126	3

Table 3.4: Comparison of the Selection Functions for Gold and the Ore

3.3.2 Secondary Classifier Performance

A classifier cyclone performance curve is a plot of Y vs. d, where Y is the weight fraction of feed size d reporting to the underflow (Plitt, 1976). Y overall is calculated from:

$$Y_{overall} = \frac{Uu_{w,i}}{Uu_{w,i} + Oo_{w,i}}$$ **3.1**

where U, O are the cyclone U/F and O/F mass flowrates, and $u_{w,i}$ and $o_{w,i}$ are the mass fraction of size class i in the U/F and O/F, respectively.

Y for individual mineral, Y_m is given by equation 3.2.

$$Y_m = \frac{Uu_{w,i}u_{m,i}}{Uu_{w,i}u_{m,i} + Oo_{w,i}o_{m,i}}$$ **3.2**

$u_{m,i}$ and $o_{m,i}$ are the assays of mineral m of size class i.

43

Figure 3.4 is the performance curve for the secondary cyclone plotted as mass recovery to the underflow versus the mean (geometric) particle size. Only the upper part of the traditional "S" shape of the curve is apparent. Gold's recovery to the underflow is high for all classes, and slowly starts to decrease at around 38 μm (400 mesh). The ore exhibits a similar trend, at lower recoveries than gold, and the descent is more severe and begins at around 106 μm (150 mesh).

It is assumed that in all classifiers, fines are entrained in the coarse product liquid in direct proportion to the fraction of feed water reporting to the coarse product (Wills, 1988). This phenomenon in cyclones causes fines to report to the underflow. A correction can be made to the original recoveries (Y) by including a water recovery term (R) into the equation:

$$Y_c = \frac{Y-R}{1-R} \qquad\qquad \textbf{3.3}$$

The water recovery to the underflow calculated from the circulating load and the densities of the SCOF and SCUF, R, is 44.7%. This includes surging, when the full content of the cyclone is discharged to the SCUF, and as such overestimates R when the cyclone is operating properly. The corrected performance curves for total solids and gold are illustrated in Figure 3.4 and show that short circuiting is more apparent in the ore's performance curve as the corrected recovery goes to 0.

The corrected cut size, d_{50c}, can be determined from the corrected performance curve using the approach devised by Plitt (1976), who suggested the following
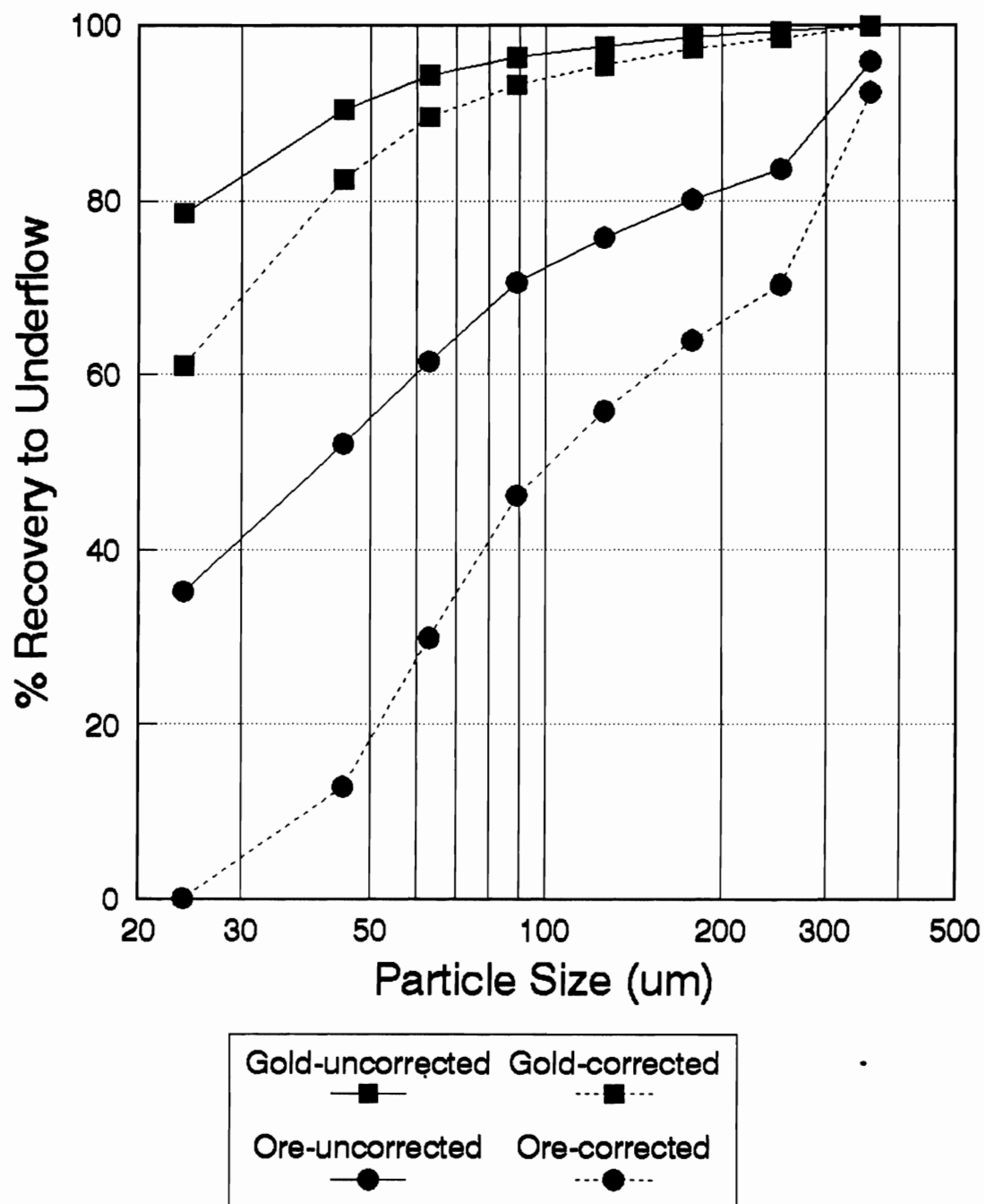
Figure 3.4: Secondary Cyclone Efficiency Curves

equation to represent a corrected classification curve :

$$Y_c = 1 - \exp{-0.693\left(\frac{d}{d_{50c}}\right)^m}$$ **3.4**

where d_{50c} is the corrected cut-size and m is a measure of separation sharpness

Equation 3.4 can be rearranged to form a linearized equation:

$$\ln\left[\left(\ln\frac{1}{(1-Y_c)}\right)\right] = m*\ln(d) + \ln(0.693) - m*\ln(d_{50c})$$ **3.5**

A plot of $\ln[1/(1-Y_c)]$ versus d on a log-log scale should yield a straight line

of slope m and $d_{50c} = d$ at $1/(1-Y_c) = 2$. Figure 3.5 shows this plot for both gold and

the ore, and Table 3.5 presents the model parameters. To minimize the effect of the

normal experimental errors, only values of Y_c between 0.1 and 0.9 were used as

suggested by Plitt. The measured d_{50c} of the ore is thus 75 μm. The gold corrected

cut-size cannot be determined as accurately, but is approximately equal to 15 μm.

Alternatively, however, the d_{50c} of gold can also be estimated by extracting the effect

of solids density from Plitt's cyclone model (Plitt, 1976):

$$d_{50c} = \frac{K}{(\rho_s - 1)^{0.5}}$$ **3.6**

where K is a constant and ρ_s is the solids density in g/cm^3

Thus, if the d_{50c} of the ore, whose specific density is approximately 4.9, is 100

μm, then the corrected cut-size for gold, which has a specific density of 19, is 35 μm.

Clearly this value does not agree with the d_{50c} estimated from equation 3.5, 15 μm.

46
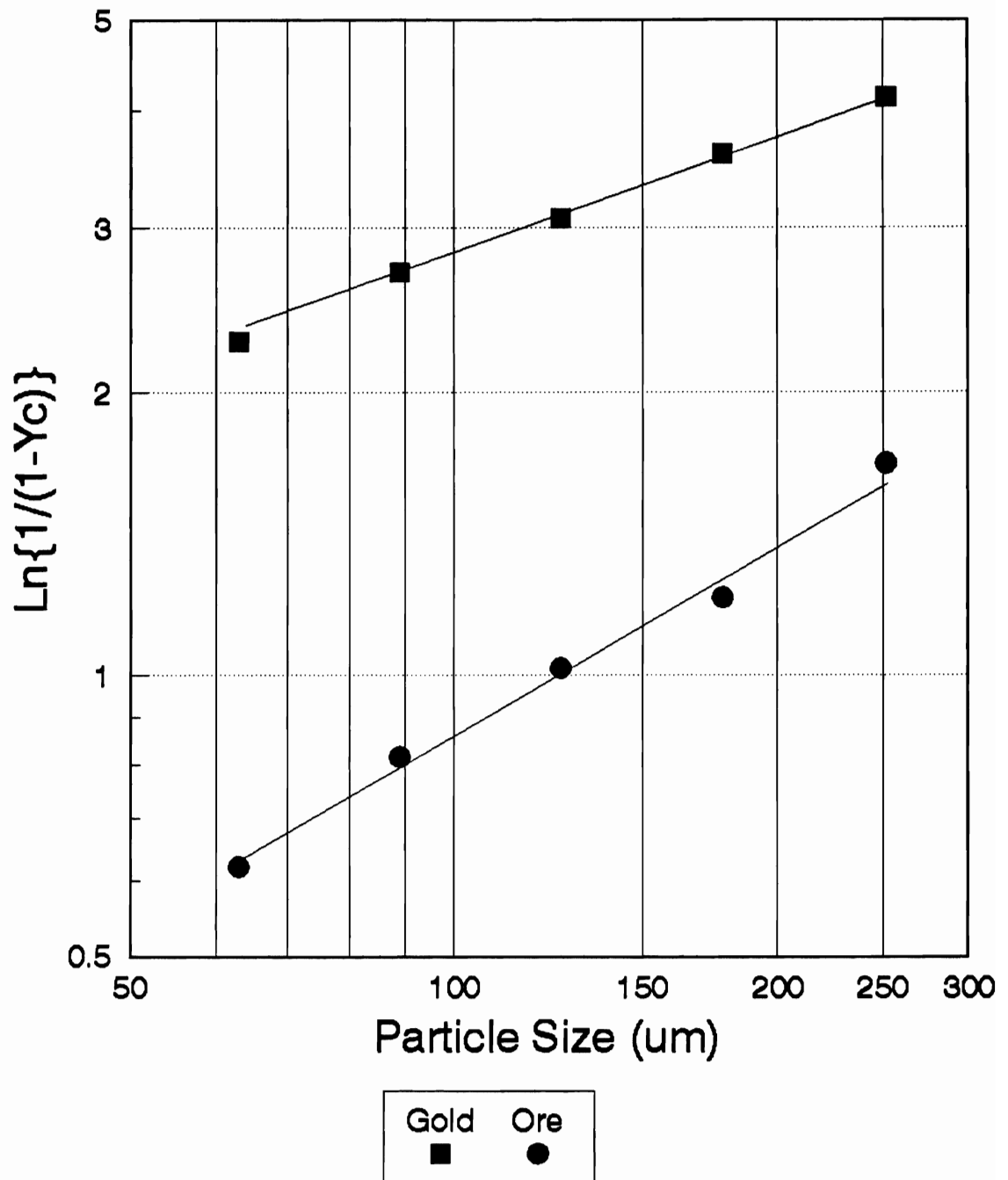
Figure 3.5: Regression of Equation 3.5
to Calculate d50c of Ore and Gold

Parameter	Gold, μm	Ore, μm
d_{50c} from Eq. 3.5	approx 15	75
d_{50c} from Eq. 3.6	35	75
m (slope)	0.91	2.34

Table 3.5: Calculated Model Parameters

From hydrodynamic theory, the value of the exponent in equation 3.6 can be 0.5, 0.62, or 1.0, corresponding to laminar, intermediate, and turbulent flow conditions, respectively. Finch et al (1977) examined the behavior of various minerals (in cyclones) and concluded that a better range of values for the exponent are from 0.75 to 1.5.

If the corrected cut-size for gold is assumed to be 15 μm (Equation 3.5), then the value of the exponent in equation 3.6 should be 1.1, which lies within the range reported by Finch et al (1977).

The parameter, m, is a measure of classification sharpness. An m of over 3 represents sharp classification, whereas an m below 1 represents a poor classification. Clearly, gold's classification efficiency is poor (m=0.9) in comparison to the ore's efficiency (m=2.34); ie. the proportion of coarse gold reporting to the SCOF and of fine gold reporting to the SCUF is high. Gold in the coarse particle sizes may readily report to the SCOF because it is not liberated or is flaky. Fine gold is better liberated and generally more spherical and will thus report to the SCUF.

3.4 Phase 3: Knelson Test Results

Although the KC was used primarily as a means of estimating gold content accurately, the response of each stream (recovery, concentrate grade) is in itself very informative. Table 3.6 summarizes the results of the test work and Appendix I presents the complete metallurgical balances for each test.

Sample Identification	Calculated Feed Grade	Concentrate Grade (g/t)	% Gold Recovery
Primary Ball Mill Discharge 1	17.3	480	46
Primary Ball Mill Discharge 2	26.4	1300	35
Sluice Concentrate 1	30.5	660	49
Sluice Concentrate 2	40.1	190	30
Sluice Tail 1	14.1	370	43
Sluice Tail 2	36.7	680	26
Secondary Cyclone Overflow 1	41.6	185	16
Secondary Cyclone Overflow 2	25.0	150	24
Primary Cyclone Feed 1	21.2	340	43
Primary Cyclone Feed 2	28.1	350	39
Primary Cyclone Underflow 1	25.0	670	40
Primary Cyclone Underflow 2	28.7	700	47
Primary Cyclone Overflow	21.9	48	7
Regrind Mill Discharge	162.7	5583	71
Secondary Cyclone Underflow	127.5	3000	54

Table 3.6: Summary of Knelson Test Work Performed on Grinding Circuit

In the primary grinding circuit, the KC was able to recover 46 and 35% of the gold from the BMD1 and 2 samples, and 40 and 47% from the PCUF1 and 2

samples.

The gold recovery associated with the PCOF was only 7% and is clearly incorrect. The back-calculated feed assay associated with this test, 22 g/t, is too high, because of the high tail assay associated with this test, 21 g/t. At steady-state conditions, the assay should be equal to that of the fresh feed, 5 g/t. Perhaps the gold load in the circuit was still building up at the time of sampling, in which case the grade should actually be lower.

As expected, the KC performed well with the RMDS and the SCUF because these are recycle streams and are made up of sluice concentrate. Gold recovery is higher with the RMDS (70% vs. 52%) sample presumably because of the increased gold liberation in that stream.

The recoveries associated with the SCOF1 and 2 were 16 and 24% respectively which is quite poor and may be attributed to the fineness of the gold. The KC has been reported to perform poorly on cyclone overflow (Banisi, 1989).

Figure 3.6 shows that there is significantly more +53 μm (270 mesh) gold in the SCUF and RMDS streams than in the SCOF. In fact, roughly 75% of the gold in these two streams reports to the +53 μm (270 mesh) classes. Most of the gold is distributed between 53 and 150 μm, for which the KC performs well. For the SCOF, over 70% of the total gold is below 38 μm, which may explain the KC's poor performance.

Figure 3.7 presents some size-by-size gold recoveries for the SCOF2, RMDS,

50
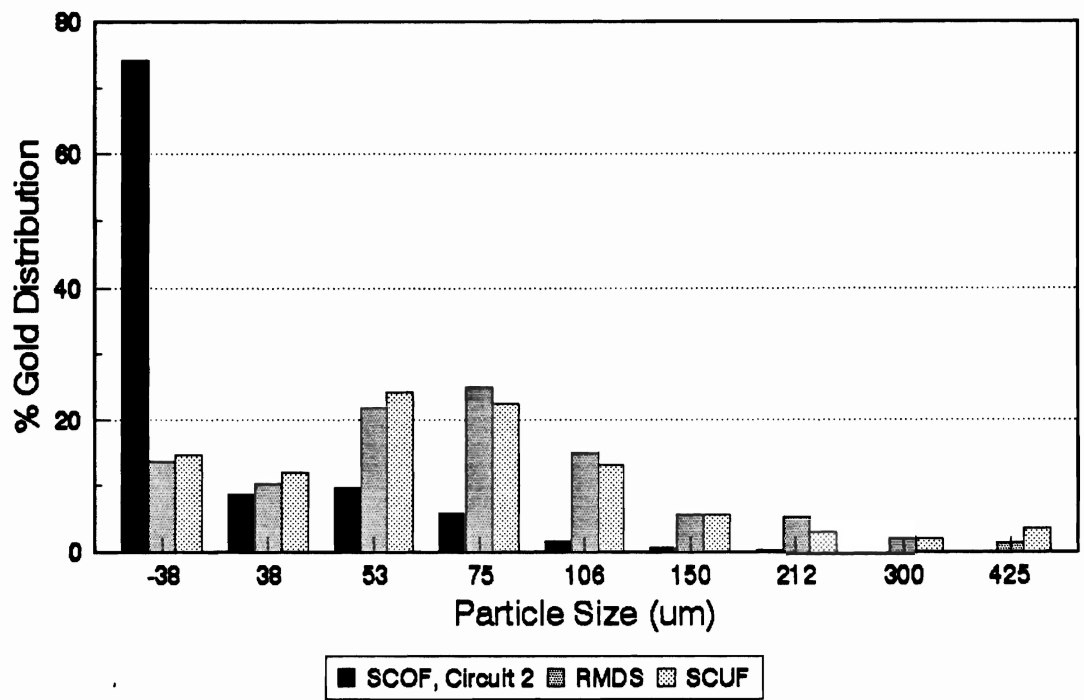
Figure 3.6: Gold Distribution in Regrind Circuit
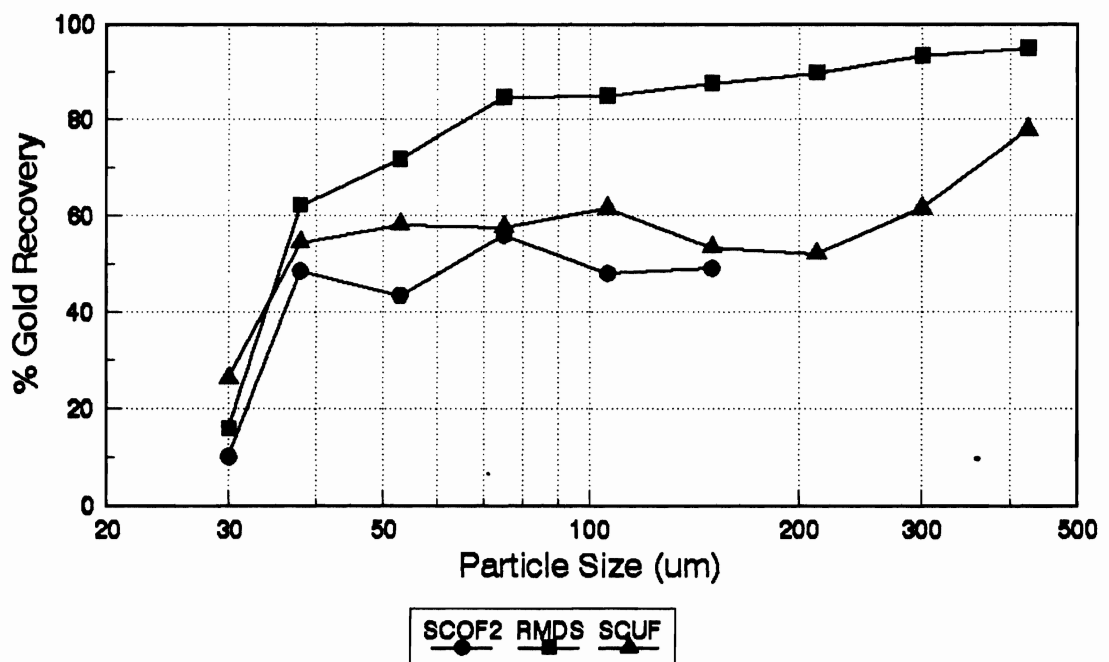
Figure 3.7: Size-by-Size Gold Recovery
for K.C. Tests on Regrind Circuit

and SCUF. The R_{50}[1] is between 38 and 25 μm. The recovery of -38 μm gold was generally the poorest for all streams tested, and in particular from the SCOF stream, which further indicates that the gold associated with this stream is extremely fine. This limiting particle size is coarser than what has been reported with the KC thus far (Banisi, 1990) probably because of the high density of the gangue at AELR, which is 80% sulphides. The gold recovery in the 53 to 300 μm range for the RMDS and SCUF, where most of these streams' gold is distributed, is 85 and 60% respectively. The recoveries are higher with the RMDS because of higher liberation and the finer gangue size of the RMDS material.

There is an abundance of free gold needlessly being locked up in the regrinding loop. This is due to gold's high density affecting its behavior in the classifier and its malleability lowering its breakage kinetics. As a result, most of the free gold is reporting to the SCUF, and only very fine gold (15 μm, from the classifier performance curve) is successfully removed from the circuit. The KC can effectively recover the gold from the regrind mill discharge and secondary cyclone underflow, but performs poorly with the secondary cyclone overflow where the gold is too fine to be recovered effectively.

3.5 Preliminary Tests and FC Feed Selection

The FC is a relatively new technological development and thus few results are

---

[1]R_{50}: The particle size at which gold's recovery is 50%, by analogy with the d_{50}

available to quantify its performance. Given a particular ore type, an operator can readily adjust three variables, feed flowrate, density, and flushing frequency. A fourth variable, bowl geometry, may also be included but is not as readily adjusted[2]. The effect of these variables on gold recovery, preferably size by size, is information needed to optimize the operation of the FC. Already some important questions can be raised. For example, what is the best stream from which to recover gold, and down to what size will gold be recovered? Also, what are the optimum conditions (time, flowrate, density) at which to run the FC?

Section 3.5.3 will deal with the issue of test time, or feed mass. Following this, Section 3.5.4 will present the results of processing various streams with the FC and size-by-size performance will be assessed. Section 3.6 will deal with the issue of optimizing FC performance.

3.5.1 Experimental Procedure and Design

The experimental arrangement used for the test work is shown schematically in Figure 3.8. The arrangement consisted of a mixer, baffled mixing tank, pump, and an ultrasonic flowmeter. A 1" ARO diaphragm pump (Model AR 666053-311) was used to pump the slurry. Pumping rate was controlled by varying the air pressure to the pump. The air pressure was controlled with an air pressure filter-lubricator regulator unit manufactured by Parker pneumatic. The ultrasonic flowmeter, which

---

[2]The 14° bowl was selected for this test work, for reasons that will be described shortly.

Ultrasonic flowmeter

Falcon B6 Concentrator

Tail Discharge

Mixing Tank and Diaphragm pump

Concentrate Removal
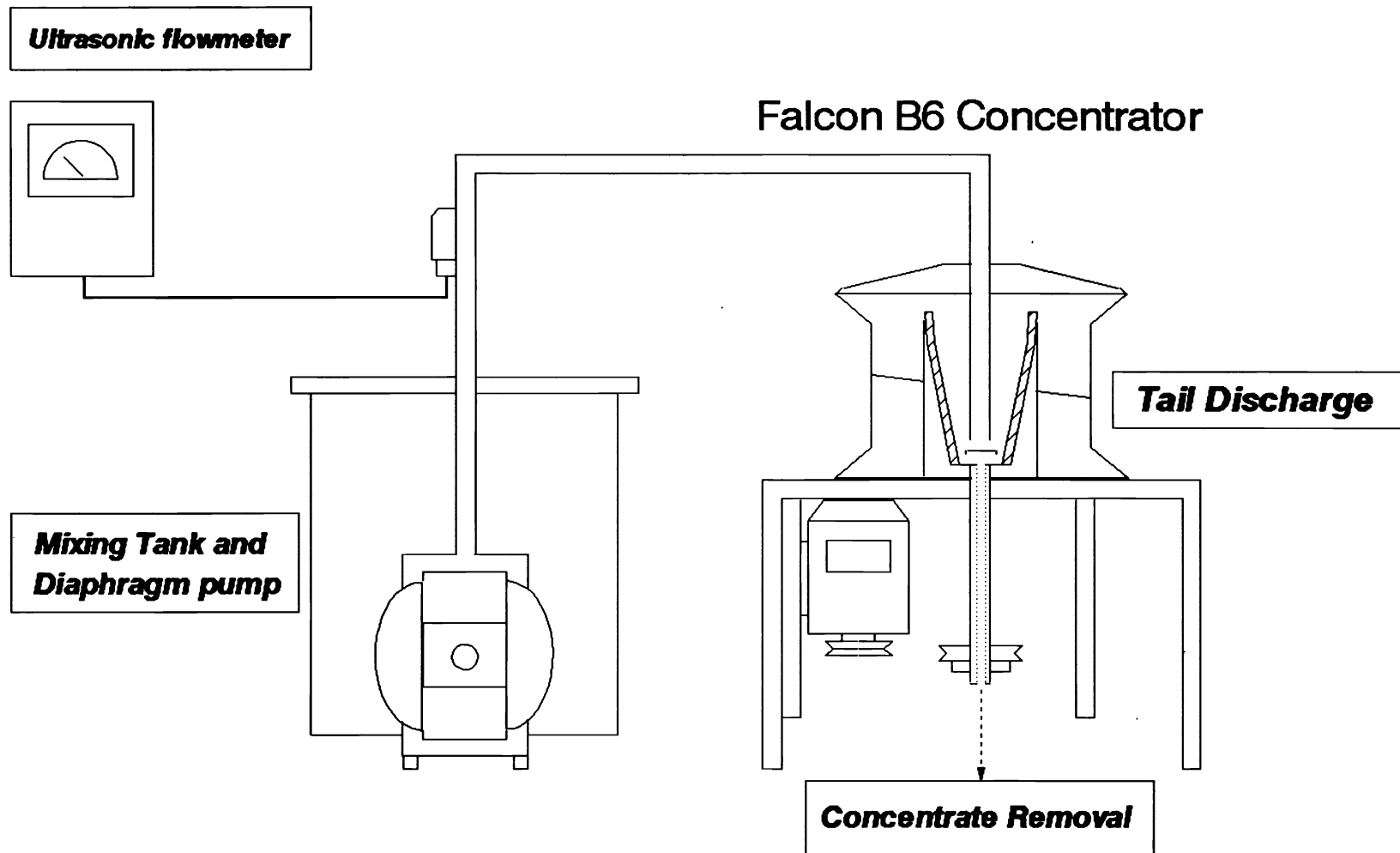
Figure 3.8: Experimental Arrangement for Falcon Tests

consisted of an ultrasonic transmitter/sensor (model FD5000) and a blind flowrate

indicator (model FD302s) was manufactured by Omega Engineering.

The following notes outlines the procedure used to calibrate the flowmeter:

1) The slurry was mixed and recirculated in/to the mixing tank for 10 minutes.

2) The pumping rate was set to the desired flow.

3) The flowrate was measured with a stopwatch and a 1000 ml graduated cylinder.

4) The flowmeter reading was compared to this value.

5) If the values did not agree to $\pm$ 2 L/min, then a second reading was taken.

6) If the values still did not agree, then the zero on the flowmeter was adjusted.

A FC model B6 was used to perform the test work. The bowl shape is similar

to that of a hydrocyclone in that the lower region is angled slightly from the vertical

and the upper region is straight vertical. By increasing the bowl angle (from 8

degrees to 14 degrees) and decreasing the height of the retention zone, material

rejection will be increased. A schematic of a typical bowl is shown in Figure 3.9.

The AELR staff had already tested the 8 and 10 degree rotors, and found that they

performed poorly with their flotation concentrate. The degree of upgrading was too

low (2:1 and even 1:1 on some occasions) because of the high density of the pyrite

gangue and thus the 14 degree rotor, designed to recover gold from dense sulphide

ores, was used.

Operation of the FC was straightforward. After the machine was turned on,

the feed was introduced and timed samples of the FC tails were extracted at regular

Solids Bed Deposited on Rotor Walls

Bowl Angle
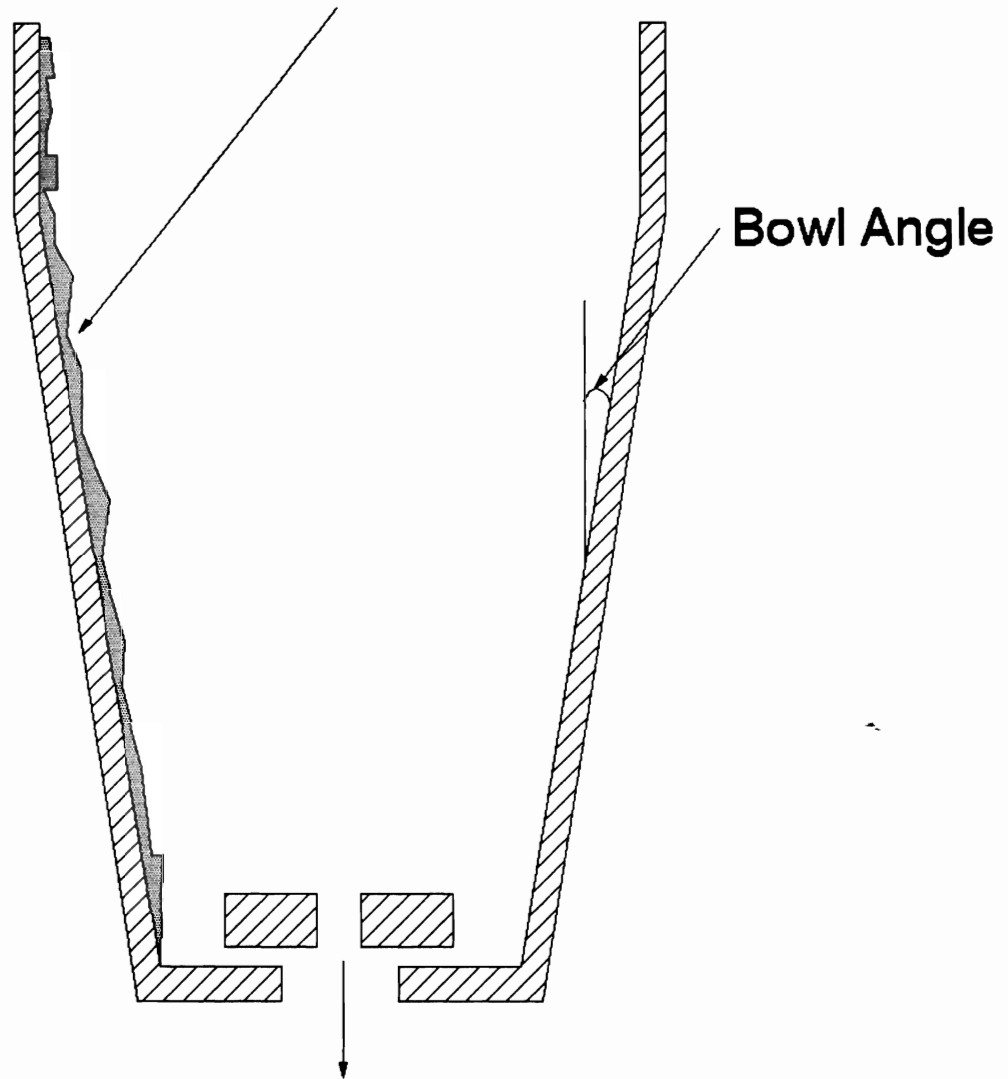
Concentrate Discharge

Figure 3.9: Schematic of a Typical Falcon Rotor

intervals throughout the experiment. At the end of the test, the unit was stopped and the concentrate was collected. The tail and concentrate samples were weighed wet and dry to determine the percent solids. Roughly 100 g of each sample was then sent to assaying. Samples of the various streams (BMD2, SCOF, RMDS, and flotation concnetrate) were extracted from the circuit, then dried. Next, a 20.0 kg sample of each material was mixed with the appropriate amount of water to obtain the desired percent solids, and processed with the FC. Table 3.7 highlights some of the important experimental data. A more complete listing is presented in Appendix IVa.

Test	Sample	Dry Sample Mass (kg)	Percent Solids	Flowrate (l/min)
1	Flot. Conc.	10.0	20.0	20
2	Flot. Conc.	20.0	20.0	20
3	Flot. Conc.	40.0	20.0	20
4	Flot. Conc.	60.0	20.0	20
5	Flot. Conc.	100.0	20.0	20
6	PCOF	15.0	20.0	10
7	PCOF	15.0	20.0	15
8	PCOF	15.0	20.0	20
9	PCOF	15.0	20.0	30
10	SCOF	20.0	20.0	20
11	RMDS	20.0	20.0	20
12	BMD2	20.0	20.0	20

Table 3.7: Summary of Experimental Conditions

The tests labelled "Flot. Conc." were designed to determine the time (or sample

mass) required for the FC to overload[3]. The results will be discused in Section 3.5.3. Different sample masses of the same material were processed with the FC. A bypass valve and a length of flexible 2.5 cm hose were installed together on the feed pipe to the flotation concentrate thickener to permit on-line operation of the FC. This posed some flowrate control problems due to inherent flowrate fluctuations in the thickener feed. The large sample masses required for these tests, however, made it impractical to perform the experiments otherwise. The mass of sample treated was estimated from the volumetric flowrate of the tails, the solids density, and the FC operating time. Next, 20 kg samples of the SCOF, SCUF, RMDS, and BMDS were taken and processed with the FC. All the samples were extracted over a short period of time (1 hour) in order to minimize the effect of long-term feed grade fluctuations. This test series, which compared the performance of these various streams, will be discussed in Section 3.5.4. The group of tests labelled "PCOF" were designed to study the effect of flowrate on performance. The results of these experiments will be discussed in Section 3.6.

3.5.2 Estimating Error in Gold Recovery

Overall gold recovery was estimated from the two-product formula:

$$R = \frac{cC}{cC + tT} \qquad \qquad 3.7$$

---

[3]Overloading in the FC occurs when the bed of solids becomes saturated and can no longer recover additional gold effectively. Recovery then decreases sharply.

where c,t are the assays of the concentrate and tails, and C,T are the masses.

The measured assay values will always be in error, be it due to improper sample preparation, or bad assaying methodology, or random error. It is important to determine how these errors propagate into the estimate of gold recovery. Errors in C and T are minor and can be disregarded, but a measure of the recovery variance due to variations in the assays can be estimated by performing a Taylor expansion of equation 3.7 (Laplante, 1991):

$$\sigma_R^2 = \left(\frac{\delta R}{\delta c}\right)^2 \times \sigma_c^2 + \left(\frac{\delta R}{\delta t}\right)^2 \times \sigma_t^2 \qquad \textbf{3.8}$$

The expressions for the two derivatives in equation 3.8 are as follows:

$$\frac{\delta R}{\delta c} = \frac{CTt}{(cC+Tt)^2} \qquad \textbf{3.9}$$

$$\frac{\delta R}{\delta t} = \frac{-cCT}{(cC+Tt)^2} \qquad \textbf{3.10}$$

3.5.3 The Effect of Mass Processed

Figure 3.10 and Table 3.8 present the results of the test work ("flot conc" in Table 3.7). The sample masses were calculated from the volumetric flowrate, the solids density, and the percent solids in the slurry. Recoveries were calculated from the procedure described below.

The assays were first mass balanced with Norbal2 (Spring,1985). Appendix

59
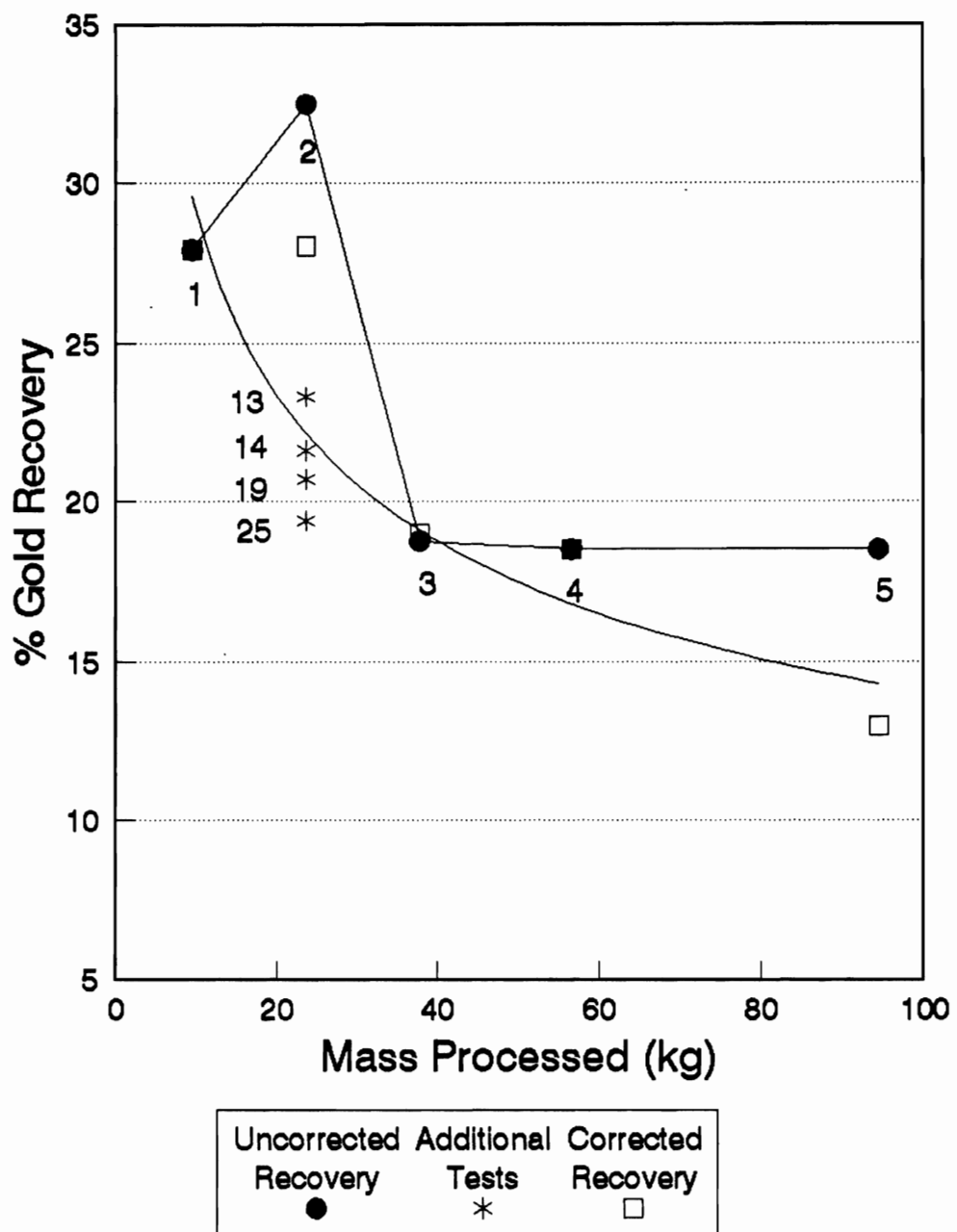
Figure 3.10: Incremental Au Rec. vs. Feed Mass
Feed:flot. conc., Flowrate: 20 l/min, 20% solids

V presents the results of the mass balance, including the weighing factors. By back-calculating each of the individual test feed assays from the unadjusted concentrate and tail assays, a "global feed" assay, or the assay of the original sample extracted from the stream, and common for all tests, was calculated as the average of each of the individual test feeds. Each test was then mass balanced individually using the

Test #	Test Time (min)	Calc. Sample Mass(kg*)	Recovery ± S.D.	Balanced Recovery'	Yield (%)
1	2.00	9.44	27.92±0.97	27.94	6.89
2	5.00	23.60	32.47±12.22	28.05	4.79
3	8.00	37.75	18.76±3.09	19.01	2.25
4	12.00	56.63	18.50±4.15	18.49	1.50
5	20.00	94.38	18.49±5.20	12.98	0.93

*Based on solids density 4.2, 20% solids, 20 l/min

Table 3.8: Gold Recovery vs. Mass Processed for the Flotation Concentrate

following variances: feed, 2 $(g/t)^2$; concentrate, 0.5 $(g/t)^2$; tails, 20 $(g/t)^2$. This average feed assay was then adjusted. In Figure 3.10, the first curve presents the unbalanced results, and the second, the balanced results. There is good agreement between all points, except for tests 2 and 5. In general, it appears that gold recovery is at a maximum (30%) up to 2 minutes (9 kg of feed) of operating time, after which it drops to below 20% and continues to decrease. Can this drop in gold recovery be attributed to saturation of the solids bed, or is it the result of gold being eroded from the bed at a rate equal to feed gold capture? The first explanation seems more plausible since Table 3.9 shows that both the concentrate weight and grade become

61

constant (concentrate weight: 800 to 850 g; grade: 1600 to 2000 g/t) at longer times despite an increase in feed mass.

The second hypothesis can be easily tested by a simple experiment which will be described in the next section.

Test #	Concentrate Mass (g)	Concentrate Grade (g/t)	Calculated Feed Grade(g/t)
1	648	550	137
2	1128	974	169
3	848	1724	207
4	806	2111	165
5	881	1566	115

Table 3.9: Concentrate Results for Flotation Concentrate

3.5.3.1 The Effect of Bed Erosion

For feed masses greater than approximately 25 kg, gold recovery drops. This is perceived as a failure to recover additional values because of bed saturation. There may be, however, another plausible explanation for a drop in gold recovery, which is gold being rejected from the solids bed by the abrasive action of the slurry. Thus, whereas additional values would be recovered, an equivalent loss of already recovered material would result in little or no net gain. To test this explanation requires additional work, which the following section will discuss.

A 40 kg sample of solids, consisting of 20 kg of flotation concentrate and 20 kg of cyanidation tails, 0.3 g/t Au, was separately processed. The flotation

concentrate sample was processed first and the FC concentrate was left in the bowl; the barren tail sample was then processed immediately. Gold recovery from this test test was compared to that from a similar test (identical operating conditions) where only 20 kg of flotation concentrate was processed. Table 3.10 presents the results of these tests (with and without the barren feed):

Test 13
Feed: 20 kg of flotation concentrate, 116 g/t

Concentrate	Tail:
Weight: 565 g	Grade: 95 g/t
Grade: 850 g/t	
Recovery: 20.7%	

Test 14
Feed: 20 kg of flotation concentrate, 151 g/t
then 20 kg of cyanidation tails, 0.3 g/t

Concentrate:	First Tail:
Weight: 834 g	Weight: 19.17 kg
Grade: 834 g/t	Grade: 119 g/t
Recovery: 23.3%	Recovery: 75.5%

Second Tail:
Weight: 20 kg
Grade: 2.5 g/t
Recovery: 1.46%

Table 3.10: Results of Tests to Determine Effect of Bed Erosion

Gold recovery is similar for both tests although feed grade is slightly larger for test 14. The amount of gold lost[4] in the 20 kg of barren feed for test 14 is only 1.46% of the feed, or 5.9% of what had been recovered. If gold lost to erosion is assumed to follow first order kinetics with respect to the eroding mass (ie. the barren

---

[4]Exclusive of what was already in the barren feed, 0.3 g/t

material in this case), then the rate constant is equal to

$$-\ln\frac{\dfrac{23.3}{(23.3+1.46)}}{20\ kg} = 3.0 \ x \ 10^{-3} \ kg^{-1}$$

3.5.4 Testing Various Streams

Preliminary tests were performed with the FC using samples of flotation concentrate, primary cyclone overflow, secondary cyclone overflow, regrind mill discharge, and primary ball mill discharge to determine the amount of gold that can be recovered from these streams. Since the main objective of the AELR work was to produce a smeltable gravity concentrate, the final FC concentrate grade was closely monitored by requesting the assaying lab to perform multiple assays on the products. From these multiple assays, then, estimates of the error in gold recovery were calculated using the "propagation of errors" technique described in section 3.5.2. Table 3.11 presents the results of this test work. The results were calculated from the raw data in Appendix IVa and IVb. The recovery was calculated from the measured concentrate and average tail assays, and the sample mass corrected for material left unprocessed in the mixing tank (approximately 1 kg). The best performance was observed with the flotation concentrate where the FC was able to recover 32% of the gold and produce a concentrate assaying 900 g/t gold. The 32% was reduced to 28% when the grade data was adjusted, and additional tests could not reproduce this performance (recoveries were between 18 and 23% Au). The recovery

is higher than the economic break-even point, 22%, but the concentrate grade is far from being suitable for direct smelting (300000-500000 g/t) and further upgrading would be required at which point recovery would drop further. The FC performed poorly with the RMDS and SCOF samples, recovering only 15-17% of the gold and producing a 500 to 700 g/t gold concentrate. The BMDS results were very poor, presumably because the feed was too coarse for the FC.

Test no.	Stream Sample	Recovery	Conc. Grade g/t	Yield %	Upgrade
8	PCOF	12.3 ± 6.6	15.0	2.7	4.6
10	SCOF	14.8 ± 1.0	546.4	1.9	8.0
11	RMDS	16.6 ± 2.4	661.8	2.3	7.3
2	Flot Conc	32.5 ± 12.2	973.6	5.9	5.5
12	BMD2*	2.3 ± 1.2	21.7	2.3	1.0

* Flowrate: 20 L/min; Feed Density: 20%; recovery based on 16 kg for BMDS, 19 kg for Flot Conc and 20 kg for others

Table 3.11: Comparison of Overall Gold Recovery for Various Samples

The error in recovery due to variations in the tails and concentrate assays was calculated and is shown in Table 3.11. Most of the error in recovery is due to the large fluctuations in the tailings assays (shown in Table 3.12). For example, the standard deviation (s.d.) associated with the FC tail for this test was quite large, 127.8 ± 71.1 g/t, and thus the s.d. for recovery was large 32.5 ± 12.2%. Duplicate assays of each tail sample are very consistent, and show that fluctuations are due to FC operation, not assaying errors. Subsample extraction time was held

Sample	Tail Mass(g)	Assays	(g/t)	Average Assay	S.D.	Degrees of Freedom
8) PCOF	396.3	2.67	2.95	2.41	0.32	7
	402.1	2.34	2.19			
	400.5	1.98	2.19			
	410.4	2.67	2.25			
2) FLOT CONC	955.0	85.44	83.55	127.8	71.12	7
	713.9	60.51	60.65			
	991.4	131.2	133.1			
	1103	231.9	236.2			
10) SCOF	1596	64.46	61.51	59.46	3.75	11
	1552	63.63	62.13			
	1603	52.80	59.25			
	1616	56.85	52.87			
	1550	59.93	60.55			
	1602	61.30	58.29			
11) RMDS	982.2	125.5	132.8	137.5	35.37	9
	1025	110.3	111.0			
	995.1	198.5	201.8			
	958.9	107.7	107.8			
	1013	139.1	140.9			
12) BMD2	472.2	27.03	30.86	21.77	10.37	9
	322.2	8.85	8.78			
	349.0	32.09	30.10			
	177.9	28.39	29.83			
	161.2	10.42	11.38			

**Table 3.12: Tail Masses and Assays for Preliminary F.C. Tests
(Each tail sample was assayed twice; both assays are shown)**

constant in each test at 15 seconds. The tail assays for the flotation concentrate test appear to be increasing with time, which may explain the high standard deviation. In the remaining tests, however, the fluctuations appear to be mostly random. The flotation concentrate tail results also seem to indicate slightly unstable feed conditions, as evidenced by the inconsistent tail masses. As noted earlier, the FC was operated on-line for this test and the feed conditions were not as effectively controlled. The SCOF and RMDS tail samples yield much more constant masses and assays. The more stable feed flowrate may account for this behavior.

The BMD2 results are very unstable both in terms of mass and assays. The decreasing tail weights show that the % solids of feed went down with time due to severe settling in the feed tank; four kilograms of solids out of 20 had settled to the bottom of the tank and were left unprocessed by the separator. Also, liberation problems were suspected due to the coarseness of the feed.

Table 3.13 and Figure 3.11 show the metallurgical balance and the size-by-size gold recoveries for the flotation concentrate test at 20 l/min, 20 % solids. The data were obtained by wet screening with 8 inch Tyler screens at 75, 53, 38, and 30 μm (200, 270, 400, 500 mesh). The remaining fractions were generated with microscreens. Some caution must thus be taken in interpreting the results in the -30 μm classes because of the experimental difficulties involved in microscreening.

The overall gold recovery from the metallurgical balance is 27%, which is lower than the figure calculated from the head assays and the product masses, 32%,

Flot. Conc. Size (um)	F.C. Conc. 19000 Feed Mass Mass (%)	F.C. Conc. 19000 Mass (g)	F.C. Conc. 19000 Grade (g/t)	F.C. Conc. 19000 Rec (%)	F.C. Tail Mass (%)	F.C. Tail Total Mass	F.C. Tail Grade (g/t)	F.C. Tail Rec (%)	F.C. Feed Mass (%)	F.C. Feed Mass (g)	F.C. Feed Grad (g/t)	F.C. Feed Dist (%)
75	2.61	29.42	656	97.75	0.02	3.57	124	2.25	0.17	33.00	599	0.51
53	13.30	150.0	1246	27.33	15.91	2843	175	72.67	15.75	2993	228	17.57
38	24.10	271.8	991	26.44	29.17	5213	144	73.56	28.87	5485	186	26.18
25	20.89	235.6	896	34.29	12.47	2229	181	65.71	12.97	2464	250	15.82
15	12.51	141.2	862	33.69	7.20	1287	186	66.31	7.52	1428	253	9.28
11	4.93	55.60	830	17.19	7.13	1274	175	82.81	7.00	1330	202	6.90
5	21.67	244.4	790	20.93	28.10	5022	145	79.07	27.72	5266	175	23.73
Totals	100	1128	929	26.93	100	17872	159	73.07	100	19000	205	100

Sample Mass: 20 kg, Flowrate: 20 l/min, % solids: 20

Table 3.13: Results of FC Test with Flotation Concentrate (Test 2)
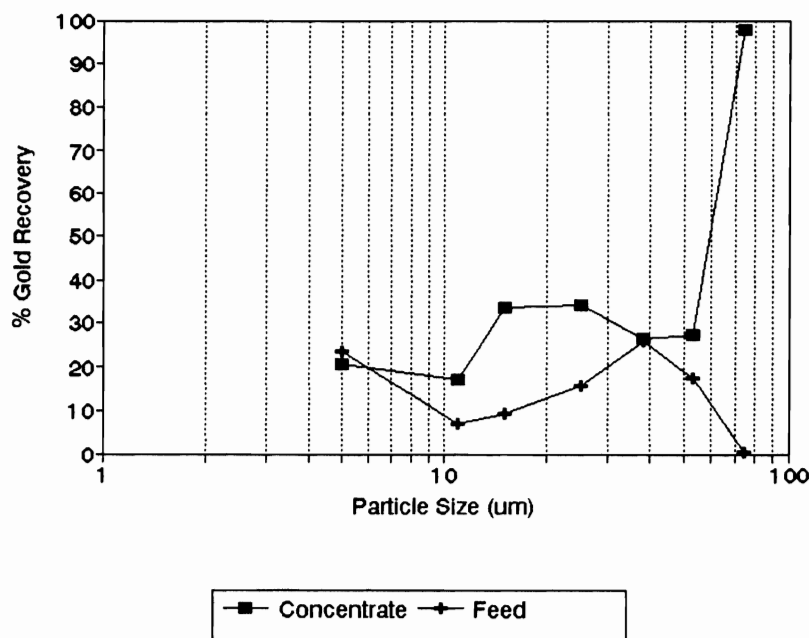
Figure 3.11: Size-by-Size Gold Recovery and Distribution
for the FC Tests with the Flotation Concentrate

but within the calculated experimental error. The FC appears to be recover +75 μm particles quite effectively, but not selectively. The impact on overall recovery is low because of the low mass in this size class. The FC recovery in the mid-sizes is roughly 25%, with a higher 30% recovery in the 15 to 30 μm size ranges. Gold recovery below 15 μm, however, drops down to about 18%, presumably because of decreasing particle size. Overall recovery calculated from size-by-size data is 26.9%, much lower than "raw" recovery, 32%, but in good agreement with the "corrected" recovery (with NORBAL2) of 28%.

3.6 Phase 5: Optimizing Falcon Performance

The preliminary test work has shown that at 20% solids and 20 l/min, the FC can recover 20-28% of the gold, at a grade of 900 g/t, from the flotation concentrate and 17% from the regrind mill discharge at a grade of 0.07% Au. Can the FC do better under a different set of operating conditions (feed flowrate, and % solids)? The 14 degree bowl designed for treating high density gangues was used for this work. First, however, a suitable material had to be selected on which to perform the test work. The regrind mill discharge and the flotation concentrate appeared to be the best because they yielded the richest concentrates and highest recoveries (Table 3.11).

3.6.1 Stream Selection

From the laboratory KC tests, it was shown that the regrind mill discharge

contained an abundance of gravity recoverable gold. In fact, the KC was able to recover 70% of the gold. When the same material was processed with the FC, gold recovery was only 20%. The gold in this product was shown to be predominantly distributed in the 53-150 μm, where the KC yields recoveries of 70 to 80%. KC performance in the -38 μm, where only 14% of the gold is distributed, was quite poor. With the FC and the flotation concentrate, the FC was not able to perform as well in the 53-150 μm range, but did perform better in the 15-38 μm range, where over half of the gold is distributed. Since gold in the flotation concentrate is distributed in the finer classes, then it is a more suitable feed for the FC than the regrind mill discharge. From a plant perspective, the flotation concentrate is also a better choice, since the regrind mill is not always used. From an experimental perspective, the flotation concentrate is preferred because its finer gold is easier to assay than that of the RMDS. As a result, most of the optimizing work was performed with the flotation concentrate. A second, more limited test series was also performed using the PCOF as feed. This work is warranted since a cyclone overflow would be a prime candidate for the FC in most applications because of its fineness.

3.6.2 Experimental Design

In this this section, the effect of flowrate and % solids will be examined. The previous test work showed that optimum feed mass was around 20 kg; this was fixed. Similarly, only the 14 degree bowl was used and thus bowl geometry was held fixed,

again because of the nature of the gangue.

A 3^2 factorial design experiment for flowrate and % solids was performed with the FC. The three flowrate chosen were 10, 20, and 30 l/min, and the three percent solids chosen were 10, 20, and 30%. The 3^2 testing combinations were randomized, and three experimental repeats were performed, one for each midpoint, for a total of 12 tests.

To complete all the tests with material of the same feed grade required the collection of twelve 21 kg samples of flotation concentrate over a very short time, less than 1 hour. These samples were readily available, dewatered, from the flotation concentrate disc filter. The samples were thus collected, dried in an oven at below 100° Celcius, to minimize hardening of the material and generation of SO_2. The large mass was then divided into 12 weighed portions of 21 kg. Each sample was then slurried with an appropriate amount of water to give the desired % solids, and the FC tests were performed as usual. Three samples of the tails were taken throughout the test and the complete concentrate was removed. Each of these products was dried, weighed, and subsampled. At the end of the test work, the samples were pulverized at McGill University, then sent back to AELR's assaying facilities for gold determination. The three tail samples were assayed separately.

For the PCOF, feed density was set at 20% solids, and feed rate was at 10, 15, 20 and 30 l/min. A mass of 15 kg was processed for each test. Sample extraction and preparation was similar to the flotation concentrate tests.

3.6.3 Results and Discussion

3^3+2 Design with Flotation Concentrate: Table 3.14 presents a summary of the experimental conditions. The complete data set can be found in Appendix VI. The mass of sample processed, which is shown in the table, is the difference between the initial feed mass, 21 kg, and the amount of material that remains unprocessed due to settling in the tank. The mass of this material was measured for the first two tests; it averaged 1.5 kg. Because the twelve 21 kg samples originate from the same lot, they should have the same grade. Table 3.15 presents the feed grade calculated from the concentrate and tail assays, and their respective masses. They are highly variable, much more than what would be expected from the common feed stock. Sampling and assaying errors are therefore significant and the assays will have to be adjusted.

The same mass balancing procedure that was used in Section 3.2.4 was used here: a "global feed assay", f, was assumed to be the average of all the back-calculated feed assays, then each test was adjusted individually. The following absolute standard deviations were used: feed, 20 g/t; concentrate, 50 g/t; tail, 50 g/t. Norbal2 can be used to perform these corrections but there is a simpler and quicker technique available, the method of Lagrange multipliers. The method is based on calculating a "Lagrangian", L, and using it to correct the feed, concentrate, and tail grades. The Lagrangian is defined by the following equation:

$$\frac{Ff-Tt-Cc}{F^2\sigma_f^2+T^2\sigma_t^2+C^2\sigma_c^2} \qquad 3.11$$

72

Test #	Flowrate (l/min)	% Solids	Sample Mass (kg)
15	10	10.0	19.7
16	10	20.0	19.4
17	10	30.0	19.5
18	20	10.0	19.5
19	20	20.0	19.5
20	20	30.0	19.5
21	30	10.0	19.5
22	30	20.0	19.5
23	30	30.0	19.5
24	10	20.0	19.5
25	20	20.0	19.5
26	30	20.0	19.5

* Original Feed mass: 21 kg

Table 3.14: Summary of Experimental Conditions for Optimization Tests

Test Number	Feed Grade Au, g/t	Test Number	Feed Grade Au, g/t
1	98.10	7	117.6
2	123.2	8	180.1
3	150.7	9	179.3
4	162.8	10	100.9
5	118.7	11	124.6
6	120.2	12	291.0

Table 3.15: Back-Calculated Feed Grade for Optimization Tests

The three correction equations are defined as follows:

$$f' = f - LF\sigma_f^2 \qquad\qquad \textbf{3.12}$$

$$c' = c + LC\sigma_c^2 \qquad\qquad \textbf{3.13}$$

$$t' = t + L\sigma_t^2 \qquad\qquad \textbf{3.14}$$

The concentrate, feed, and tail grades are represented by the letters f,c, and t respectively, and their masses are represented by the letters F, C, and T. The standard deviations of the individual assays are represented by 'σ'.

Table 3.16 presents the key results; details are in Appendix VI. The adjustments are quite reasonable in most cases, with the tail assays being adjusted more so than the concentrate assays, which is consistent with equations 3.12-3.14, which state that corrections are proportional to mass. The adjustments to test 2 and 11 tail assays are higher than the rest because the measured tail assays were particularly high. The measured assay is a weighted average of the three tail subsample assays.

The concentrate assays vary quite considerably from test to test and even between repeats, which makes interpretation of the data somewhat difficult. The highest grade is roughly 900-1000 g/t Au at the higher flowrates, 20 to 30 l/min, where recovery is also the highest at 24% (Figure 3.12). This is not unlike the values reported in the section discussing the preliminary FC test results and perhaps more realistic because the data have been mass balanced. Considerable upgrading would

74
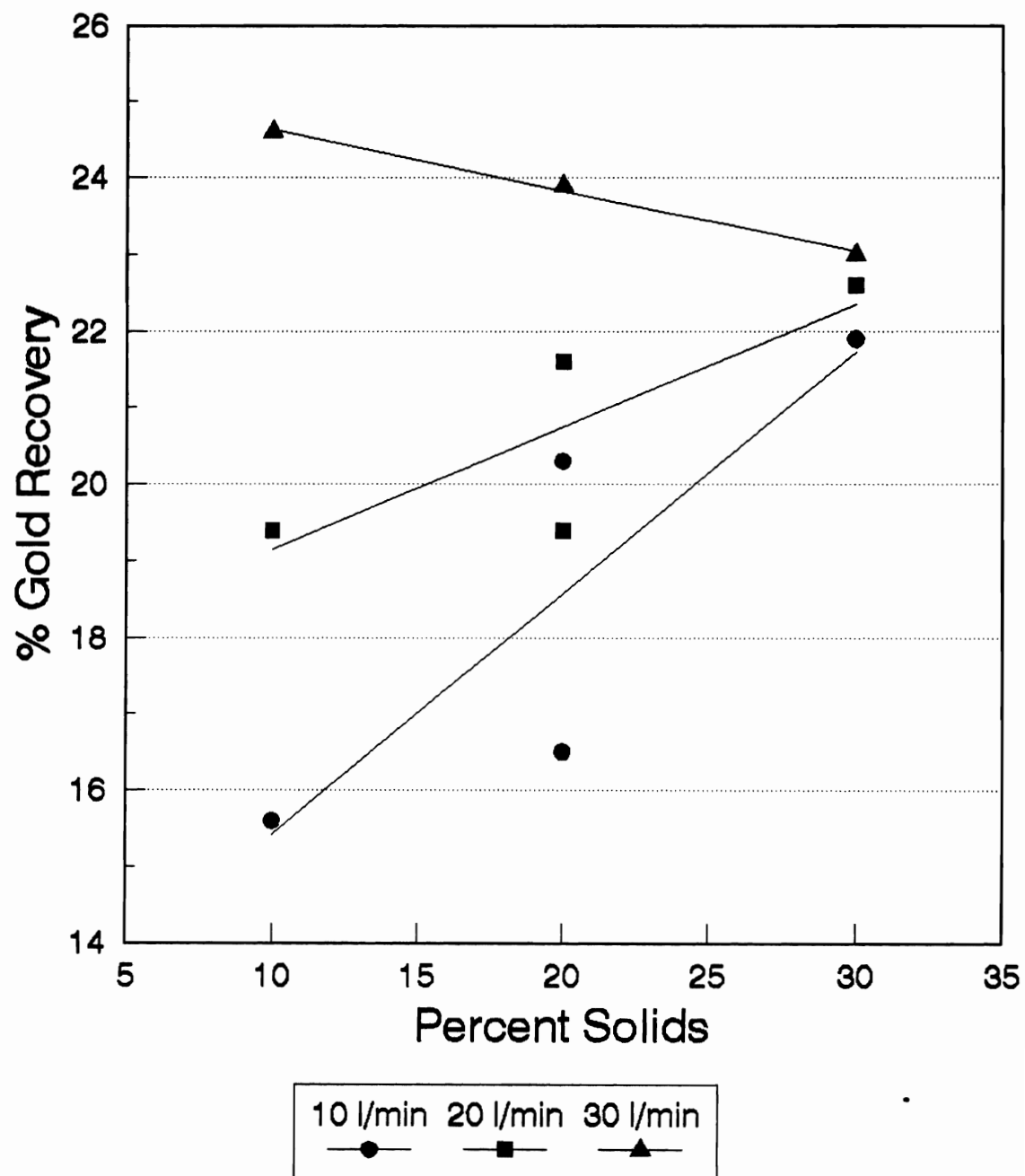
Figure 3.12: Effect of Flowrate and Density
on Gold Recovery

Feed: 20 kg, flotation concentrate

be required for direct smelting, and further processing of the tails may be required

if gold recovery is to be increased.

Test #	Flowrate	% Solids	f	c	c'	t	t'
15	10	10	98.1	533.3	533.8	83.0	100.0
16	10	20	123.2	620.9	620.6	103.8	95.1
17	10	30	150.7	987.6	987.8	120.5	126.8
18	20	10	162.8	876.5	876.3	137.2	131.0
19	20	20	118.7	854.7	854.6	96.8	92.7
20	20	30	120.2	666.8	666.6	98.1	92.5
21	30	10	117.6	955.2	955.1	92.1	89.2
22	30	20	180.1	1048	1048	143.0	142.6
23	30	30	179.3	900.5	900.5	144.6	145.0
24	10	20	100.5	765.3	765.7	84.1	98.1
25	20	20	124.6	689.1	688.8	105.7	95.6

Test 26 has been removed because the assays are suspect.
f', c', t' are the adjusted assays for feed, concentrate, and tails.

Table 3.16: Adjusted and Unadjusted Assays for Optimization Tests

Table 3.17 presents the concentrate masses and gold recoveries. The average

mass recovered for all tests is 704 $\pm$ 105 g. The results are consistent in most cases,

but there are a few exceptions. For example, tests 16 and 24 were run under

identical conditions but the masses are quite different (723 vs. 973).

The results of Figure 3.12 can be fitted to the following regression:

$$R_{Au} = 13.2 \pm 5.3 + 0.66 \pm 0.26 Q + 0.53 \pm 0.13 S - 0.02 \pm 0.006 QS$$

$(\rho^2, \text{ correlation coefficient} = 0.87)$

76

where Q is flowrate, S is percent solids, and QS is the product term.

The regression and Figure 3.12 show that the optimum performance can be achieved at the maximum flowrate and minimum density. It is probably better not to dilute the stream, however, in order to minimize dewatering requirements. A feed density of 30% would be preferable, at which the effect of flowrate is minimal

Test #	Flowrate	% Solids	Concentrate Mass (g)	Corrected Gold Recovery
15	10	10	659	15.6
16	10	20	723	20.3
17	10	30	679	21.9
18	20	10	675	19.4
19	20	20	565	21.6
20	20	30	758	22.6
21	30	10	576	24.6
22	30	20	800	23.9
23	30	30	896	23.0
24	10	20	973	16.5
25	20	20	900	19.4

Table 3.17: Concentrate Results for Optimization Test Work with Falcon

Effect of Flowrate for the Primary Cyclone Overflow: Tables 3.18 and 3.19 present the experimental results, and Appendices IVa and IVb present all the raw data. The mass of sample processed for the tests was assumed to be 14.5 kg, the difference between between the original feed mass and mass left unprocessed, which was

approximately 500 g. The adjustments are reasonable in all the tests with the tails

being adjusted more than the concentrates, as expected.

Test	Flowrate (l/min)	f g/t	f' g/t	c g/t	c' g/t	t g/t	t' g/t
6	10	2.7	2.9	12.7	12.7	2.4	2.7
7	15	2.7	3.0	14.7	14.7	2.4	2.7
8	20	3.4	3.1	15.7	15.7	2.9	3.4
9	30	3.3	3.1	14.7	14.7	2.9	3.3

S.D.'s Used: f, 0.5 $(g/t)^2$; c, 0.2 $(g/t)^2$; t, 1 $(g/t)^2$

Table 3.18: Adjusted and Unadjusted Assays for Effect of Flowrate Tests

Test	Flowrate (l/min)	Concentrate Mass (g)	Corrected % Gold Recovery
6	10	355	10.6 ± 3.5
7	15	402	13.7 ± 4.3
8	20	472	16.6 ± 3.4
9	30	476	15.7 ± 3.5

Feed: 14.5 kg PCOF, 20% solids

Table 3.19: Results for Effect of Flowrate Tests with PCOF Samples

Overall, the results are quite poor and clearly the PCOF is not a suitable feed

for the FC. The highest upgrading achieved was 5:1 (15:3 g/t) at 10 and 20 l/min,

and recovery appears to increase with increasing flowrate from 10 to 20 l/min; further

increases in flowrate do not affect recovery.

3.7 Conclusions

There is an abundance of free gold needlessly being locked up in the

regrinding loop, as was attested by the high circulating load. This is due to gold's high density affecting classifier performance. As a result, most of the free gold is reporting to the underflow where it gets reground. Only very fine gold (15 μm) is successfully removed from the circuit. The KC can effectively recover gold from the regrind mill discharge and secondary cyclone underflow (70% + gold recovery), but falls short with the secondary cyclone overflow (20% gold recovery) because the gold is simply too fine to be recovered. KC performance was only briefly covered in this chapter but research should be pursued because the results were certainly very promising.

The results of the optimization tests showed that the FC will overload when the feed mass exceeds 20 kg. Recovery then drops sharply as more material is fed. Some of the gold will be removed from the bed with increasing test time (mass), but most of the drop in recovery is due to bed saturation.

Several streams were tested (PCOF, Flotation Concentrate, RMDS, SCUF, BMD2 and SCOF) to determine the best stream from which to recover gold with the FC. The FC performed poorly with the recycled streams (RMDS), recovering only 16 $\pm$ 2% of the gold, but did better with the flotation concentrate, where it recovered 22 $\pm$ 3% of the gold. The FC did fail to make grade (target: 200000-300000 g/t) with the flotation concentrate, producing only a 900 g/t concentrate.

For a constant feed mass of 20 kg, especially at low percent solids, recovery increases with increasing flowrate between 10 and 30 l/min. The effect of feed

79

density is not clear: at low flowrates (10 l/min) recovery increases with increasing density; the effect decreases with increasing flowrate, and might actually reverse at 30 l/min.

On a size-by-size basis, the FC recovered approximately 30% of the gold in the 15 to 25 μm fractions of the flotation concentrate where approximately 15% of the gold was distributed (slightly better than the KC in the same classes of the regrind mill discharge, where 15% of the gold was also distributed).

Based on the present results, it is certainly difficult to justify the purchase of a FC. The FC performed poorly with the regrind mill discharge material, recovering only 17% of the gold and producing a 700 g/t gold concentrate. It did perform slightly better with the flotation concentrate, however, by recovering 22% of the gold; this is still inadequate. Significant reprocessing of the tails would certainly be required to increase recovery, which is not a particularly attractive prospect.

Chapter 4

Gold Recovery from Meston's Flotation Tails

4.1 Introduction

The objective of this work is to evaluate the FC's performance as a scavenging unit, and to eventually reduce gold losses in the tails from the Meston Resources concentrator. Preliminary work was begun with a sample of slimes from the former back-fill circuit at Meston to recover gold. This chapter will present the results of this work as a further application of the FC.

Whereas at AELR the objective was to recover free gold to smeltable grade from a high density gangue, the objective here is to gold-bearing sulphides and other (mostly) locked gold species from a low density gangue.

4.2 Meston Circuit

The Meston Resources concentrator, located near Chibougamau, P.Q., treats ore from the Joe Mann Mine. The gold occurs in two generations. First generation gold, about 25% of the total gold, is mostly associated with silicates, contrary to AELR's ore which is mostly associated with pyrite. It is very fine (1-10 μm), which makes grinding to complete gold liberation impractical. Cyanidation must thus be used in conjunction with flotation and gravity concentration to improve recovery. Second generation gold is associated with sulphides and silver. It is coarse, contains approximately 20% silver (electrum), is easily liberated and responds well to gravity recovery (Laohapanit, 1989). Total gold recovery at the time of the test work was 88%, of which 35-40% is in the

gravity concentrate, 35-40% in the flotation concentrate, and approximately 10% in the cyanidation circuit. The remaining gold reports to tails. Flotation tails are deslimed in what used to be a backfill circuit; the fine fraction goes to the tailings pond directly, whereas the coarse fraction is cyanided first. Figure 4.1 is a schematic of the Meston circuit and illustrates the details of the circuit. After three stages of crushing the ore is ground in a 3.4 m x 4.0 m rod mill. The rod mill discharge is pumped to two 76 cm cyclones in closed circuit with two 3.1 m x 3.7 m ball mills. The cyclone overflow is fed to the flotation circuit. Gold is recovered from the ball mill discharge using sluices, 76 and 30 cm KCs, and a shaking table located in the gold room. The sluice and KC tails are returned to the cyclones. Further details of the gravity circuit are given in Liu (1989).

The cyclone overflow is fed to four Denver DR 300 rougher flotation cells, and then to two six-cell banks of Denver DR 30's. The rougher tails is distributed to four six-cell banks of Fagergren 66 scavengers. The scavenger tails are upgraded in a two-stage cycloning circuit (previously used to produce back-fill), and the coarse fraction cyanided. The rougher concentrate is upgraded through two stages of two six-cell banks of Denver DR 24 cleaners. The scavenger concentrate and cleaner tails are cycloned in closed circuit with a 2.2 m x 2.2 m regrind mill to obtain better mineral liberation and create fresh surfaces needed for selective flotation; the cyclone overflow is then fed to three six-cell banks of Fagergren 66 retreaters for recleaning.

Primary and Secondary Grinding

Flotation

Desliming

Rod Mill

Sluice

1.7 mm Screen

Knelson Concentrator Circuit

To Gold Room

Rghr

Scav

Final Tails

Clnr 1

Clnr 2

Final Concentrate

Retreat

To Cyanidation
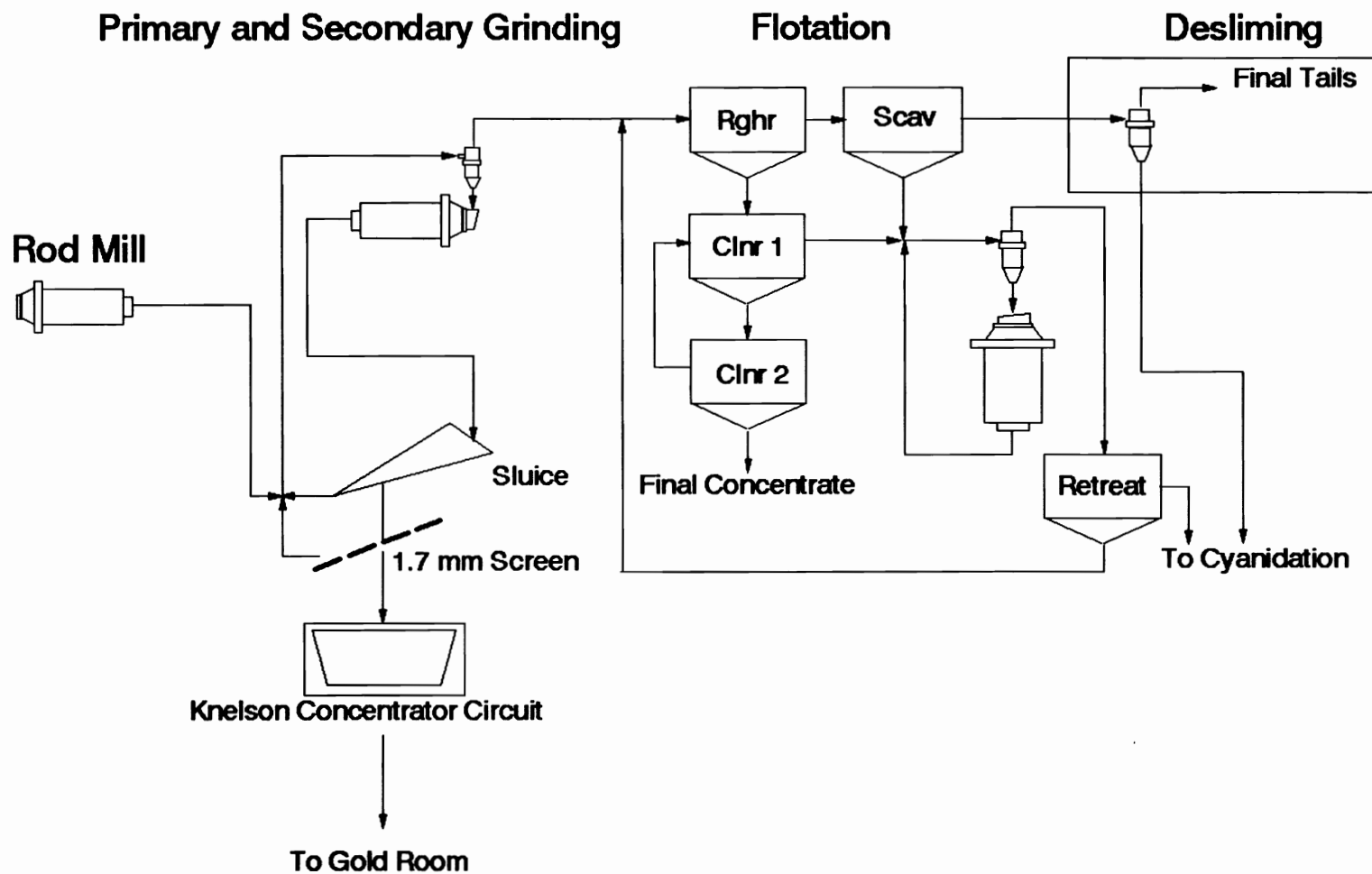
Figure 4.1: Meston Resources' Plant Flowsheet

It is important to note the difference between the AELR and the Meston material since they are not expected to behave the same way in the FC. The AELR flotation concentrate, a very fine, high grade material, contains over 70% sulphide and does not respond very well to gravity separation. The FC recovered only 20 % of the available gold from a 20 kg sample of this material (Chapter 3). The Meston fine flotation tail is much finer, 98% -75 μm, contains under 2% sulphides (0.7% S), and is composed mostly of silicates and hard-to-float middlings. The separation, then, is based on the difference in specific gravity between these gold and sulphide middlings and the silicates. The density of the gold middlings, may be higher than that of the pyrite middlings. Some fine gold may also be present.

4.3 Experimental Procedure

A 20 kg sample of Meston flotation tails (slimes) was shipped to McGill University for processing with the FC. Three different bowls were tested (8, 10, 14 degrees) at two flowrates (10, 20 L/min) and three percent solids (10, 20, 30). Nineteen experiments were performed (15 runs and 4 randomly chosen repeats). Test work consisted of three 2 x 3 factorial designs, one for each bowl. Due to the limited sample mass, a full experimental design could not be performed. High priority was thus assigned to the 8 and 10 degree bowl tests. The 14 degree bowl was not expected to perform as well in this application in this application where

85

pyrite recovery was targeted.

All tests were performed with roughly 10 kg of solids (half the sample). At the end of each experiment, both the FC concentrate and tails were dried, proportionally sampled, not to alter the head grade, then assayed for total sulphur (pyrite) at Assayers Laboratories in Rouyn-Noranda and gold at the laboratory of Meston Resources. The remaining portion of the products was re-used for the subsequent experiments. The first half of the 20 kg stock sample was used for test 1. The second half was used to replace the mass removed for assaying (450 g per test).

4.3.1 Sampling and Mass Balancing Considerations

Because most of the concentrate and tails samples of each test were recycled to the next one, the experimental procedure was slightly modified, as will now be described.

After the FC was operated, and the concentrate and tails products were dried, weighed, representative samples were extracted for assaying. For a given proportion of the total concentrate mass removed for assaying purposes (roughly 10%), the same proportion of the total tail mass was removed; thus a constant feed composition was maintained from test to test. Following this, then, the assays were mass balanced using the method of Lagrange multipliers used previously, with the following variances being used: for pyrite, 0.003 $\%^2$ for feeds and 0.01

$\%^2$ for concentrates and tails; for gold, 0.003 $(g/t)^2$ for feeds and 0.01 $(g/t)^2$ for concentrates and tails. The results were balanced using the back-calculated average feed grade from each test: pyrite, 0.80%; gold: 0.81 g/t. Finally, pyrite and gold recovery were calculated from these adjusted assays.

It is important to understand the sources of mass loss, since ideally all tests should be performed at a constant feed mass. Two major sources of mass loss were discovered during the test work. The first loss arose from incomplete processing of the sample; roughly 1.5 kg remained in the mixing tank. The second loss, spillage, is hard to measure, and was estimated making the basic assumption that it is constant for each test. Thus, given a feed mass of 8500 g in test 1 and a feed mass of 8310 g in the final test 16, total losses were 230 g, or 13 g per test. The adjusted feed masses were then used to calculate recovery. The feed masses in the final three experiments (14 degree bowl) were not adjusted, however, because the feed stock was exhausted and thus the tests were performed without replacing the mass removed.

Table 4.1 shows the feed assay results before and after mass balancing. The remaining data can be found in Appendix VII. The unbalanced assays are quite erratic, and, as expected, the balanced assays less so. The adjustments are, in general, reasonable, with a few exceptions. The adjustments to tests 1, 10, 12, 14, 15, and 18 are much larger. Assaying problems were suspected, due to the low grade of the material, making these particular results questionable. The samples

87

Test #	Operating Conditions	Feed Mass (g)	Pyrite Feed Grade (%) f	f_{corr}	Gold Feed Grade (g/t) f	f_{corr}
1	Flowrate:10 l/min % solids:10 Bowl: 8 degrees	8500	1.07	0.87	0.64	0.77
2	20, 20, 8	8487	0.68	0.78	0.80	0.80
3	20, 10, 8	8475	0.73	0.79	0.87	0.82
4	20, 20, 8	8462	0.78	0.81	0.78	0.80
5	20, 30, 8	8449	0.64	0.77	0.66	0.77
6	10, 30, 8	8437	0.62	0.77	0.87	0.82
7	10, 10, 8	8424	0.79	0.81	0.77	0.80
8	20, 20, 8	8411	0.78	0.80	0.76	0.79
9	10, 20, 8	8399	0.85	0.82		
10	20, 10, 10	8386	1.00	0.86	0.96	0.84
11	10, 20, 10	8373	0.97	0.85	0.69	0.78
12	20, 20, 10	8361	0.69	0.78	1.03	0.85
13	10, 30, 10	8348	0.93	0.84	0.73	0.79
14	20, 30, 10	8335	1.00	0.86	1.15	0.88
15	10, 10, 10	8323	1.02	0.86	0.72	0.78
16	20, 20, 10	8310	0.54	0.75		
17	10, 10, 14	8084	0.83	0.82		
18	10, 20, 14	7754	0.80	0.81	0.57	0.75
19	20, 20, 14	5924	0.74	0.80	0.85	0.81

Table 4.1: Comparison of Balanced and Unbalanced Feed Grades

for tests 9, 16, and 17 were contaminated during sample preparation and thus were

not assayed for gold, hence the blank entries.

4.4 Results

The results of this test work are illustrated in Figures 4.2 and 4.3, for pyrite and Figures 4.4 and 4.5, for gold, for the 8 and 10 degree bowls, respectively. Overall results are summarized in Table 4.2. Only three tests were performed with the 14 degree bowl, which yielded the lowest sulphide and gold recoveries. Detailed results are found in Appendix VII.

Feed Rate (L/min)	Sulphur (pyrite)		Gold	
	8° bowl	10° bowl	8° bowl	10° bowl
10	13	17	44	41
20	23	19	44	73

TABLE 4.2: Gold and Sulphur (pyrite) Recovery from fine flotation tail of Meston Resources; each point is the average of 3 tests at 10, 20 and 30% solids)

Gold recovery is higher than sulphur's; there is some evidence that gold recovery is better with the 10° bowl at the higher flow rate. Data for the 8 and 10° bowls were regressed to correlate recovery with operating parameters: bowl angle, feed density, dry feed rate and flow rate, and a synergetic term for flowrate and density. Of all the operating parameters, none were found significant for sulphur. For gold, the following regression was obtained:

$$R_{gold} = -40.2 + 413 \pm 185 \tan \alpha + 1.67 \pm 0.66 \ Q,$$

where R_{gold}: gold recovery, %; α: bowl angle, °; Q: feed flowrate, L/min

If the results of all tests with the 8 and 10° bowls are averaged, a gold recovery of 50% is achieved at a concentrate grade of 4.0 g/t in a weight yield of

Pyrite Recovery from Meston Tails
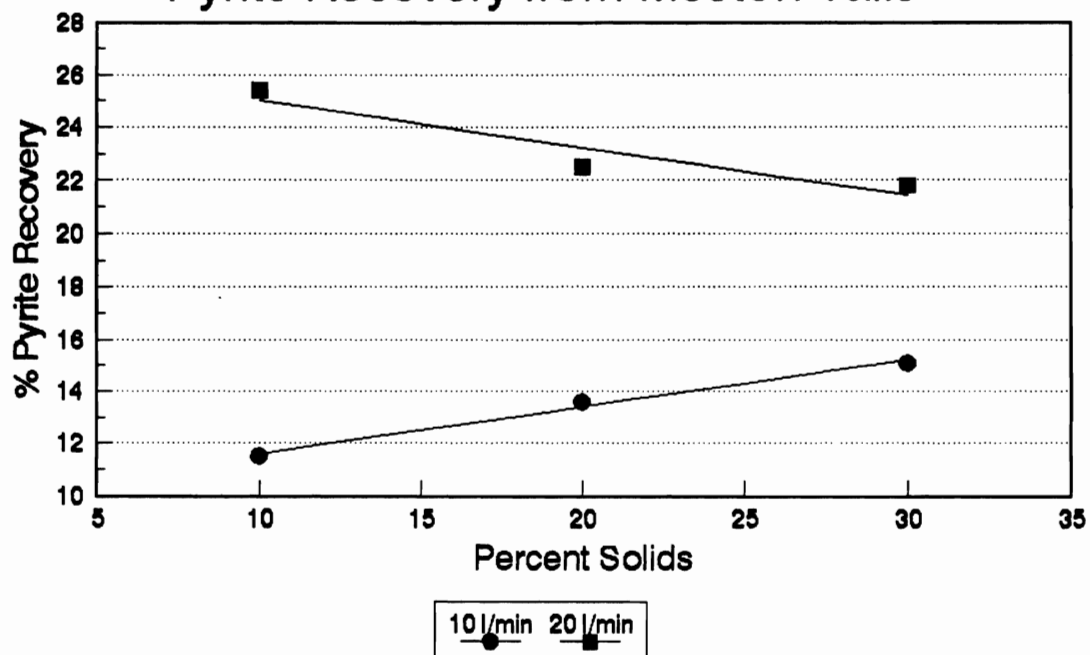
Figure 4.2: Pyrite Recovery for 8 Degree Bowl
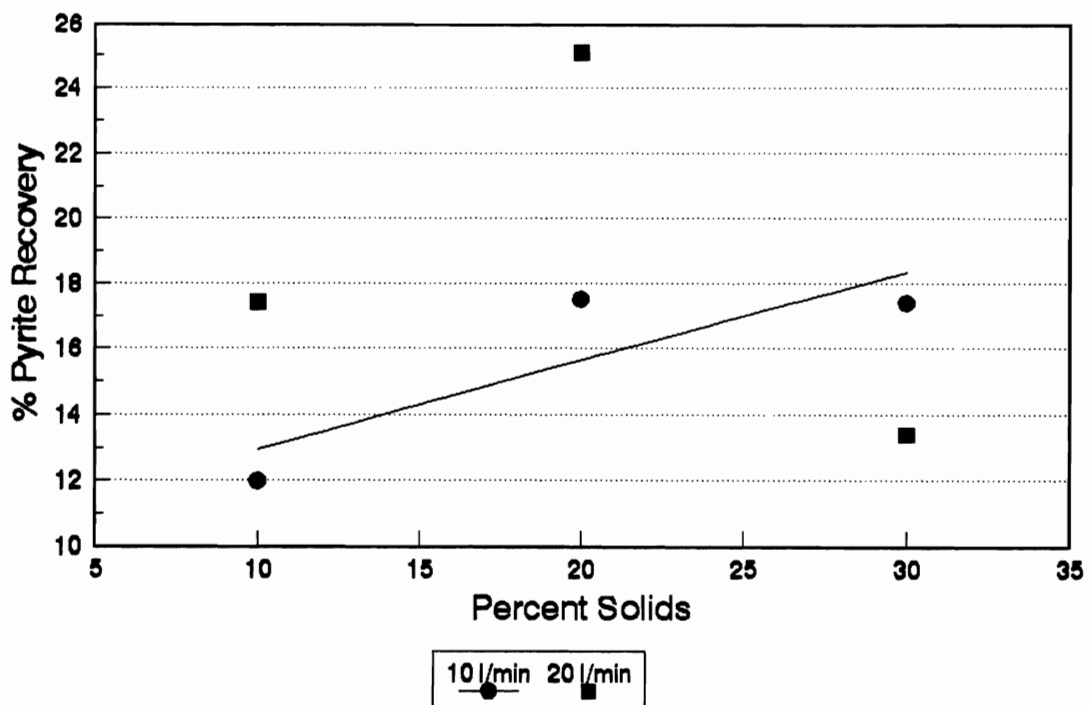
Figure 4.3: Pyrite Recovery for 10 Degree Bowl

Gold Recovery from Meston Tails
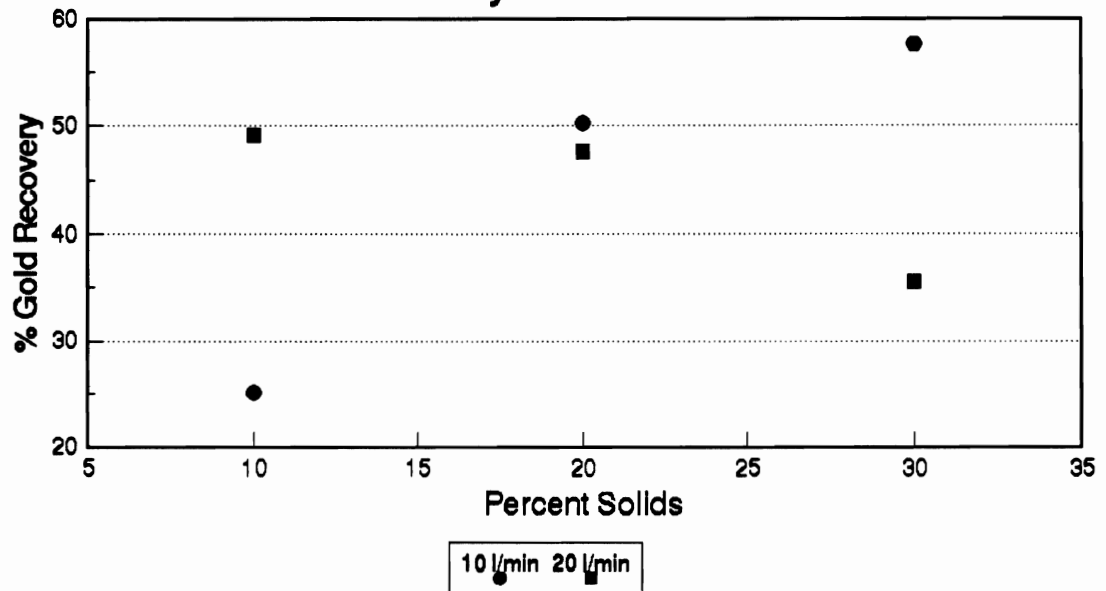
Figure 4.4: Gold Recovery for 8 Degree Bowl
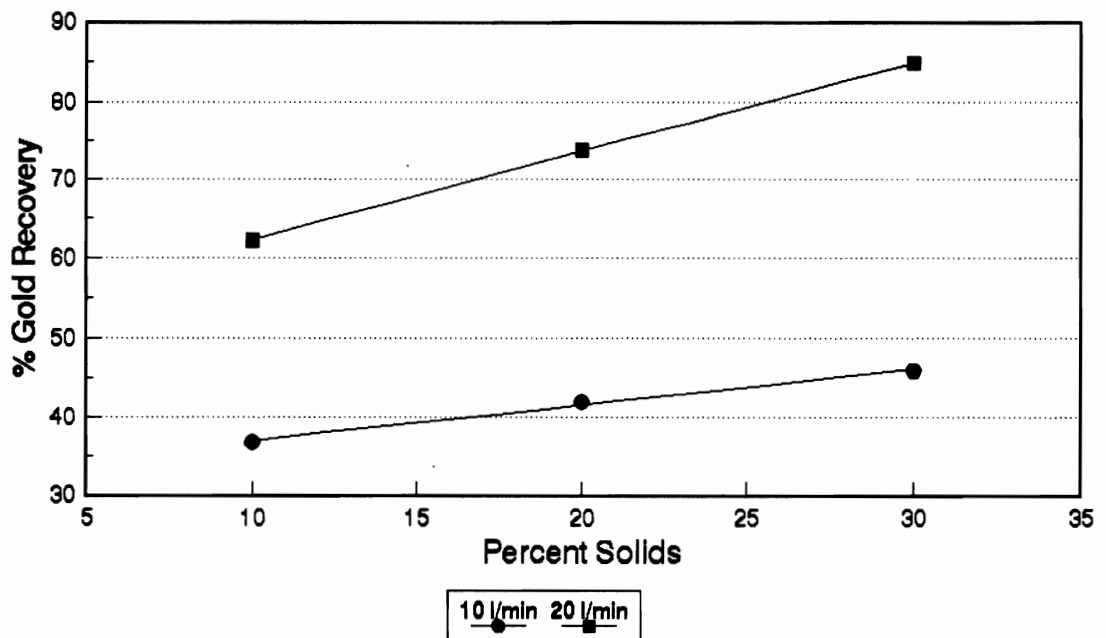
Figure 4.5: Gold Recovery for 10 Degree Bowl

10%. The existing cyanidation circuit would be capable of handling such a product.

Figure 4.6 shows the FC tails' gold grades as a function of the pyrite grades and shows a very poor correlation between the two ($R^2 = 0.11$). This implies that the middlings are not predominantly sulphide/gold. This suggests that the flotation circuit is operating properly as most of the gold reporting to the tails is not associated with sulphides.

4.5 Conclusions

The FC can effectively recover 50% of the gold and 20% of the pyrite from the final flotation tails.

The low grade of the products makes assaying very difficult and as such, the correlation between recovery and the operating variables are difficult to quantify. Despite this difficulty, however, it appears that higher recoveries are favored at the higher flowrates (at least 20 l/min).

The tailings material contains very little pyrite/gold middlings, and consequently the separation is based on the physical differences between the gold/silica and pyrite/silica middling particles. Because the gold/silica middlings are heavier, they are preferentially recovered over the pyrite middlings.

There is still some recoverable gold remaining in the flotation tails slimes Although the FC can recover a significant portion of this material, there are other in-house alternatives which should be considered as well as potential improvements:

1) The backfill circuit configuration and the deslimer cyclone geometry should be investigated to determine if more gold cannot be classified into the coarse product (which is already cyanided).

2) The gravity circuit should be reinvestigated to determine if additional gold can be recovered upstream.

3) A mineralogical investigation of the scavenger tails should be considered to determine the performance of the scavengers. Perhaps are they operating too selectively and releasing a considerable amount of flotable gold to tails?

This chapter presented the results of a preliminary investigation, and since the basic findings were promising then certainly further test work is warranted and a mineralogical investigation of the products, preferably size by size, is needed.

All the test work so far has dealt with gold, a difficult material to sample and assay, particularly when dealing with grades that were lower than 1 g/t. In Chapter 5, the factorial test work work will be repeated with an artificial ore consisting of liberated silica and magnetite. This effectively eliminates the assaying errors since these two phases can be separated by magnetic separation, and increases the level of certainty in the data.
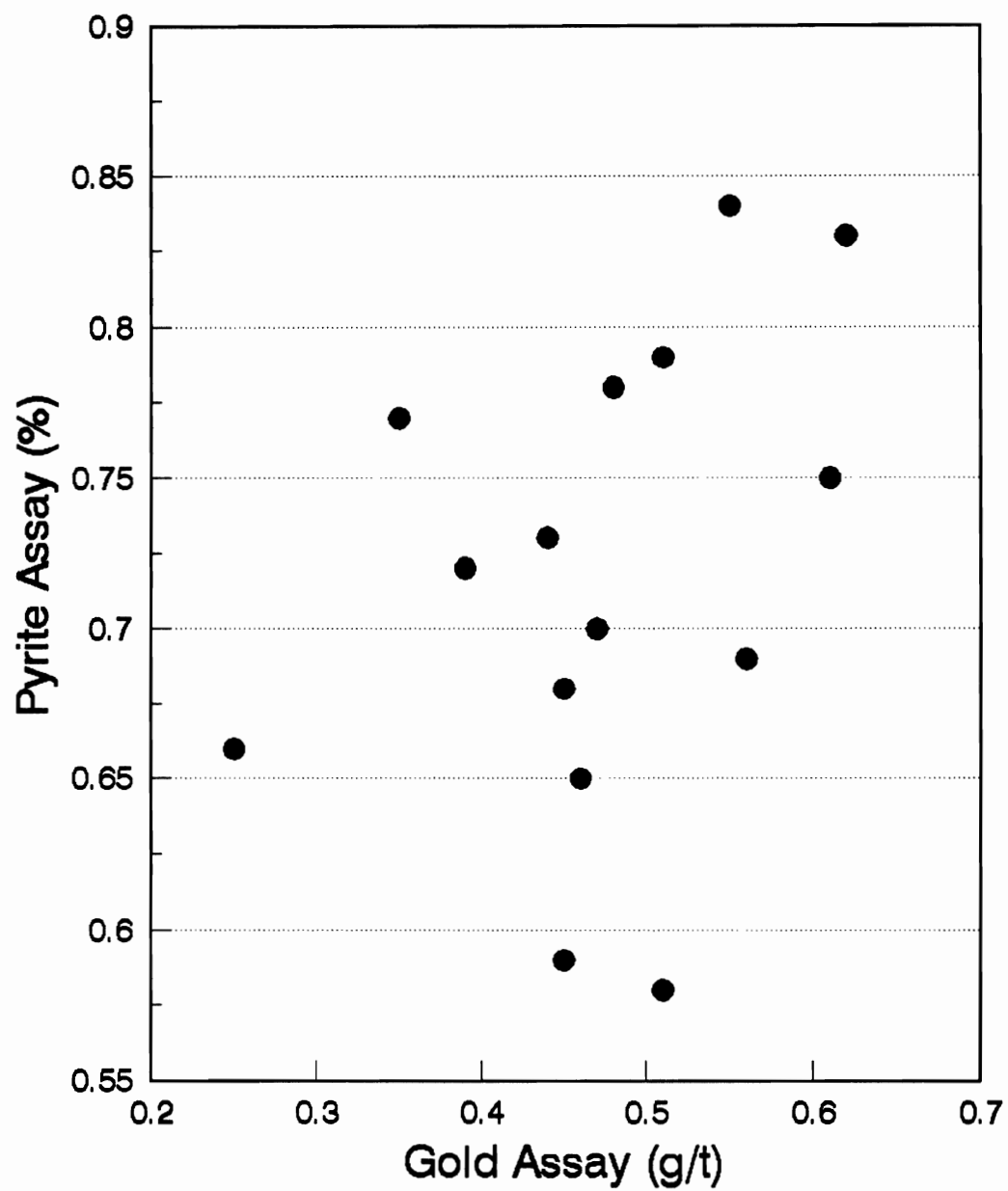
Figure 4.6: Comparison of F.C. Tails Grade

Chapter 5

Fundamental Investigation of Falcon Concentrator

5.1 Introduction

The purpose of this Chapter is to present the results of a fundamental investigation of the FC performed with a prepared feed consisting of liberated magnetite and silica. The discussions presented will focus on the mechanisms involved in the recovery process, which is important information needed to understand how the FC works.

Section 5.2 will present the results of a systematic variable test program used to study the effect of the operating variables on FC performance.

Sections 5.3 and 5.4 will examine the mechanism of bed formation and discuss how the effect of particle size affects the selection of particles recovered in the bed.

Section 5.5 will present the results of test work performed to study overloading; ie. feeding over a long period of time to monitor the decrease of recovery. The issue has already been examined for gold in Chapter 3, but the results require further confirmation and size-by-size data were lacking. The kinetics of recovery will also be addressed.

Section 5.6 will present the results of a multi-pass test performed with the FC. For this test, a sample of the prepared feed was processed with the FC, and the tails were then reprocessed twice.

Gold-bearing material, because of its low grade, is difficult to sample and as a result, assaying errors tend to be large. These errors have already been discussed in Chapters 3 and 4 and were shown to lead to significant variations in the calculated gold recovery, thus causing uncertainties in the results. Repeating the test work as well as multiple assaying did help, as was demonstrated in Section 3.5.3, but the major

96

drawbacks were the cost of assaying, approximately $10 per assay, and the long delay before the results were returned, typically 4 to 8 weeks. If only general results are required, however, then another testing alternative, which will be demonstrated in this Chapter, is to use an artificial feed consisting of two liberated, easily separable minerals, such as silica and magnetite, to perform the test work. Assaying costs are eliminated because magnetite is easily recovered by magnetic separation, and the delay time is effectively reduced to a few days. The magnetic and non-magnetic fractions can be screened to generate size-by-size data. The main drawback to this approach is that the density difference between magnetite (5.2 g/cc) and silica (2.7 g/cc) is lower than that of gold-sulphide-silicate systems.

5.2 Discussion of the Systematic Variable Tests

Three 3-level nested factorial experiments were performed to study the effect of gangue particle size, bowl type, % solids, and flowrate. Figure 5.1 illustrates the design and shows the range of the parameters investigated. The complete size distributions of the silica are presented in Appendix VIII.

5.2.1 Experimental Procedure

A sample of an iron ore cobber concentrate (P_{80}= 425 μm) from the Iron Ore Company of Canada (IOC) was ground and processed with a Davis Tube separator. The magnetite was recovered and further upgraded with the separator. Finally, the FC feed was prepared (9500 g of silica of the required size with 400 g of magnetite concentrate).

Bowl	8 Degrees	10 Degrees	14 Degrees
Gangue Particle Size (micrometres)		425 212 75	
Flowrate (L/min)		10 20	
% Solids		10 20	
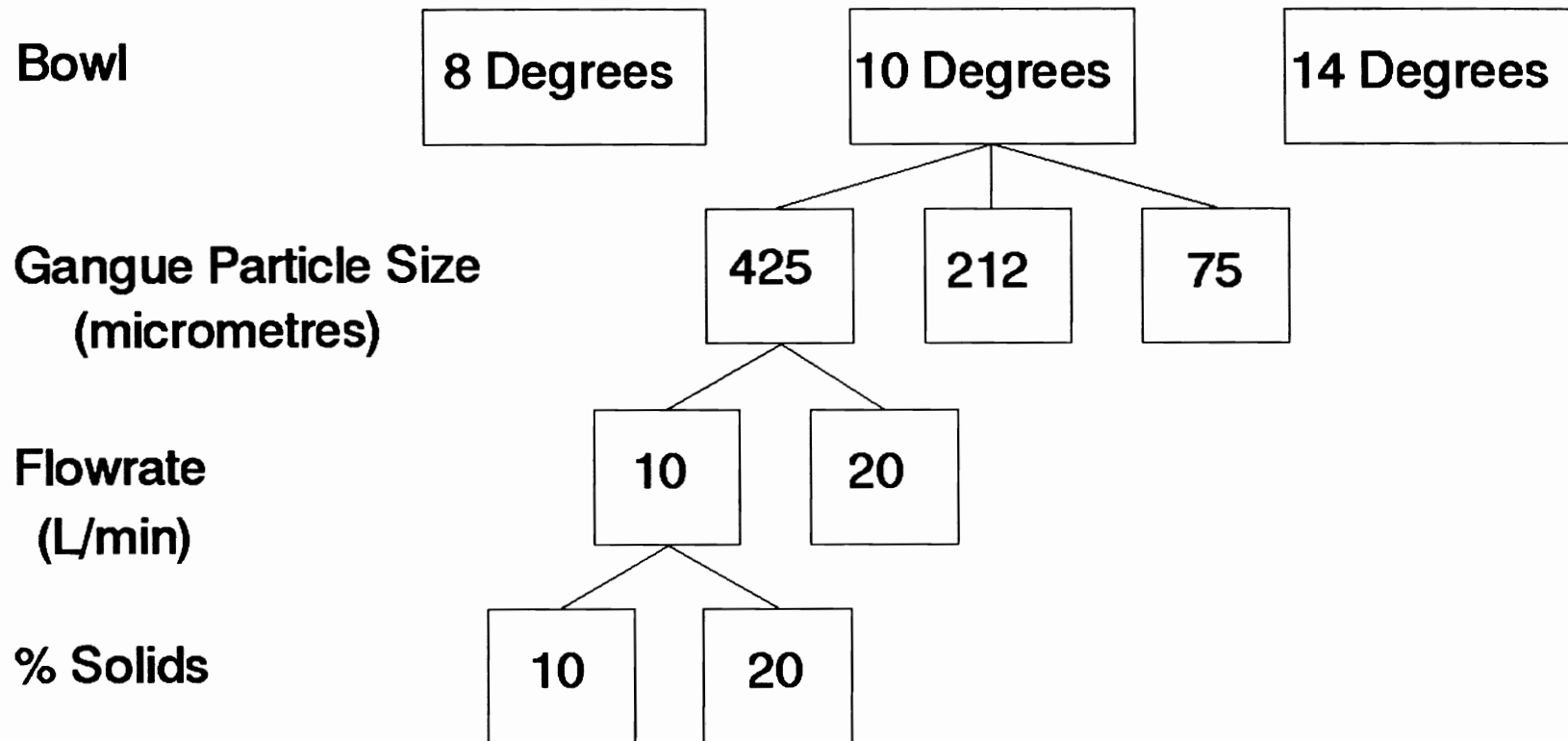
Figure 5.1: Experimental Design used for Test Work

For the 8 and 14 degree bowl tests, the samples of prepared feed were processed with the FC, as per the usual procedure, and the FC products were completely recovered dried, weighed and sampled. The samples were then processed with a High Gradient Magnetic Separator (HGMS) for roughing, and a Davis Tube (DT) for final cleaning. The Davis Tube concentrate was dried, weighed and then screened from 600 to 53 μm. Finally the overall and individual size-by-size recoveries were calculated from the magnetite content in the tails and concentrate.

An alternative procedure was used for the 10 degree tests to determine if experimental time could be further reduced. For these experiments, only the concentrates were recovered and processed with the magnetic separator. Recovery was to be calculated from these and the original feed data, thus the feed was assumed constant. The procedure was later found to be less accurate because it did not take into account the material left unprocessed in the tank, but the data will nevertheless be presented.

5.2.2 Results

Table 5.1 presents the total mass of magnetite in the FC feeds for each test. The magnetite content for the 10 degree bowl trials was first assumed to be constant at 400 g, the initial mass of magnetite put into the material.

The assumed magnetite content of the feed for the 10 degree bowl experiment is not correct and is in fact too high. This difference in magnetite content can be readily accounted for by the magnetite remaining unprocessed in the slurry tank. In fact, 1500

	Mass of Magnetite in Feed (g)	
Test Number	8 Degree Bowl	14 Degree Bowl
1	246	246
2	261	353
3	254	253
4	237	242
5	264	256
6	238	258
7	269	251
8	254	257
9	256	258
10	257	241
11	290	240

Table 5.1: Comparison of Magnetite Weights for the Individual Feeds

grams of solids, containing 10% magnetite (measured), remained at the bottom of the slurry tank. The mass of magnetite fed to the FC was actually 250 g, contrary to the assumed 400 g. Thus it would appear that back-calculating the magnetite content of the feed from the concentrate and tails is a better procedure since it provides a direct measurement of the actual feed. The magnetite recovery for the 10 degree bowl tests was thus recalculated on the basis of the average magnetite content of the individual test feeds (241 g), which is clearly more accurate than the initial procedure, but less accurate than the procedure used with the two other bowls.

The original data can be found in Appendix IX, and Table 5.2 presents the magnetite recoveries for all the tests.

Particle Size, μm	% solids	Flowrate l/min	8 Degree Bowl	10 Degree Bowl	14 Degree Bowl
425	10	20	23.2	18.5	13.1
	30	20	26.6	23.2	19.5
	10	10	32.5	31.0	9.1
	30	10	36.1	33.0	18.3
212	10	10	37.1	35.5	15.2
	30	10	42.5	38.8	17.9
	10	20	40.1	41.5	16.3
75	10	10	77.9	51.2	22.2
	30	10	52.6	51.7	31.5
	30	20	78.7	73.2	21.8
	10	20	65.4	74.8	36.2

Table 5.2: Calculated Magnetite Recoveries for Factorial Design Experiments

The effect of particle size is quite apparent in the data, and clearly as the P_{80} of the silica gangue decreases, magnetite recovery increases.

There is a significant difference between the magnetite recoveries for the 14 degree bowl tests, and the other bowl tests. The differences in recoveries between the 8 and 10 degree bowls are not as apparent, although the data do suggest lower recoveries with the 10 degree bowl tests. As the bowl angle is increased, recovery becomes more selective, and less material will be recovered.

The effect of flowrate and percent solids is not as apparent as the other effects, and the test work showed some conflicting results. It is thus difficult to suggest that any relationship exists between flowrate, density and recovery.

101

A multilinear regression was performed and Table 5.3 presents the regression results. The results for test 2 were found to be a questionable because the calculated mass of magnetite in the feed was too high (353 g) and were not included in the regression. The bowl type is reflected by the value of X: bowl 1 (8 degrees), X=-1; bowl 2 (10), X=0; bowl 3 (14), X=1. The cross-effects terms, for example: (flowrate factor) * (% solids factor), were found to be insignificant and thus dropped from the model.

	Bowl Parameter X	Silica P80	Flowrate	% Solids
Value	-12.42	-9.1	2.6	2.4
S.D.	2.5	2.6	2.0	2.0
t-ratio	-5.0	-3.6	1.3	1.2

Table 5.3: Results of Multilinear Regression

The correlation coefficient for the model was 0.6, indicating that there is some correlation between the selected operating variables and recovery. In addition, by comparing the t-ratio (Value/S.D.) to the t-value at 95% confidence (1.96), it is clear that the most significant factors affecting performance are the type of bowl and the P_{80} of the gangue. As the particle size of the silica decreased, recovery increased, and as the bowl angle increased, recovery decreased. The strongly negative value of the bowl parameter, -12.4, can be attributed to the large decrease in recovery between the 8, 10 degree bowl tests, and the 14 degree bowl tests.

The low t-ratios associated with flowrate and percent solids implies that they are

not significant at 95% confidence. This is unlike results of Chapters 2 and 3 which showed a definite effect of feed flowrate and density. These effects may be well masked by those, more important here, of bowl type and gangue size distribution. These larger particles, exhibiting a greater resistance to motion, are maybe less responsive to hydrodynamic forces.

Figure 5.2 shows the relationship between magnetite recovery and particle size at 30% solids and 10 l/min, at a feed size of 425 μm. Although overall recovery changes from 35% (8 and 10 degree bowls) to 18% (14 degree bowl), the size-by-size behavior is similar for all three bowl types. In the coarser classes, 300 to 500 μm, recovery is high (55% for 8 and 10 degree bowls, 20% for 14 degree bowl). It then drops and remains relatively constant (30% for 8 and 10 degree bowls, 9% for 14 degree bowl) between 100 and 200 μm, but increases again in the 53 to 100 μm sizes (55% for 8 and 10 degree bowls, 45% for 14 degree bowl). The coarser particles may be preferentially recovered because they are less likely to be carried out by the slurry flow and the finer particles may be recovered via capture sites on the surface of the bed, in which they are partially shielded from the shearing action of the slurry flow.

5.3 Examination of the Bed Formation in the Falcon Concentrator

The results of an examination of the the particle bed will be presented in this section to help understand how particles are recovered in the FC. Section 5.3.1 will discuss the experimental procedure used and Section 5.3.2 will present the results. Section 5.3.3 will present a brief discussion of Bagnold's work with sand dunes to help

understand the dynamic topology of the bed in the FC.

5.3.1 Experimental Procedure

A 10 kg sample of prepared feed (5% magnetite, $P_{80\ silica}$= 212 μm) was processed with the FC. The unit was temporarily stopped after 10, 30, and 70 seconds of operation. The thickness of the solids bed was measured with a specially designed probe and a photograph of the bed was taken at each time interval. A schematic of the probe is shown in Figure 5.3. It consists of a 30 cm rod on with marks made at every 2 cm. The thickness of the solids is measured by adjusting the tip of the pointer so that it just touches the surface of the solids. The length of the pointer provides a measure of bed thickness. This process is repeated with no solids in the bowl and the thickness is the difference between the two readings. The pointer length was measured with a Vernier caliper with a precision of $\pm$ 0.05 mm.

5.3.2 Results

Figure 5.4 shows the solids profile and plates A to C are the photographs of the bed. The profiles appear quite irregular because of the presence of furrows presumably where slurry preferentially flows. Plate A was photographed after 10 seconds of operation, and shows that the bed has not yet completely formed and no magnetite has yet been recovered. After 20 seconds of operation, however, the bed is completely formed and some magnetite has deposited on the surface of the bed (Plate B). Bed thickness has increased and apparently achieved a maximum, as indicated in Figure 5.4.
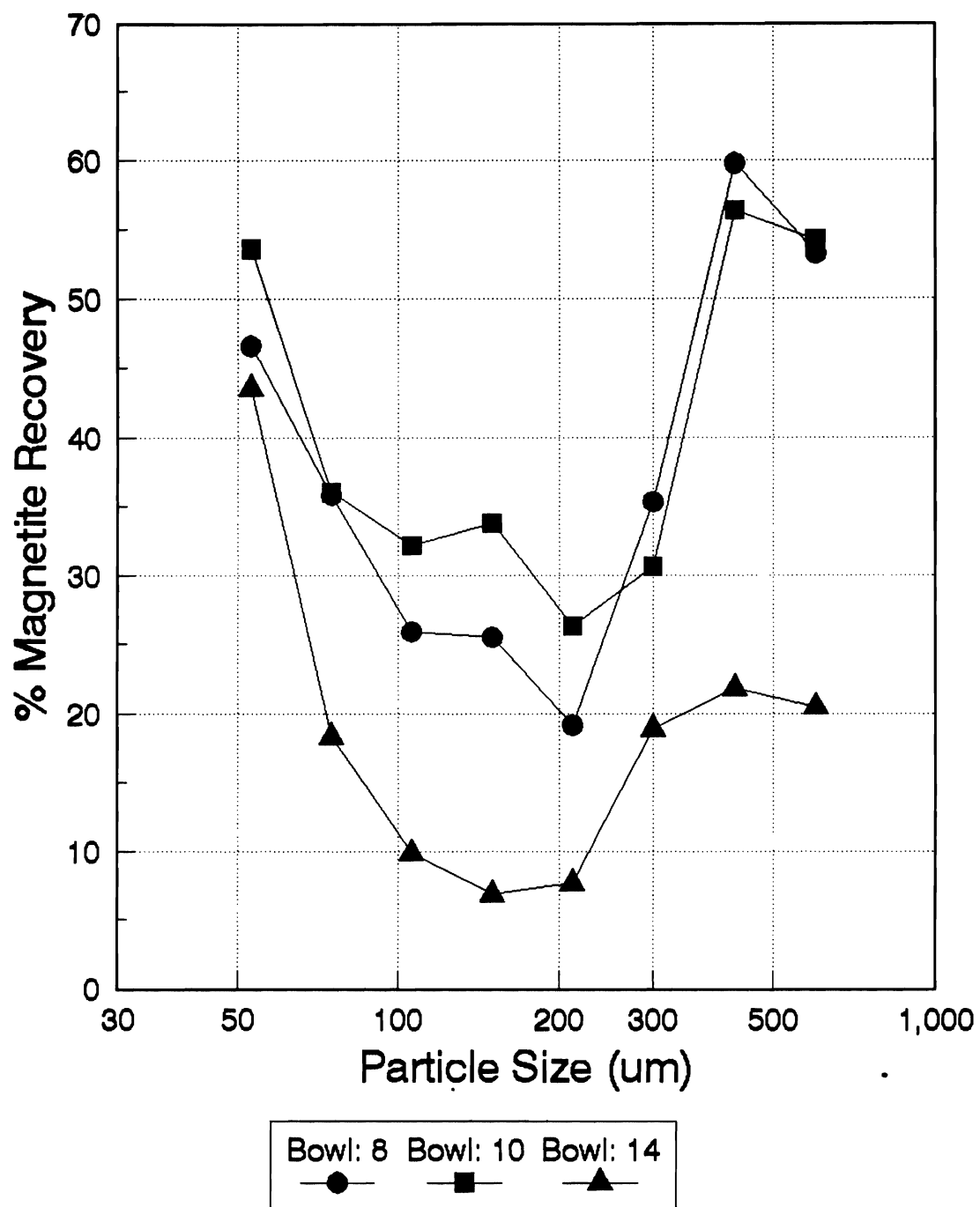
Figure 5.2: Size-by-Size Magnetite Recovery
Feed: 30% solids, 10 l/min, 425 um gangue

Pointer
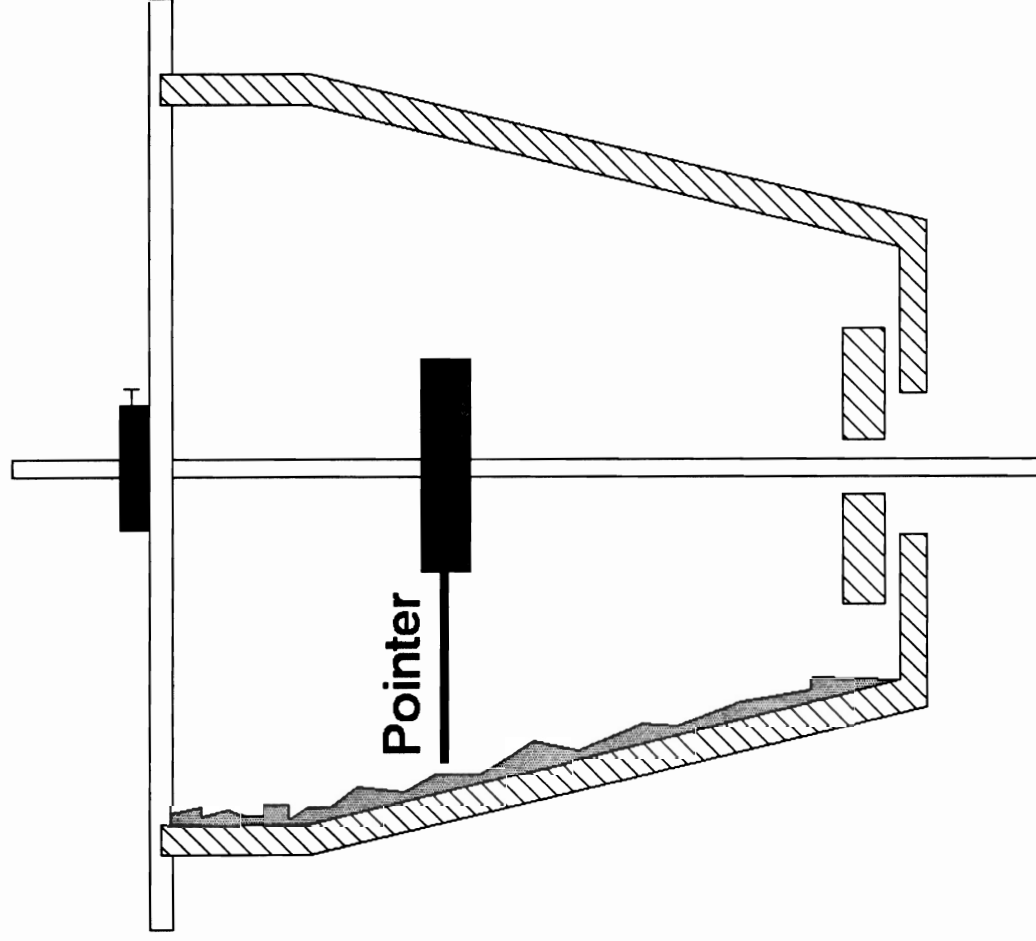
Figure 5.3: Sketch of Probe used to Measure Bed Thickness

The uneven wall profile reflects

the accuracy of the system used to measure the thickness
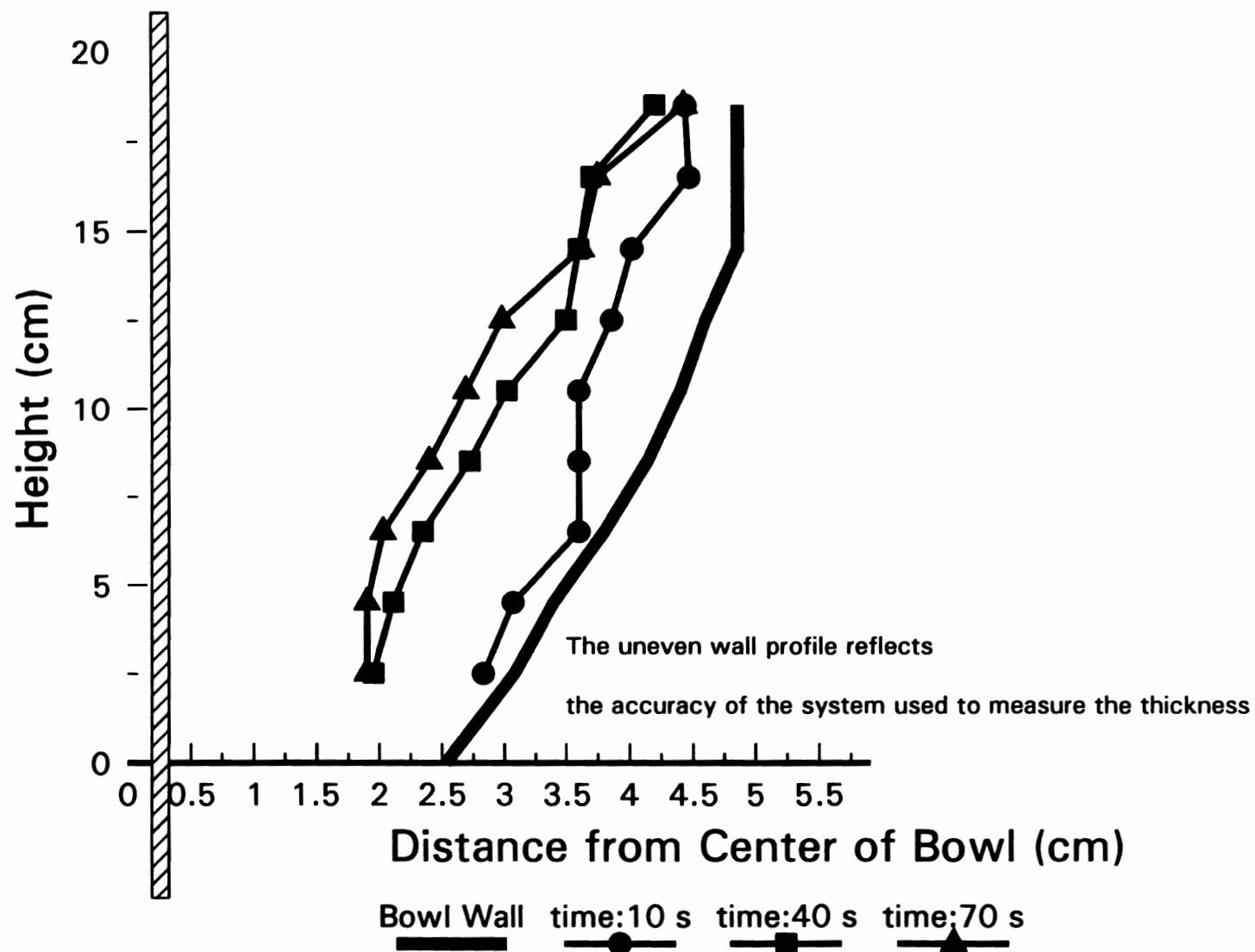
Figure 5.4: Solids Profile in 10 Degree Bowl

Plate A: Concentrate Bed after 10 seconds of Falcon Operation
(Feed: Silica/Magnetite)

Plate B: Concentrate Bed after 20 seconds of Falcon Operation
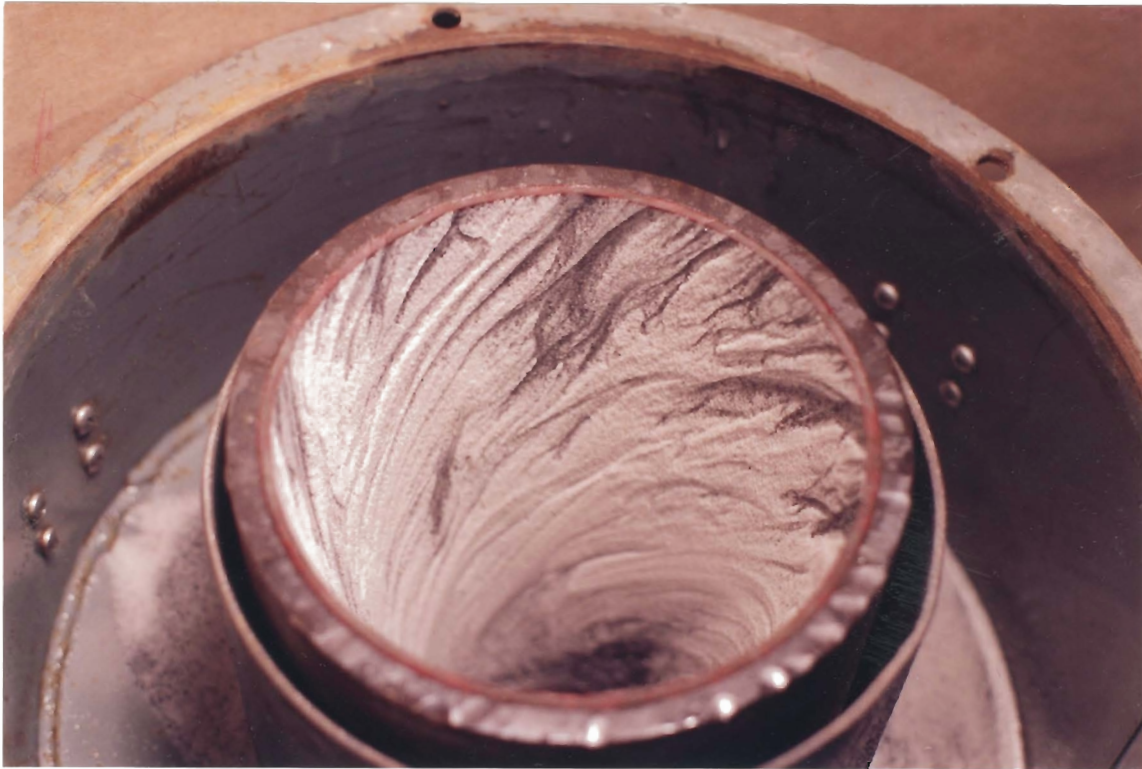
Plate C: Concentrate Bed after 70 seconds of Falcon Operation

Little change in bed thickness occured between 20 seconds and the end of the test, which characterises the end of bed formation, although more magnetite is still being recovered. Plate C shows the final state of the bed. Clearly there is more magnetite which has been recovered since Plate B.

5.3.3 Discussion

The furrows on the surface of the bed are formed by the action of the slurry raking through the solids. The factors that affect riffle formation also affect the way in which a particle will be recovered. Bagnold (1973) has written an excellent monograph on the formation of sand dunes in the desert, which has some similarities to the way in which solids bed is formed in the FC. He concluded that the major factors affecting the height, shape, and repetition distance of sand dunes, although not mutually exclusive, are five-fold:

1) The flow of air (water in this system), which causes the primary motive power to the individual grains in saltation, and which is in turn controlled by the intensity of the saltation.

2) The saltation, which causes grain movement by impact.

3) The surface grains, which are moved to a greater or lesser extent according to their **size** and **density**, and which by their relative movement are sorted out and heaped into ripples and ridges.

4) The resulting surface relief which causes place-to-place variations in the rate of

ejection of new grains into the saltation.

5) The state of the material's movement- whether deposition or removal is taking place, or whether no movement is occuring.

In the case of sand dunes, the driving force, wind, is running perpendicularly to the direction of the dune. The wind pushes the sand and causes it to pile up. In the case of the FC, the slurry is travelling in the same direction as the orientation of the grooves and riffles. It is not the riffles which are at issue, but rather the grooves formed by particles raking through the bed. The same physical factors that affect riffle formation, for example particle size, affect the mechanisms of groove formation and, more importantly the selection of particles that will be recovered.

5.4 Particle Size Effects in the Falcon Concentrator

The results so far have demonstrated that particle size (that of the gange) affects recovery more than bowl type, % solids, and flowrate. This section, then, will investigate the effect of particle size more closely.

As the particle size of the silica in the feed was increased, the recovery of magnetite decreased. The question arises now as to whether recovery is affected more by the particle size of the silica in the feed, or the particle size of the silica in the bed. It is certainly clear from the previous discussion and that of Holtham (1991) in Section 2.3.1, that the nature of the particle bed will affect the transport of solids and thus recovery.

A set of three experiments was performed and both the gangue and bed particle

sizes where independently varied to determine the impact of particle size on magnetite recovery. The results of this test work will be presented in this section.

5.4.1 Experimental Procedure

All the tests were performed as per the standard procedure with 10 kg of sample, at 20 l/min and 20% solids, with the following additional points being included to the description of the procedure:

1) The P_{80} of the silica in the feed and bed for each test was as follows: test 1- feed 212 μm, bed 212 μm; test 2- feed 212 μm, bed 425 μm; test 3- feed 425 μm, bed 212 μm.

2) A 10 kg sample of pure silica of the required particle size was processed with the FC to form the solids bed prior to processing the actual feed.

3) The regular silica/magnetite mixture was fed to the FC.

3) The complete FC tails and concentrate were removed, dried, and weighed. A 1 kg sample of both products was then processed with the magnetic separators, dried, weighed, and screened from 30 (600 μm) to 500 mesh (30 μm).

4) The size-by-size magnetite recovery was then calculated from the concentrate and tail results.

5.4.2 Results

The complete results of the test work, and the calculated recoveries, both overall and size-by-size, are in Appendix X.

The overall magnetite recoveries are shown in Table 5.4. For a given feed size

distribution, then, as the bed P_{80} is increased, recovery increased (16.0 to 28.8%). As the bed particle size increases, the capture sites will be larger, and thus be able to accomodate more magnetite.

Gangue Particle Size, μm	Bed Particle Size, μm	Magnetite Recovery
212	212	16.0
212	425	28.8
425	212	10.7

Table 5.4 Overall Magnetite Recovery for Particle Size Tests

For a given bed size distribution, as the gangue P_{80} is increased, recovery decreased (16.0 to 10.7%). The recoveries are lower than the corresponding recoveries of Table 5.2, because most of the bed is made of barren feed (it was formed when the first 10 kg of pure silica was fed). As the gangue particle size increases, more silica will be recovered and thus less magnetite will be recovered since less capture sites are available. The increased scouring action of the gangue is also expected to decrease magnetite recovery.

Figure 5.5 presents the individual size-by-size recoveries for each test. In the mid-size range, the increase in recovery with respect to an increase in bed particle size is quite appreciable. In the finer classes, there is little difference as recovery is already high for the worst operating conditions (above 80%). In the coarser size classes, recovery differences are again low, presumably because coarser particles, which are recovered when they impact the bed and bury themselves on it, are shielded from the scouring action of the feed. The most important recovery differences are in the range

113
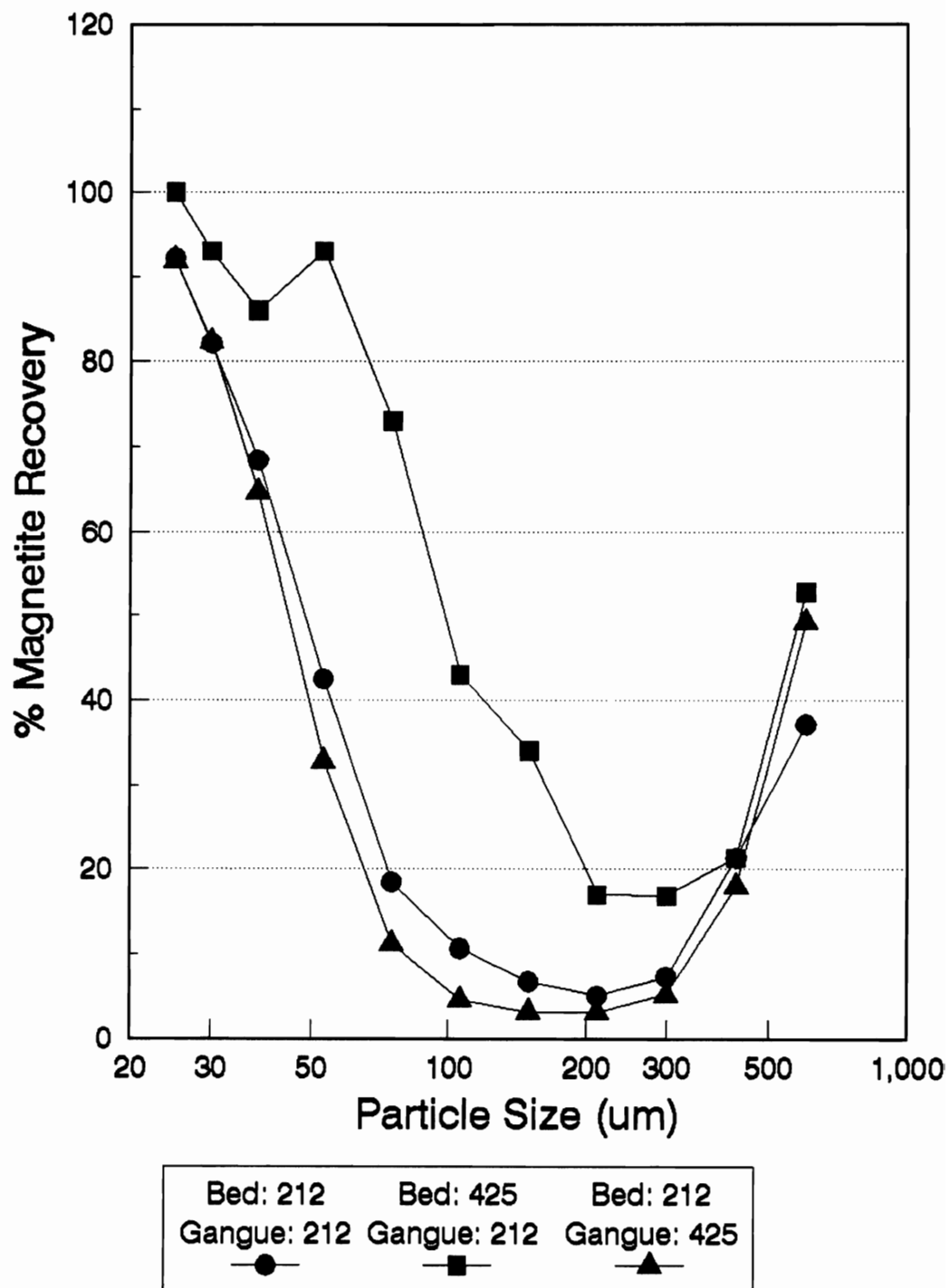
Figure 5.5: Size-by-Size Recoveries for Tests
to Study Effect of Particle Size

of 70 to 150 μm, which corresponds to particles that are roughly one quarter to one half the size of the top gangue particles. It would appear that the coarser bed is more effective in providing capture sites for these.

5.5 Overload Tests with the Falcon Concentrator

The purpose of this section is to present the results of an investigation of the mechanism of recovery in the FC and to determine if it can be described by first order kinetics.

It has been shown that recovery in the FC is dependent on the amount of material fed to it. The recovery process is thus rate dependent and a fundamental investigation of the FC should include a discussion of the kinetics of particle capture.

In Section 3.5.3, Figure 3.12 (Gold recovery vs. mass processed) suggests three phases of gold recovery. Initially, recovery is close to 100% as nearly all the feed is captured to create a bed. This phase typically lasts less than 20 seconds with a B6 FC. In the next mode, gold recovery decreases rapidly, as the recovery becomes more selective, to a certain recovery where it remained for a brief transition period. During this period, capture sites are still largely free. In a third phase, capture sites begin to saturate and recovery begins to drop again. These observations need to be verified, and a clearer definition of the curve is required.

5.5.1 Experimental Procedure

Two tests were performed as per the standard procedure with 32 and 38 kg of

sample, at slurry flowrates of 20 l/min for the first test, 30 l/min for the second, and 20% solids for both. The following additional points are included in the description of the procedure:

1) The FC feed was processed batchwise with initially 40 l of water being mixed with 10 kg of the sample in the mixing tank. When the level in the tank reached 30 l, an additional 5 kg of solids and 20 l of water were added. This procedure was repeated until the remaining material was processed.

2) The tails were sampled continuously for the complete duration of the test. The sampling time for each increment was approximately 20 to 40 seconds.

3) Each tail sample was then subsampled (1000 g), magnetic separation was performed on the subsamples, and the magnetite content of the original sample was calculated.

4) The size distribution and size-by-size magnetite content of the feed was back-calculated from the total of the individual tails and the concentrate.

5) Cumulative and incremental recoveries were calculated for each time increment by assuming that the feed to each increment is the same. The mass of feed for each increment was assumed to be that of its tails, which is a legitimate assumption given that the bed is virtually complete after 20 seconds. Only for the first tail sample would this be wrong. The incremental recovery is that of each time increment and the cumulative recovery is that from the beginning of the test up to the end of the given increment.

5.5.2 Results

Appendix XI presents the test data for both tests.

116

Figure 5.6 shows incremental magnetite recovery versus time for the 20 l/min test. Because the original data were unreasonably noisy, they were grouped into smaller clusters, the average for each cluster was calculated, and the results were arranged as shown in the figures. The results for the size classes above 105 μm have not been included because the data were questionable, due to the very small mass of magnetite present.

Upon initial feeding of the machine, a bed quickly grows, unselectively, and rapidly approaches its final profile, as shown in Figure 5.4. Material is then recovered selectively, in a mode that is extremely size and density dependent. The recovery sites saturate and recovery drops dramatically. The zone of zero recovery was never reached.

Figure 5.7 shows cumulative magnetite recovery versus time for the same test. Cumulating the recovery decreases the errors of each increment, and yields a smoother profile without averaging data. It is also quite apparent that as the particle size increases, recovery decreases. The highest recoveries are associated with the -25 μm particles. Laplante and Huang (1992) also saw a similar relationship with a gold-pyrite system. Recovery was highest for the coarsest (+500 μm) and finest classes (-25μm) and lowest for the intermediate sizes. Particles report to the bed in two different ways. Fine particles are captured when they lodge themselves in capture sites created by the asperities of the concentrate bed. Coarse particles can bury themselves in the concentrate bed, which they can also erode away. Recovery at intermediate sizes is lowest. Figure 5.5 showed this U-shape recovery curve, and figures 5.6 to 5.9 confirm this.

Figures 5.8 and 5.9 show the results for the 30 l/min test. The same trends are

117
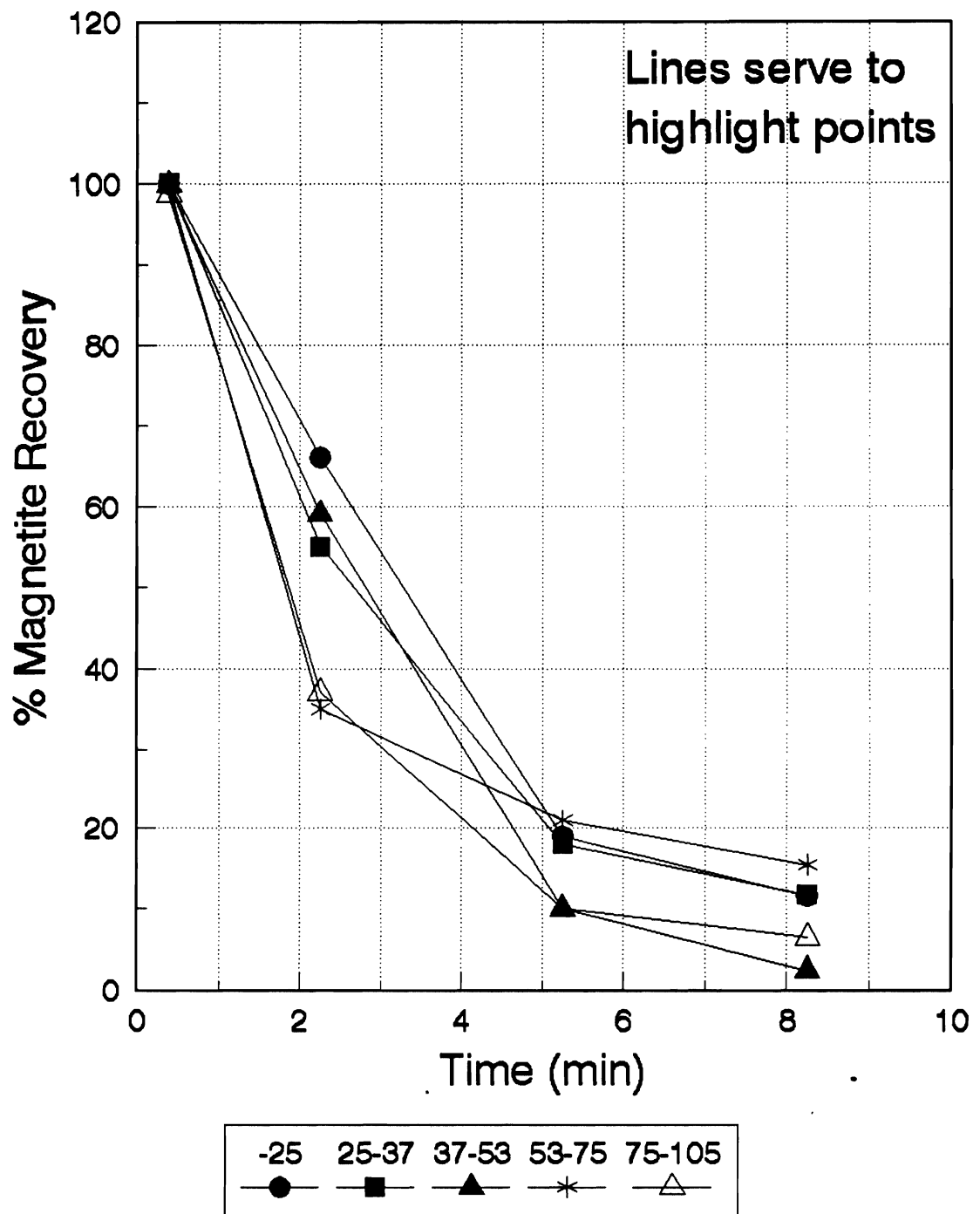
Figure 5.6 Incremental Recovery vs. Time
for the First Overload Test

Feed: 20% solids, 20 l/min, 32 kg
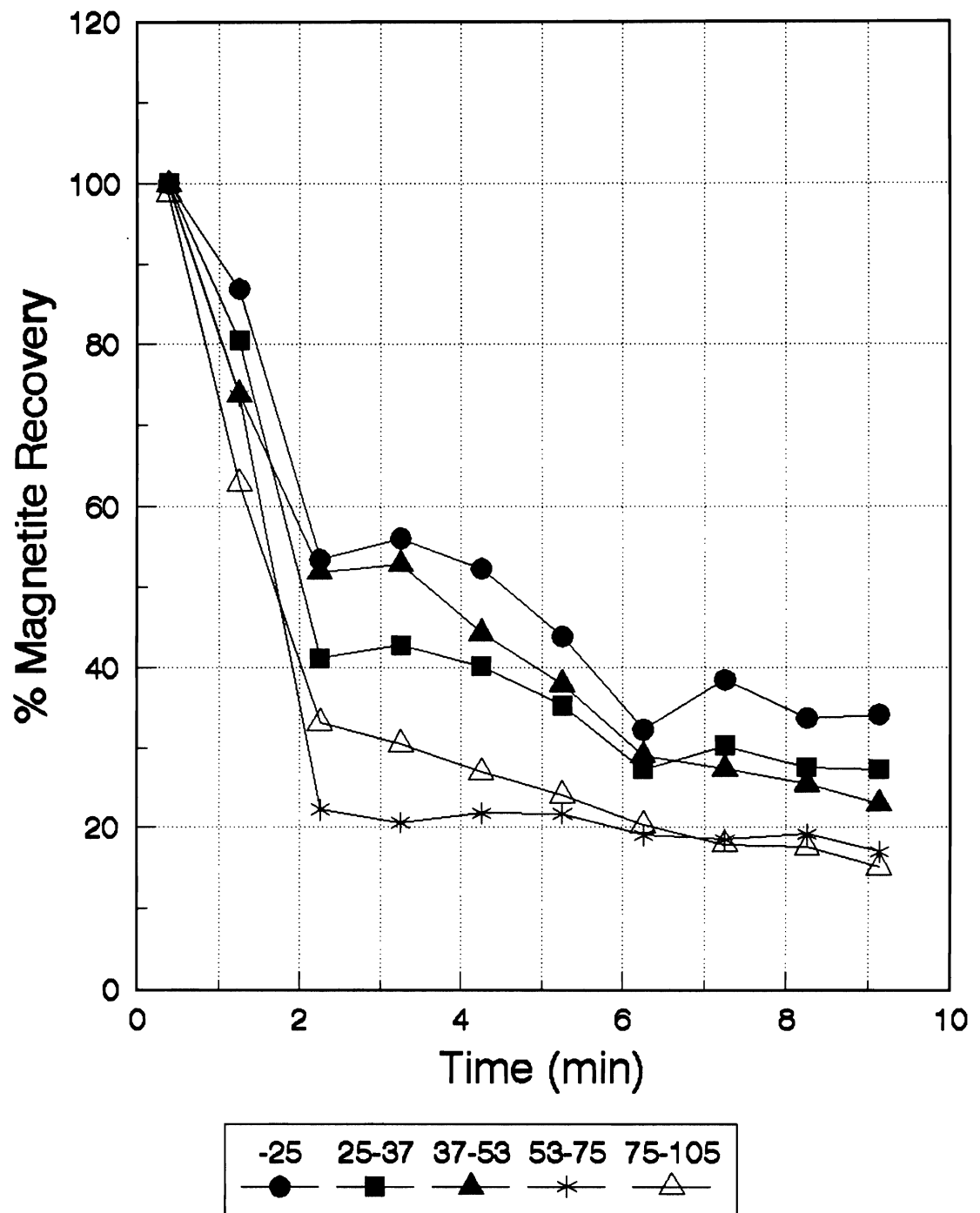
Figure 5.7 Cumulative Recovery vs. Time
for the First Overload Test
Feed: 20 % solids, 20 l/min, 32 kg
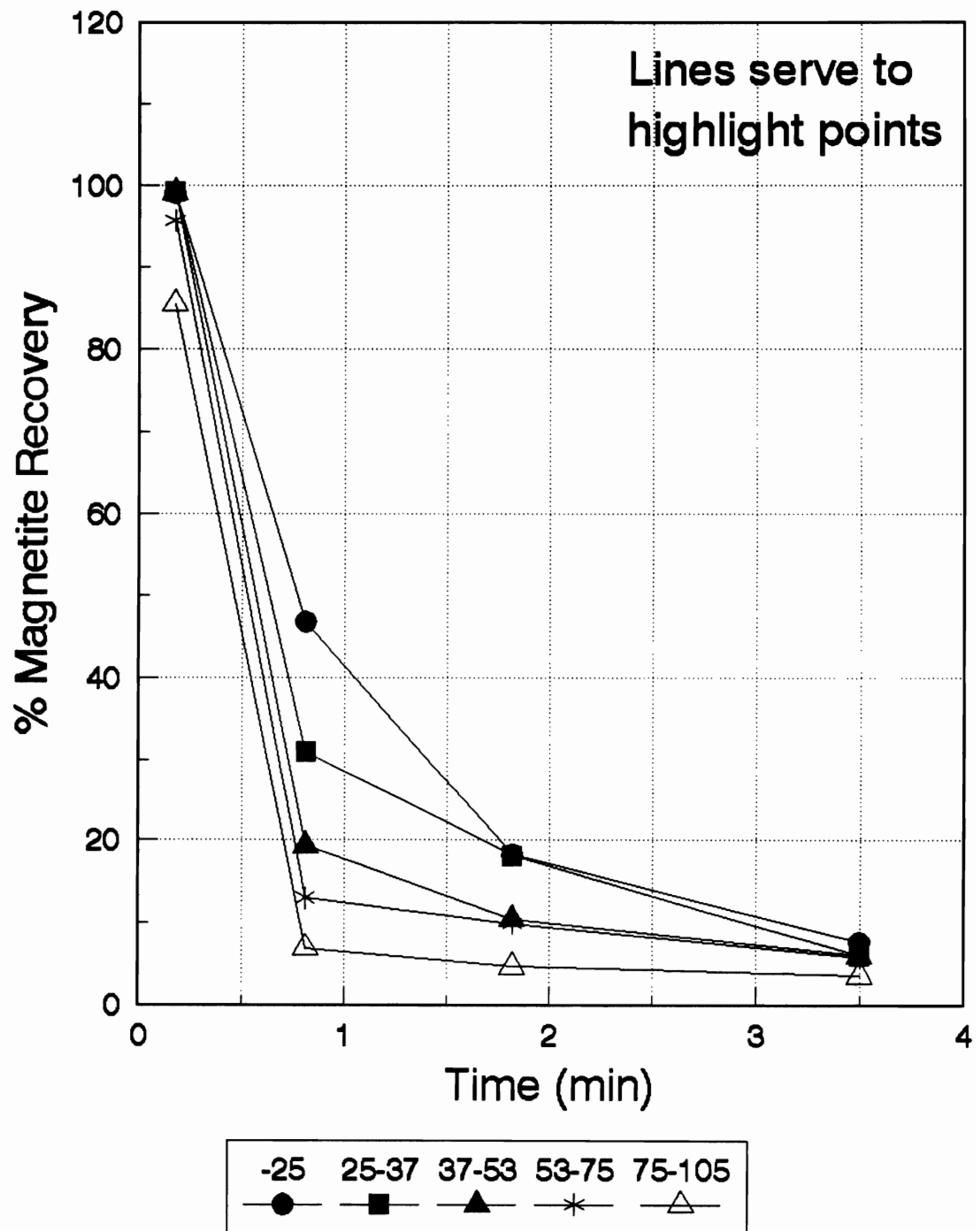
Figure 5.8 Incremental Recovery vs. Time
for the Second Overload Test
Feed: 20% solids, 30 l/min, 32 kg
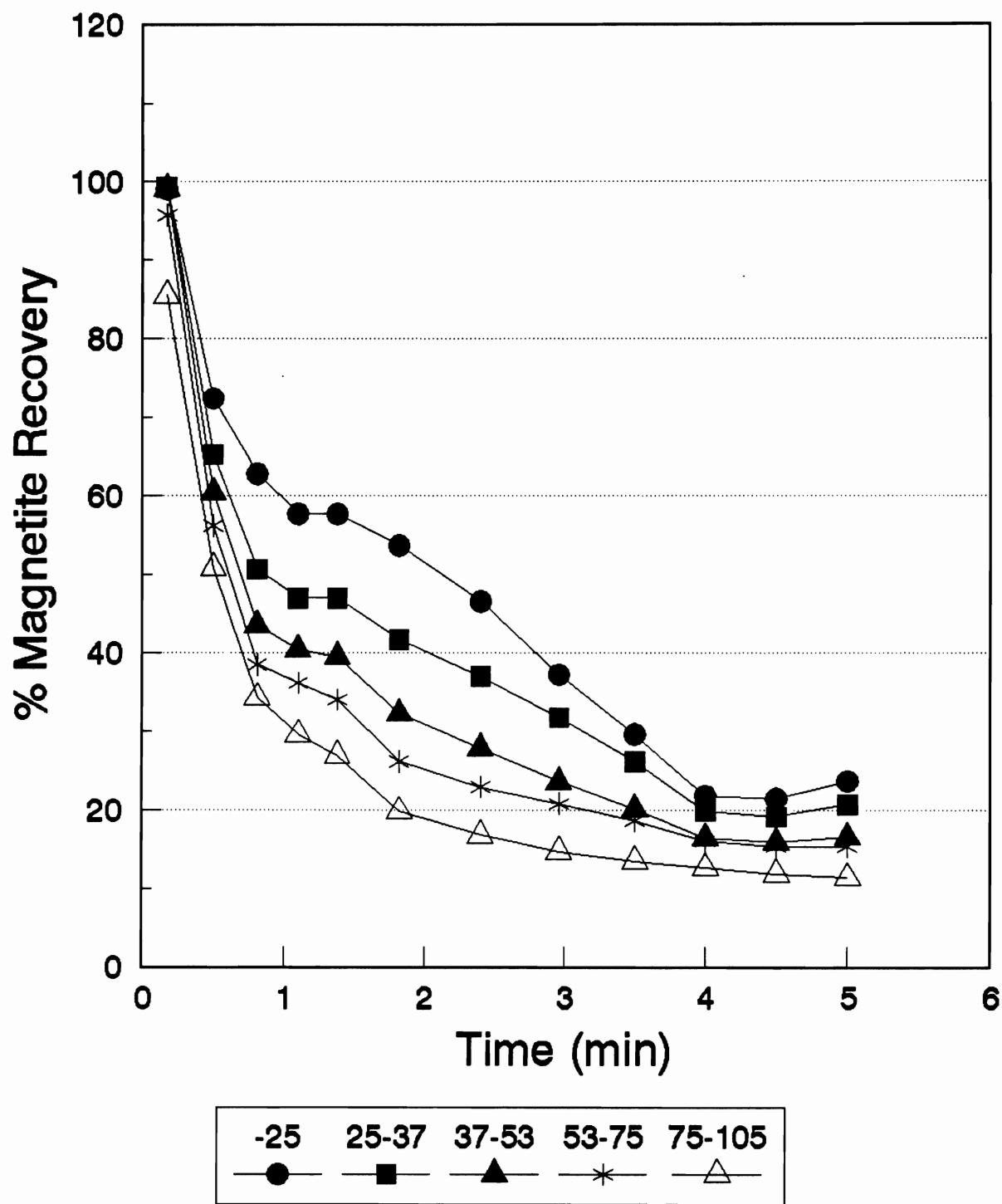
Figure 5.9 Cumulative Recovery vs. Time
for Second Overload Test
Feed: 20% solids, 30 l/min, 32 kg

apparent, which confirms the above results, but the more importantly, recoveries are lower. Two factors may account for this. First, because this test was performed at a higher flowrate. Second, this test was performed with more feed, more magnetite, and thus for a constant bed loading, more magnetite will be lost. The cumulative recovery shows the same particle size effects: recovery increases with decreasing particle size down to -25 μm.

5.6 Multi-Pass Separation with the Falcon Concentrator

When a certain mineral product, such as iron ore, has to be prepared to a certain market specification using separation processes of only moderate efficiency then single-pass separations are not adequate. Quite often a number of re-treatment steps and recirculation of different product streams are required to achieve the desired end product. For example, the Iron Ore Company of Canada uses three stages (roughers/ cleaners/ recleaners) of spiral separation to achieve a final iron concentrate grading 4% SiO_2 or less. The cleaner and recleaner tails are continuously recirculated to the roughers to minimize fines losses.

The purpose of this section is to present the results of a multi-pass test performed with a sample of prepared silica/magnetite material to determine how the FC would behave in a staged separation. Unlike the IOC example, the purpose the multi-stage separation will be to investigate recovery mechanisms and to determine if particles not recovered in a first pass are less recoverable, were not recovered because of the random nature of the recovery process, or were not recovered because of bed overloading.

In the first case, recovery for a second pass should be lower than the first. For the second case it should be equal, and for the case of overloading it should be higher.

5.6.1 Experimental Procedure

A 20 kg sample of the prepared silica/magnetite feed ($P_{80, silica}$ = 212 μm) was processed with the FC at a flowrate of 20 l/min and feed density of 20 % solids. The following additional points are included in the procedure:

1) The concentrate was removed from the unit after each stage.

2) The FC tails were reprocessed two additional times, and size-by-size magnetite recoveries were calculated for each stage from 600 to 25 μm (30 to 600 mesh). The individual stage and cumulative recoveries were calculated from the amount of magnetite recovered to each stage concentrate and the total amount of magnetite processed. The unprocessed fraction was not used in the calculation.

3) The unprocessed magnetite remaining in the mixing tank was screened, and the proportion of the magnetite that was left unprocessed for each stage was calculated.

5.6.2 Results

Appendix XII presents all the data for the test work.

Figure 5.10 shows the incremental recoveries versus particle size for each cycle. stage. Recovery generally increases with decreasing particle size. Recovery is the highest for the third cycle (there is also a slight increase from the first to the second cycle), an indication that bed saturation is a strong factor in limiting overall particle size.

123
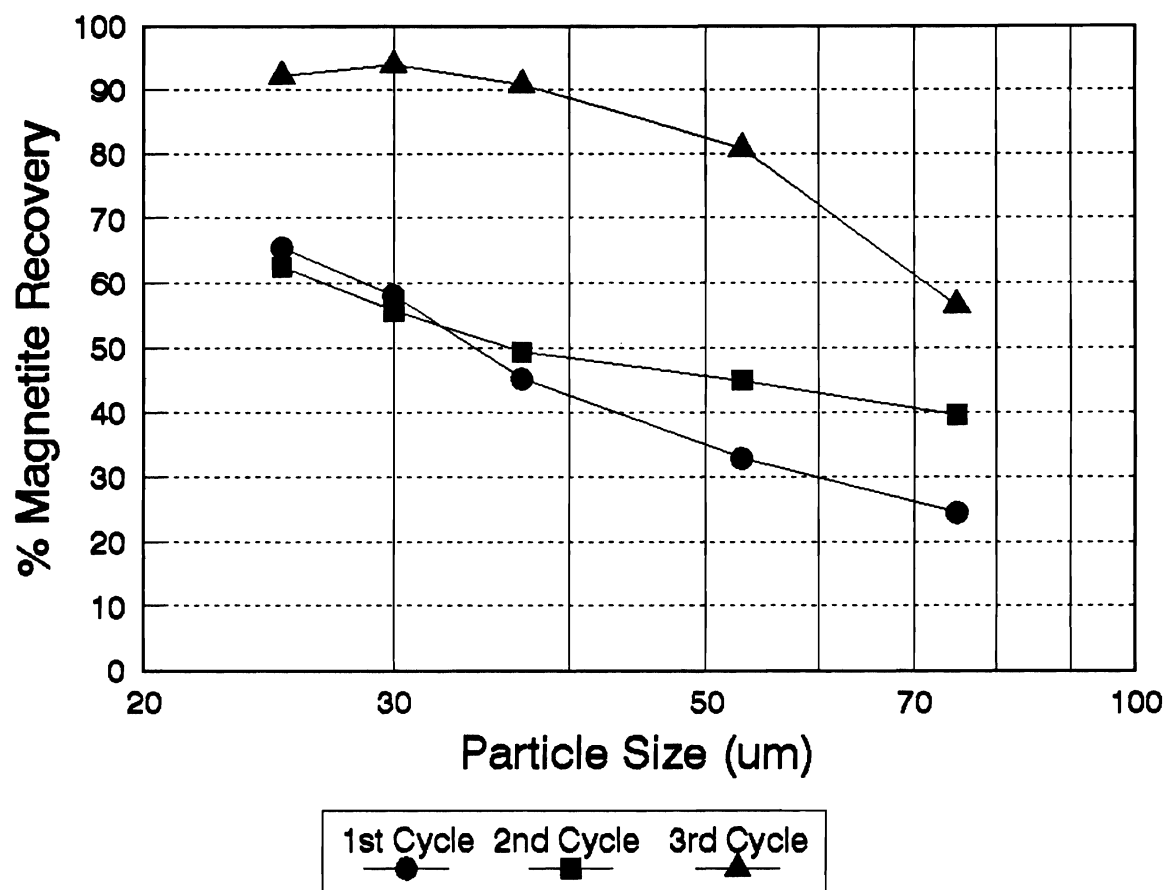
Figure 5.10: Three Cycles of Falcon Processing
Feed: 20% solids, 20 l/min, 20 kg

5.7 An Analogy with Gold Recovery from CIP Circuits

Unlike most gravity separation devices, the FC is a semi-batch unit and the overload component is an important aspect of its metallurgical performance. It is impractical to model its operation from existing gravity separation methods, such as jigging or spirals since they do not overload, as defined in Section 5.5.2. The adsorption of gold onto activated carbon is a phenomenon which exhibits strong overloading characteristics and will be thus used in this section to describe the FC. The use of physico-chemical reaction theory to describe phenomenon which are essentially physical, such as flotation and grinding kinetics, has been successfully used in the past and can thus be readily applied here, with a few simplifying assumptions.

Carrier et al (1991), considered the following first order reaction to describe the rate of gold adsorption:

[Active Site] + [Free Aurocanide] < = > [Adsorbed Aurocyanide]

The rate of adsorption is related to the number of active sites available on the carbon, and the concentration of gold on the carbon and in the solution by the following equation:

$$\frac{dM_{ci}(t)y_i(t)}{dt} = K_a x_i(t)[N - y_i(t)]M_{ci}(t) - K_d y_i(t)M_{ci}(t) + C_{i+1}(t)y_{i+1}(t) - C_i y_i(t) \qquad \textbf{5.1}$$

where x, y are respectively the gold contents in solution and on the carbon; K_a and K_d are adsorption and desorption rate constants, N represents the effective capacity of the carbon for gold (Williams et al, 1985); $M_{ci}(t)$ is the mass of carbon in the CIP tank at a specific time, and C_{i+1} and C_i are the amounts of carbon added or removed from the

tank at stage "i". The adsorption coefficient, K_A, is a lumped parameter whose value is dependent on the physical characteristics of the individual particles, the flowrate of the slurry, and the percent solids in the feed.

Assuming that the rate of mass removal with time is constant (ie. dM/dt=0), that no carbon is added or removed, and that there is a constant number of capture sites available, then equation 5.1 can be simplified further to equation 5.2:

$$\frac{dy_i}{d} = K_a^* x_i [N - y_i] - K_d^* y_i \qquad\qquad \textbf{5.2}$$

From equation 5.1 and several other mass balance considerations, Carrier was able to simulate a complete CIP circuit. The results of the simulations were interesting and have some relevance to operating the FC in a semi-continuous or continuous mode.

For a given amount of gold to be recovered in a selected number of adsorption stages, the carbon inventory in the tanks is a major operating variable. Basically, the higher the inventory, the higher the gold recovery. For high carbon inventory, the gold lock-up in the CIP circuit is higher and thus a larger amount of less loaded carbon will be transferred. For lower inventories, a higher fraction of the carbon has to be transferred to maintain similar recoveries. The implication for the FC is that as for material with low feed grades, the bed turn-over rate can be low and still maintain a high recovery. For a high grade feed, however, the bed turn-over rate should be increased to minimize losses.

Nicol et al (1984) also derived a similar model to describe the CIP process. Their

findings were similar to those of Carrier. In addition, they analyzed the efficiency of each stage, ie. the percentage of gold extracted in each stage, and found it to be constant if the concentration of carbon remained the same. When the stage efficiency decreases as the carbon progresses then this is an indication of a cumulative 'poisoning' effect. The implication for the FC is that for a constant bed mass, the individual stage recoveries in the "normal" or operating region should remain the same. The results of the test work in this section certainly support this claim.

5.8 Conclusions

The main focus of this chapter was to understand how the FC works. An artificial feed consisting of two liberated, easily separable phases was used to perform the test work. A better understanding of the FC was gained, but the effect of flowrate and feed %solids still remains unclear.

For a given bowl type, the most significant parameters affecting FC performance are the density and size distribution of the material, both the feed and the bed. By testing different particle sizes of the silica gangue in the feed and in the bed, it was found that the bed particle size was most significant.

The dynamics of solids bed formation was examined. The results showed that the bed builds up quickly and that recovery occurs predominantly on the surface via capture sites. From the results of the overload test, three recovery stages in the FC loading cycle were suggested:

1) Initial non-selective recovery phase were recovery is very high, but of short duration.

2) Rapid decrease in recovery as bed saturation is approached.

3 Final near-zero recovery as bed reaches saturation point.

For both systems, maximum loading occurs not only because the recovery rate drops dramatically as the number of free capture sites decreases, but also because of removal of captured material by desorption for gold, and by bed erosion for the FC. The maximum mass recovered corresponds to a dynamic equilibrium between the loading and removal rates.

When processing a high-grade material with a semi-continuous or continuous FC, the bed turn-over rate should be high to minimize losses. Conversely, for lower grade material, the bed turn-over rate should be lower.

The results of the multi-pass test confirmed that the the failure to recover all the magnetite in a single pass can be attributed mostly to overloading. As such, then, reprocessing the tails would seem to be an effective method of increasing recovery.

Chapter 6

Conclusions

6.1 Introduction

The work presented in the thesis was both practical and fundamental. Some information on how the FC works was presented, and the test work of two case studies was discussed. This chapter will present some general conclusions about the FC. Next, conclusions about the test work conducted at AELR and at Meston Resources will be discussed, and finally suggestions for future work (general, AELR, Meston Resources) will be outlined.

6.1.1 General Conclusions about the Falcon

The batch Falcon is essentially a rotating bowl in which a slurry is fed from a central well. Initially, a bed of feed is recovered, unselectively, on the walls of the bowl. After the bed rapidly reaches a steady state, material is then selectively recovered on the surface of the bed via capture sites. The actual concentrate bed is thus covered by a layer of feed particles that saltate their way out of the recovery zone. After a certain time the capture sites become saturated and no further recovery is possible. Slight erosion of the bed may occur by the incoming slurry, leading to erratic performance.

Particles report to the bed in two different ways: i) Coarse particles are captured because they can burry themselves in the concentrate bed, and ii) Finer particles are captured when they lodge between the interstices created by the coarser particles on the surface of the bed. The recovery of mid-size particles (53 to 150 μm) is poorer ($<$ 50%) than that of fine particles ($<$ 53 μm, 70%+) because it is more dependent on the

bed topology. As the size of the surface particles increase, recovery increases, because of the larger volume of the capture sites. As the volume of the capture sites increases, concentrate grade may be decrease because gangue particles may also be more readily recovered.

Bowl geometry is separation specific. The 8 and 10° bowls are better units to recover heavy minerals (5-7 g/cm^3), whereas the 14° bowl is designed to recover gold from lighter minerals (2.6-5 g/cm^3).

6.1.2 Conclusions about Agnico-Eagle, Division Laronde (AELR) Test Work

Contrary to the KC, the FC is not a particularly effective cleaning device. It does not operate by the same mechanism as the KC, and the effective range of particle size for which it produces the best results is finer and much narrower (about 15 to 37 μm vs. 37 to 600 μm for the KC). The preferential accumulation of free gold over the size range 53 to 150 μm in regrind mill discharges and secondary cyclone underflows makes the KC a suitable unit for the production of a smeltable gravity concentrate. The FC does not perform as well for this sort of application for several reasons. First, a very significant fraction of the concentrate is recovered in a non-selective manner at the beginning of each test which dilutes the product and thus leads to poor upgrading. Second, the unit overloads rapidly above feed masses greater than 20 kg (for AELR) and therefore is of very limited capacity. This is probably because of the high sulphide content of the AELR ore. Third, the design of the unit (rotor speed and geometry) is such that it cannot effectively recover the gold in the size ranges 53 to 150 μm. Thus,

several passes of the concentrate would be required (5+) to produce a smeltable concentrate, several tails reprocessing stages would be required to maximize gold recovery, and perhaps the unit would have to be redesigned to operate effectively in the right size range (slowing down the rotor, changing the bowl angle, etc.). Certainly there is some flexibility with regards to the operating variables (% solids, feed flowrate), but not enough to improve performance significantly. Generally, for a constant mass processed, recovery increases with flowrate, up to 20 and in some cases 30 l/min. The effect of density is unclear, but all tests showed poor recoveries at low feed rates and densities (10 l/min, 10% solids). Practically, the feed density is difficult to control and thus flowrate is really the sole operating variable.

6.1.3 Conclusions about Meston Resources Test Work

The batch FC is basically a scavenging device used for the recovery of fine (15-37 μm) heavy particles from a much lighter gangue (such as silica), such as encountered in flotation feeds, concentrates and tails. The unit has already demonstrated its effectiveness in recovering very fine gold-bearing pyrite and gold particles from a fine fraction of a flotation tail. The FC concentrate was not particularly upgraded, but its high pulp density and relatively low flow makes it an ideal feed for down-stream cyanidation. The KC had also been tested for this application but could not produce acceptable recoveries.

Gold recovery was higher than sulphur's; there was some evidence that recovery was better with the 10° bowl at the higher flowrate. Data for the 8 and 10° bowl were

regressed to correlate recovery with the operating parameters: bowl angle, feed density, dry feed rate and flowrate. None were found significant for sulphur, but a regression was obtained for gold which related recovery to bowl angle and feed flowrate to predict the performance of the batch FC.

6.2 Future Work and Recommendations

6.2.1 General Recommendations

The lab unit is batch, and its behavior changes markedly with mass processed. For the B6, efficiency drops sharply after about 20 kg of feed has been processed (as observed with AELR ore and the sythetic feed). To alleviate the problem, Falcon Concentrators, when testing material, has often taken the approach of reprocessing a feed up to five times to insure good recoveries. This procedure is probably warranted when attempting to simulate the performance of the continuous unit, which does not experience overload. However, there are little data available on the performance of the continuous unit, and this procedure remains to be validated.

Predicting the performance of a full scale FC (ie. B30) from a lab unit (B6) is also a procedure that has yet to be validated. However, the scale-up ratio is less than that of a KC (a diameter ratio of 5 rather than 12 for the KC), which should make scale-up easier. Again, little or no scale-up data are available yet, and these are required.

Perhaps one of the major drawbacks of the FC is that a significant fraction of the concentrate mass is recovered in a non-selective manner. Perhaps the problem can be corrected by artificially forming a bed with easily separated particles, such as magnetite.

133

Alternatively, a bed of particles coarser than the actual feed can be created and then easily removed by screening, at the end of the test. Both these approaches have yet to be tested.

The failure to recover all particles in a single stage is attributed to the random nature of the recovery process. The probability of capture is a function of feed characteristics, which is fixed; bowl profile, which can be varied somewhat; flowrate and % solids, which can more easily be manipulated; and rotor speed, which can be varied with some adjustments made to the driving system of the unit. Future work should certainly consider experimenting with the rotor speed to determine to determine its effect on recovery.

The unit is scavenging device suitable for the recovery of fine, heavy particles. Future work should include the search for more applications for the FC where this sort of recovery is targeted.

6.2.2 Recommendations for AELR

The Falcon is clearly not suitable for the application required and other types of separators should be tested. For instance, the KC has proven effective in this sort of application and should certainly be tested. It is of course not without its own problems. For instance, once a KC is installed and gold is progressively recovered, its circulating load will dramatically decrease and the feed to the KC will change and perhaps be less responsive to gravity recovery. Perhaps this behavior may be studied by processing a sample of this material with a laboratory KC and then reprocessing the tails several times

to determine how gold recovery behaves as less gold gold becomes available in the feed. Second, the KC is of limited capacity, which means that only a small fraction of the circulating load would be processed.

The Kelsey Jig is another centrifugal separator which has yet to be tested. At It is a continuous type separator and may eliminate the problem of the limited capacity of the KC.

6.2.3 Recommendations for Meston Resources

Although the FC can recover a significant portion of the gold from the fine flotation tails at Meston Resources, there are other in-house alternatives which should be considered as well:

1) The backfill circuit configuration and the deslimer cyclone geometry should be investigated to determine if more gold cannot be classified into the coarse product (which has already been tested).

2) The gravity circuit should be reinvestigated to determine if additional gold can be recovered upstream.

3) A mineralogical investigation of the scavenger tails should be considered to determine the performance of the scavengers. Perhaps they are operating too selectively and releasing a considerable amount of flotable gold to tails.

4) A regression was developed to predict the performance of the batch FC. Since a continuous FC may be preferable for this application then its performance should also be estimated. One approach is to retreat the tails several times with

135

a batch unit, as was demonstrated in this thesis, to simulate continuous operation. This method has not been confirmed with a continuous FC and should be further investigated.

Appendix I: Metallurgical Balance of Knelson Tests for AELR

BMD1		KC	Conc			KC	Tail			KC	Feed		
	Sample	Mass:	6377										
Size	Mass	Mass	Grad	Rec	Mass	Total	Grade	Rec	Mass	Mass	Grade	Dist
(um)	(%)	(g)	(g/t)	(%)	(%)	Mass	(g/t)	(%)	(%)	(g)	(g/t)	(%)
425	22.67	23.70	110	60.51	7.07	443	3.84	39.49	7.33	467	9.23	3.92
300	11.08	11.58	110	42.68	7.11	446	3.84	57.32	7.18	458	6.53	2.71
212	12.21	12.76	110	39.83	8.81	553	3.84	60.17	8.87	565	6.24	3.20
150	15.55	16.26	110	34.71	13.98	877	3.84	65.28	14.00	893	6.71	4.68
106	12.85	13.43	352	54.43	16.56	1038	3.81	45.57	16.49	1052	8.25	7.89
75	13.85	14.48	675	44.54	21.76	1365	8.92	55.46	21.63	1379	15.92	19.95
53	7.55	7.89	1560	50.64	11.92	748	16.05	49.36	11.85	755	32.18	22.09
38	2.23	2.33	3864	45.85	4.07	255	41.66	54.15	4.04	257	76.27	17.84
-38	2.01	2.10	3449	37.18	8.73	548	22.35	62.82	8.62	550	35.44	17.70
Totals	100.00	104.53	480	45.56	100.00	6272	9.55	54.44	100.00	6377	17.26	100.00

BMD2		KC	Conc			KC	Tail			KC	Feed		
	Sample	Mass:	7036										
Size	Mass	Mass	Grad	Rec	Mass	Total	Grade	Rec	Mass	Mass	Grade	Dist
(um)	(%)	(g)	(g/t)	(%)	(%)	Mass	(g/t)	(%)	(%)	(g)	(g/t)	(%)
425	36.03	17.74	466	44.52	7.66	535	19.27	55.48	7.86	553	33.62	10.03
300	13.85	6.82	466	22.12	8.32	581	19.27	77.88	8.36	588	24.45	7.76
212	12.93	6.37	466	14.07	13.47	941	19.27	85.93	13.47	947	22.27	11.39
150	62.80	7.79	466	13.97	16.61	1160	19.27	86.03	16.60	1168	22.25	14.03
106	9.77	4.81	2404	51.17	17.31	1209	9.12	48.83	17.26	1214	18.61	12.18
75	5.30	2.61	4667	51.79	14.42	1008	11.25	48.21	14.36	1010	23.28	12.68
53	3.03	1.49	7126	50.48	8.99	628	16.59	49.53	8.95	630	33.41	11.34
38	1.81	0.89	6510	35.26	5:51	385	27.61	64.76	5.49	386	42.55	8.86
-38	1.48	0.73	8144	27.17	7.70	538	29.62	72.85	7.66	539	40.62	11.79
Totals	100.00	49.25	1303	34.58	100.00	6987	17.37	65.42	100.00	7036	26.37	100.00

Tables I1 and I2: Primary Ball Mill Discharge

SC1	KC	Conc			KC	Tail			KC	Feed		
Size	Sample	Mass:	6382									
Size	Mass	Mass	Grad	Rec	Mass	Total	Grade	Rec	Mass	Mass	Grade	Dist
(um)	(%)	(g)	(g/t)	(%)	(%)	Mass	(g/t)	(%)	(%)	(g)	(g/t)	(%)
425	23.34	33.72	459	68.46	12.82	800	8.92	31.54	13.06	833	27.14	11.62
300	12.56	18.14	459	57.41	11.11	693	8.92	42.59	11.14	711	20.41	7.46
212	16.39	23.68	459	58.96	13.60	848	8.92	41.04	13.66	872	21.15	9.47
150	15.97	23.07	459	48.98	19.83	1237	8.92	51.02	19.74	1260	17.16	11.11
106	14.16	20.45	821	64.35	16.10	1004	9.26	35.65	16.06	1025	25.46	13.40
75	9.28	13.41	1287	57.82	11.96	746	16.87	42.18	11.90	760	39.29	15.33
53	4.71	6.81	1493	39.43	6.56	409	38.13	60.57	6.52	416	61.92	13.25
38	2.13	3.08	1409	23.60	2.84	177	79.40	76.40	2.82	180	102.14	9.45
-38	1.45	2.10	591	7.15	5.16	322	49.96	92.85	5.08	324	53.46	8.91
Total	100.00	144.46	658	48.84	100.00	6238	15.96	51.16	100.00	6382	30.50	100.00

SC2	KC	Conc			KC	Tail			KC	Feed		
Size	Sample	Mass:	2205									
Size	Mass	Mass	Grad	Rec	Mass	Total	Grade	Rec	Mass	Mass	Grade	Dist
(um)	(%)	(g)	(g/t)	(%)	(%)	Mass	(g/t)	(%)	(%)	(g)	(g/t)	(%)
425	26.44	35.96	110	64.74	10.52	218	9.94	35.26	11.50	254	24.19	6.94
300	11.44	15.56	110	49.49	8.53	176	9.94	50.51	8.71	192	18.08	3.93
212	12.51	17.01	110	42.39	12.42	257	9.94	57.61	12.43	274	16.18	5.01
150	16.23	22.07	110	46.21	13.80	286	9.94	53.79	13.95	308	17.15	5.97
106	12.57	17.09	272	63.51	14.57	301	8.85	36.49	14.44	319	22.95	8.26
75	10.79	14.67	368	65.67	12.43	257	10.97	34.33	12.33	272	30.23	9.29
53	5.80	7.89	462	58.17	7.22	149	17.55	41.83	7.13	157	39.85	7.08
38	2.05	2.79	527	41.33	4.12	85	24.48	58.67	3.99	88.06	40.40	4.02
-38	2.18	2.96	414	2.80	16.38	339	125.56	97.20	15.51	342	128.05	49.50
Totals	100.00	136.00	194	29.83	100.00	2069	30.00	70.17	100.00	2205	40.11	100.00

Tables I3 and I4: Sluice Concentrates

ST1	KC	Conc			KC	Tail			KC	Feed		
	Sample	Mass:	5677									
Size	Mass	Mass	Grade	Rec	Mass	Total	Grade	Rec	Mass	Mass	Grade	Dist
(um)	(%)	(g)	(g/t)	(%)	(%)	Mass	(g/t)	(%)	(%)	(g)	(g/t)	(%)
425	18.28	17.10	72.46	51.96	5.53	309	3.71	4.80	5.74	326	7.32	2.98
300	13.80	12.91	72.46	40.19	6.72	375	3.71	59.81	6.84	388	6.00	2.91
212	15.98	14.95	72.46	38.23	8.45	472	3.71	61.77	8.57	487	5.82	3.55
150	13.09	12.24	72.46	24.29	13.35	745	3.71	75.71	13.35	758	4.82	4.57
106	13.03	12.19	363	54.96	16.34	912	3.98	45.04	16.28	924	8.72	10.09
75	12.73	11.91	803	59.03	21.38	1194	5.56	40.97	21.24	1206	13.44	20.28
53	7.84	7.33	1623	49.46	12.70	709	17.14	50.54	12.62	717	33.57	30.11
38	3.16	2.96	1440	41.05	4.68	261	23.42	58.95	4.66	264	39.28	13.00
-38	2.08	1.95	12.64	0.25	10.84	606	16.46	99.75	10.70	607	16.45	12.51
Total	100.00	93.54	367	42.96	100.00	5583	8.16	57.04	100.00	5677	14.07	100.00

ST2	KC	Conc			KC	Tail			KC	Feed		
	Sample	Mass:	6687									
Size	Mass	Mass	Grade	Rec	Mass	Total	Grade	Rec	Mass	Mass	Grade	Dist
(um)	(%)	(g)	(g/t)	(%)	(%)	Mass	(g/t)	(%)	(%)	(g)	(g/t)	(%)
425	19.00	17.97	245	56.42	6.17	407	8.37	43.58	6.35	425	18.39	3.18
300	12.83	12.13	245	44.97	6.60	435	8.37	55.03	6.69	447	14.80	2.70
212	14.59	13.80	245	36.90	10.49	692	8.37	63.10	10.55	705	13.00	3.74
150	19.22	18.18	245	31.82	17.31	1141	8.37	68.18	17.34	1159	12.08	5.71
106	13.47	12.74	1454	37.60	16.80	1108	27.77	62.40	16.75	1120	43.99	20.09
75	9.87	9.33	1707	41.70	16.52	1089	20.44	58.30	16.43	1098	34.76	15.56
53	5.53	5.23	1098	14.02	9.89	652	54.03	85.98	9.83	657	62.34	16.70
38	2.36	2.23	2420	17.20	4.87	321	80.89	82.80	4.83	323	97.02	12.78
-38	3.13	2.96	1195	7.38	11.34	748	59.38	92.62	11.23	751	63.86	19.54
Totals	100.00	94.57	681	26.23	100.00	6592	27.46	73.77	100.00	6687	36.69	100.00

Tables I5 and I6: Sluice Tails

SCOF1		KC	Conc			KC	Tail			KC	Feed	
	Sample	Mass:	2582									
Size	Mass	Mass	Grade	Rec	Mass	Total	Grade	Rec	Mass	Mass	Grade	Dist
(um)	(%)	(g)	(g/t)	(%)	(%)	Mass	(g/t)	(%)	(%)	(g)	(g/t)	(%)
425	0.97	0.91	24.14	53.68	0.19	4.73	4.02	46.32	0.22	5.64	7.27	0.04
300	1.04	0.98	24.14	30.82	0.53	13.19	4.02	69.18	0.55	14.16	5.41	0.07
212	2.78	2.61	24.14	31.70	1.36	33.83	4.02	68.30	1.41	36.45	5.46	0.19
150	4.72	4.44	24.14	21.09	4.01	99.76	4.02	78.91	4.04	104	4.88	0.47
106	9.65	9.07	95.04	50.42	6.91	172	4.93	49.58	7.01	181	4.93	1.60
75	16.83	15.82	148	38.24	15.09	375	10.08	61.76	15.15	391	10.08	5.73
53	21.78	20.48	220	44.53	20.20	502	11.18	55.47	20.25	523	11.18	9.47
38	15.90	14.95	309	50.05	12.19	303	15.22	49.95	12.32	318	15.22	8.64
-38	26.33	24.79	191	5.98	39.52	983	75.83	94.02	39.04	1008	78.67	74.17
Totals	100.00	94.05	184	16.17	100.00	2488	36.19	83.89	100.00	2582	41.57	100.00

SCOF2		KC	Conc			KC	Tail			KC	Feed	
	Sample	Mass:	2540									
Size	Mass	Mass	Grade	Rec	Mass	Total	Grade	Rec	Mass	Mass	Grade	Dist
(um)	(%)	(g)	(g/t)	(%)	(%)	Mass	(g/t)	(%)	(%)	(g)	(g/t)	(%)
425	0.00	0.00	38.40	0.00	0.00	0.00	5.09	0.00	0.00	0.00	0.00	0.00
300	0.00	0.00	38.40	0.00	0.39	9.52	5.09	100.00	0.37	9.52	5.09	0.08
212	0.00	0.00	38.40	0.00	1.07	26.12	5.09	100.00	1.03	26.12	5.09	0.21
150	9.92	9.79	38.40	49.08	3.14	76.66	5.09	50.92	3.40	86.45	8.86	1.21
106	9.98	9.85	95.86	48.08	5.79	141	7.21	51.92	5.95	151	12.98	3.10
75	16.57	16.36	127	55.91	12.22	298	5.49	44.09	12.39	315	11.80	5.86
53	20.78	20.52	179	43.41	18.68	456	10.50	56.59	18.77	477	17.76	13.35
38	15.09	14.90	266	48.59	12.52	306	13.71	51.41	12.62	321	25.43	12.86
-38	27.66	27.31	149	10.11	46.18	1127	23.04	89.89	17.37	1155	28.11	63.33
Totals	100.00	98.73	153	23.80	100.00	2441	19.79	76.20	100.00	2540	24.96	100.00

Tables I7 and I8: Secondary Cyclone Overflows

141

CF1	Sample Mass (%)	KC Mass (g)	Conc Grade (g/t)	Rec (%)	KC Tail Mass (%)	Total Mass	Grade (g/t)	Rec (%)	KC Feed Mass (%)	Mass (g)	Grade (g/t)	Dist (%)
		Mass:	4706									
425	16.45	20.80	63.41	58.27	7.34	336	2.81	41.73	7.58	357	6.34	2.27
300	9.52	12.04	63.41	48.69	6.25	286	2.81	51.31	6.34	298	5.26	1.57
212	12.27	15.51	63.41	47.44	8.47	388	2.81	52.56	8.57	403	5.14	2.08
150	12.10	15.30	63.41	36.26	13.25	607	2.81	63.74	13.22	622	4.30	2.68
106	14.40	18.21	208	25.99	15.48	709	15.22	74.01	15.45	727	20.05	14.63
75	16.39	20.72	335	45.70	20.86	956	8.64	54.34	20.74	976	15.57	15.26
53	10.86	13.73	835	49.29	13.23	606	19.48	50.71	13.16	620	37.56	23.35
38	4.50	5.69	1972	61.31	4.17	191	37.06	38.70	4.18	197	93.00	18.37
-38	3.52	4.45	1219	27.52	10.93	501	28.53	72.50	10.73	505	39.02	19.78
Totals	100.00	126.43	339	43.05	100.00	4580	12.39	56.98	100.00	4706	21.17	100.00

CF2	Sample Mass (%)	KC Mass (g)	Conc Grade (g/t)	Rec (%)	KC Tail Mass (%)	Total Mass	Grade (g/t)	Rec (%)	KC Feed Mass (%)	Mass (g)	Grade (g/t)	Dist (%)
		Mass:	4295									
425	19.67	26.70	179	44.14	8.31	346	17.51	55.86	8.67	372	29.10	8.99
300	9.63	13.07	179	28.64	8.01	333	17.51	71.36	8.06	346	23.61	6.78
212	11.25	15.27	179	25.89	10.75	447	17.51	74.11	10.77	462	22.85	8.77
150	16.16	21.93	179	23.59	17.47	727	17.51	76.41	17.43	748	22.25	13.82
106	13.94	18.92	379	40.93	16.66	693	14.95	59.07	16.57	712	10.40	14.55
75	12.88	17.48	542	51.54	15.42	641	13.89	48.46	15.34	659	14.67	15.26
53	7.96	10.81	621	49.17	9.66	402	17.28	50.83	9.61	413	17.00	11.34
38	3.54	4.81	1122	58.05	3.87	161	24.25	41.95	3.86	166	36.13	7.72
-38	4.96	6.73	709	31.02	9.84	409	25.92	68.98	9.69	416	13.08	12.76
Totals	100.00	135.72	349	39.27	100.00	4159	17.59	60.72	100.00	4294	28.06	100.00

Tables I9 and I10: Primary Cyclone Feeds

142

PCUF1		KC	Conc			KC	Tail			KC	Feed	
	Sample	Mass:	8236									
Size	Mass	Mass	Grade	Rec	Mass	Total	Grade	Rec	Mass	Mass	Grade	Dist
(um)	(%)	(g)	(g/t)	(%)	(%)	Mass	(g/t)	(%)	(%)	(g)	(g/t)	(%)
425	20.93	25.88	156	67.92	10.06	816	2.33	32.08	10.22	842	7.04	2.88
300	12.44	15.38	156	58.09	9.13	741	2.33	41.91	9.18	756	5.45	2.00
212	14.66	18.13	156	59.32	10.23	830	2.33	40.68	10.30	848	5.60	2.31
150	12.88	15.93	156	48.13	14.12	1145	2.33	51.87	14.10	1161	4.43	2.50
106	14.26	17.64	408	16.76	16.39	1329	26.90	83.24	16.35	1347	31.89	20.88
75	14.81	18.31	785	40.39	21.27	1725	12.30	59.61	21.17	1744	20.42	17.30
53	7.34	9.08	2236	47.37	11.73	952	23.70	52.63	11.67	961	44.60	20.84
38	1.80	2.23	8905	52.45	2.76	224	80.48	47.55	2.74	226	168	18.40
-38	0.87	1.08	8284	33.76	4.32	350	50.13	66.24	4.27	351	75.45	12.88
Totals	100	124	666	40.05	100	8112	15.20	59.95	100	8236	24.98	100

PCUF2		KC	Conc			KC	Tail			KC	Feed	
	Sample	Mass:	7024									
Size	Mass	Mass	Grade	Rec	Mass	Total	Grade	Rec	Mass	Mass	Grade	Dist
(um)	(%)	(g)	(g/t)	(%)	(%)	Mass	(g/t)	(%)	(%)	(g)	(g/t)	(%)
425	21.39	28.52	410	63.01	9.25	637	10.77	36.99	9.48	666	27.87	9.21
300	12.41	16.55	410	49.01	9.51	655	10.77	50.99	9.57	672	20.60	6.87
212	14.18	18.90	410	40.81	15.15	1044	10.77	59.19	15.13	1063	17.87	9.43
150	19.04	25.38	410	44.07	17.80	1227	10.77	55.93	17.82	1252	18.86	11.73
106	14.26	19.01	817	52.90	18.19	1253	11.04	47.10	18.11	1272	23.09	14.58
75	10.54	14.05	1249	53.72	13.91	959	15.77	46.28	13.85	973	33.58	16.22
53	5.10	6.80	2018	47.34	7.65	527	28.94	52.66	7.60	534	54.26	14.39
38	1.75	2.33	2583	32.49	4.10	282	44.32	67.51	4.05	285	65.11	9.20
-38	1.34	1.79	2342	24.87	4.45	306	41.34	75.13	4.39	308	54.70	8.37
Totals	100	133	702	46.50	100	6891	15.64	53.51	100	7024	28.67	100

Tables I11 and I12: Primary Cyclone Underflows

143

PCOF Size (um)	KC Conc Sample Mass (%)	Mass (g)	Conc 2546 Grade (g/t)	Rec (%)	KC Tail Mass (%)	Total Mass	Grade (g/t)	Rec (%)	KC Feed Mass (%)	Mass (g)	Grade (g/t)	Dist (%)
425	1.08	0.92	6.18	8.93	0.24	5.91	9.81	91.07	0.27	6.83	9.32	0.11
300	2.28	1.93	6.18	6.17	0.75	18.46	9.81	93.83	0.80	20.39	9.47	0.35
212	5.30	4.48	6.18	3.37	3.29	80.98	9.81	96.63	3.36	85.46	9.62	1.47
150	12.78	10.80	6.18	3.51	7.60	187	9.81	96.49	7.77	198	9.61	3.41
106	17.36	14.67	14.95	7.39	8.40	207	13.30	92.61	8.70	221	13.41	5.32
75	21.88	18.49	22.49	9.37	11.44	282	14.29	90.63	11.78	300	14.80	7.96
53	23.28	19.68	51.98	11.23	14.88	366	22.08	88.77	15.16	386	23.60	16.34
38	11.86	10.02	116	13.18	9.83	242	31.54	86.82	9.89	252	34.88	15.76
-38	4.18	3.53	317	4.09	43.58	1073	24.47	95.91	42.28	1076	25.43	49.09
Totals	100.00	84.52	47.89	7.26	100.00	2461	20.96	92.57	100.00	2546	21.86	100.00

Table I13: Primary Cyclone Overflow

RMD		KC	Conc			KC	Tail			KC	Feed	
	Sample	Mass:	5177									
Size	Mass	Mass	Grade	Rec	Mass	Total	Grade	Rec	Mass	Mass	Grad	Dist
(um)	(%)	(g)	(g/t)	(%)	(%)	Mass	(g/t)	(%)	(%)	(g)	(g/t)	(%)
425	4.00	4.31	2337	94.93	0.29	14.70	36.62	5.07	0.37	19.01	558	1.26
300	6.88	7.41	2337	93.30	0.67	33.96	36.62	6.70	0.80	41.38	449	2.20
212	14.65	15.79	2337	89.71	2.28	116	36.62	10.29	2.54	131	313	4.88
150	18.84	20.30	5134	86.69	8.61	437	36.62	13.31	8.83	457	263	14.26
106	17.83	19.21	5082	84.40	18.22	923	19.55	15.60	18.21	943	123	13.72
75	18.38	19.80	7887	83.72	29.12	1476	20.58	16.28	28.90	1496	125	22.13
53	12.20	13.14	8983	70.64	21.07	1068	45.94	29.36	20.88	1081	155	19.83
38	4.68	5.04	8753	58.85	7.60	385	80.09	41.15	7.54	390	192	8.90
-38	2.55	2.75	6248	15.89	12.14	615	148	84.11	11.94	618	175	12.82
Totals	100.00	107.76	5583	71.38	100.00	5069	47.60	28.62	100.00	5177	163	100.00

SCUF		KC	Conc			KC	Tail			KC	Feed	
	Sample	Mass:	5660									
Size	Mass	Mass	Grade	Rec	Mass	Total	Grade	Rec	Mass	Mass	Grad	Dist
(um)	(%)	(g)	(g/t)		(%)	Mass	(g/t)	(%)	(%)	(g)	(g/t)	(%)
425	11.73	15.31	1235	77.79	2.04	113	47.85	22.21	2.26	128	190	3.28
300	5.35	6.98	1235	61.38	2.05	113	47.85	38.62	2.13	120	117	1.89
212	6.96	9.08	1235	52.08	3.90	216	47.85	47.92	3.97	225	96	2.90
150	13.19	17.22	1876	53.95	10.42	576	47.85	46.05	10.48	593	101	8.07
106	18.37	23.98	2422	61.43	19.52	1079	33.78	38.57	19.49	1103	86	12.74
75	23.01	30.03	3108	57.59	29.14	1611	42.66	42.41	28.99	1641	99	21.85
53	13.74	17.93	5666	58.22	19.31	1068	68.30	41.78	19.18	1086	161	23.53
38	4.18	5.45	8556	54.45	6.18	342	114.28	45.55	6.13	347	247	11.55
-38	3.48	4.54	6067	26.18	7.46	412	188.36	73.82	7.37	417	252	14.19
Totals	100.00	130.53	3051	53.69	100.00	5529	62.13	46.31	100.00	5660	131	100.00

Tables I14 and I15: Regrind Mill Discharge and Secondary Cyclone Underflow

145

Appendix II: Norbal2 Results of Knelson Tests for AELR

Residual sum of squares: 16.44316

	Stream	Absolute Solids Flowrate	Meas	Pulp Mass Flowrate Calc	S.D.	Adjust
1	BMF1	37.00	37.0	37.0	0.0	0.0
2	BMF2	37.00	37.0	37.0	0.0	0.0
3	BMD1	216.40		216.4		
4	BMD2	221.00		221.0		
5	SLC1	6.80	6.8	6.8	0.8	0.0
6	SLC2	8.50	8.5	8.5	1.0	0.0
7	SLT1	209.60		209.6		
8	SLT2	212.50		212.5		
9	SOF1	9.30	9.3	9.3	4.0	0.0
10	SOF2	6.00	6.0	6.0	4.0	0.0
11	PCF1	218.90	218.9	218.9	100.0	0.0
12	PCF2	218.50		218.5		
13	PUF1	179.40		179.4		
14	PUF2	184.00	184.0	184.0	80.0	0.0
15	PCOF	74.00		74.0		
16	SCUF	105.00	105.0	105.0	100.0	0.0
17	RMDS	105.00	105.0	105.0	100.0	0.0

	Stream	Relative Solids Flowrate
1	BMF1	100.00
2	BMF2	100.00
3	BMD1	584.86
4	BMD2	597.30
5	SLC1	18.38
6	SLC2	22.97
7	SLT1	566.49
8	SLT2	574.32
9	SOF1	25.14
10	SOF2	16.22
11	PCF1	591.62
12	PCF2	590.54
13	PUF1	484.86
14	PUF2	497.30
15	PCOF	200.00
16	SCUF	283.78
17	RMDS	283.78

Assay Data

Au g/t	Meas.	Calc.	Std. Dev.	Adjust.	% Rec
========	=======	=======	===========	=========	=======
BMF1	1.752	1.752	0.088	-0.000	100
BMF2	8.971	8.971	0.449	-0.000	512
BMD1	19.491	19.492	0.975	0.001	6507
BMD2	25.676	25.674	1.284	-0.002	8753
SLC1	30.367	30.377	1.518	0.010	319
SLC2	39.683	39.704	1.984	0.021	521
SLT1	19.140	19.139	0.957	-0.001	6188
SLT2	25.115	25.113	1.256	-0.002	8232
SOF1	42.149	42.123	2.108	-0.026	604
SOF2	25.390	25.384	1.270	-0.006	235
PCF1	20.116	20.115	1.006	-0.001	6793
PCF2	25.123	25.121	1.256	-0.002	8467
PUF1	23.149	23.151	1.158	0.002	6407
PUF2	29.027	29.033	1.451	0.006	8241
PCOF	5.361	5.361	0.268	0.000	612
SCUF	140.540	140.539	7.027	-0.001	%22764
RMDS	140.539	140.540	7.027	0.001	%22764

Cumulative Size Distribution Data

		PCOF					PUF2		
Size	Meas	Calc	SD.	Adj.		Meas	Calc	SD.	Adj.
======	======	======	=====	======	==	======	======	=====	======
150 μm	96.46	96.46	0.5	-0.0		48.05	48.05	0.5	-0.0
106 μm	83.52	83.52	0.5	-0.0		29.92	29.91	0.5	-0.0
75 μm	63.59	63.59	0.5	-0.0		16.02	16.01	0.5	-0.0
53 μm	46.96	46.96	0.5	-0.0		8.41	8.40	0.5	-0.0
38 μm	33.81	33.81	0.5	-0.0		4.34	4.34	0.5	-0.0

		PUF1					BMD2		
Size	Meas	Calc	SD.	Adj.		Meas	Calc	SD.	Adj.
======	======	======	=====	======	==	======	======	=====	======
150 μm	56.25	56.25	0.5	-0.0		53.63	53.63	0.5	0.0
106 μm	39.88	39.87	0.5	-0.0		36.41	36.41	0.5	-0.0
75 μm	18.66	18.65	0.5	-0.0		22.11	22.11	0.5	0.0
53 μm	6.98	6.97	0.5	-0.0		13.17	13.17	0.5	0.0
38 μm	4.22	4.22	0.5	-0.0		7.71	7.72	0.5	0.0

		BMD1					SLT2		
Size	Meas	Calc	SD.	Adj.		Meas	Calc	SD.	Adj.
======	======	======	=====	======	==	======	======	=====	======
150 μm	62.53	62.53	0.5	-0.0		53.64	53.64	0.5	-0.0
106 μm	46.08	46.08	0.5	-0.0		36.30	36.31	0.5	0.0
75 μm	24.52	24.52	0.5	-0.0		21.93	21.93	0.5	0.0
53 μm	12.68	12.68	0.5	0.0		12.92	12.92	0.5	0.0
38 μm	8.67	8.67	0.5	-0.0		7.40	7.40	0.5	0.0

		SLT1					PCF2		
Size	Meas	Calc	SD.	Adj.		Meas	Calc	SD.	Adj.
======	======	======	=====	======	==	======	======	=====	======
150 μm	63.18	63.18	0.5	0.0		54.76	54.76	0.5	0.0
106 μm	46.71	46.72	0.5	0.0		37.74	37.74	0.5	0.0
75 μm	24.84	24.85	0.5	0.0		23.44	23.44	0.5	0.0
53 μm	12.84	12.84	0.5	-0.0		14.17	14.17	0.5	0.0
38 μm	8.78	8.78	0.5	0.0		8.46	8.46	0.5	-0.0

Size	PCF1 Meas	Calc	SD.	Adj.		SLC2 Meas	Calc	SD.	Adj.
150 μm	64.43	64.43	0.5	0.0		53.41	53.41	0.5	-0.0
106 μm	48.37	48.38	0.5	0.0		38.97	38.97	0.5	-0.0
75 μm	26.84	26.84	0.5	0.0		26.63	26.63	0.5	0.0
53 μm	14.50	14.51	0.5	0.0		19.49	19.49	0.5	0.0
38 μm	10.08	10.09	0.5	0.0		15.51	15.51	0.5	-0.0

Size	SLC1 Meas	Calc	SD.	Adj.		SOF2 Meas	Calc	SD.	Adj.
150 μm	42.39	42.39	0.5	0.0		94.50	94.50	0.5	0.0
106 μm	26.33	26.33	0.5	0.0		88.66	88.66	0.5	0.0
75 μm	14.42	14.42	0.5	0.0		77.00	77.00	0.5	0.0
53 μm	7.90	7.90	0.5	0.0		58.52	58.52	0.5	-0.0
38 μm	5.08	5.08	0.5	-0.0		45.75	45.75	0.5	0.0

Size	SOF1 Meas	Calc	SD.	Adj.		SCUF Meas	Calc	SD.	Adj.
150 μm	92.68	92.68	0.5	-0.0		81.08	81.08	0.5	0.0
106 μm	85.83	85.83	0.5	0.0		61.59	61.59	0.5	0.0
75 μm	71.84	71.84	0.5	0.0		32.70	32.70	0.5	-0.0
53 μm	52.05	52.05	0.5	-0.0		13.57	13.56	0.5	-0.0
38 μm	39.46	39.46	0.5	0.0		7.39	7.39	0.5	0.0

Size	RMDS Meas	Calc	SD.	Adj.
150 μm	87.62	87.62	0.5	-0.0
106 μm	69.40	69.40	0.5	-0.0
75 μm	40.37	40.37	0.5	0.0
53 μm	19.42	19.43	0.5	0.0
38 μm	11.92	11.92	0.5	-0.0

Assays of size fractions for BMD1

Au g/t	Meas.	Calc.	Std. Dev.	Adjustment	%Rec
150 μm	6.710	5.771	20.000	-0.939	
106 μm	8.250	17.697	20.000	9.447	
75 μm	15.920	18.794	20.000	2.874	
53 μm	32.180	40.653	20.000	8.473	
38 μm	76.270	91.722	20.000	15.452	
PAN	35.440	34.892	20.000	-0.548	

Assays of size fractions for BMD2

Au g/t	Meas.	Calc.	Std. Dev.	Adjustment	%Rec
150 μm	24.580	22.706	20.000	-1.874	
106 μm	18.610	20.684	20.000	2.074	
75 μm	23.280	22.364	20.000	-0.916	
53 μm	33.410	32.354	20.000	-1.056	
38 μm	42.550	51.016	20.000	8.466	
PAN	40.620	35.327	20.000	-5.293	

Assays of size fractions for SLC1

Au g/t	Meas.	Calc.	Std. Dev.	Adjustment	%Rec
150 μm	20.990	20.713	10.000	-0.277	
106 μm	25.460	25.348	10.000	-0.112	
75 μm	39.290	39.259	10.000	-0.031	
53 μm	61.920	61.877	10.000	-0.043	
38 μm	102.140	101.788	20.000	-0.352	
PAN	53.460	53.982	20.000	0.522	

Assays of size fractions for SLC2

Au g/t	Meas.	Calc.	Std. Dev.	Adjustment	%Rec
150 μm	18.210	17.936	10.000	-0.274	
106 μm	22.950	22.888	10.000	-0.062	
75 μm	30.230	30.213	10.000	-0.017	
53 μm	39.850	39.850	10.000	-0.000	
38 μm	40.400	40.143	20.000	-0.257	
PAN	128.050	130.411	20.000	2.361	

Assays of size fractions for SLT1

Au g/t	Meas.	Calc.	Std. Dev.	Adjustment	%Rec
150 μm	5.720	5.012	50.000	-0.708	
106 μm	8.720	17.455	50.000	8.735	
75 μm	13.440	18.432	50.000	4.992	
53 μm	33.570	40.279	50.000	6.709	
38 μm	39.280	91.495	60.000	52.215	
PAN	16.450	34.534	60.000	18.084	

Assays of size fractions for SLT2

Au g/t	Meas.	Calc.	Std. Dev.	Adjustment	%Rec
150 μm	13.740	22.898	50.000	9.158	
106 μm	43.990	20.610	50.000	-23.380	
75 μm	34.760	22.094	50.000	-12.666	
53 μm	62.340	32.116	50.000	-30.224	
38 μm	97.020	51.330	60.000	-45.690	
PAN	63.860	27.359	60.000	-36.501	

Assays of size fractions for SOF1

Au g/t	Meas.	Calc.	Std. Dev.	Adjustment	%Rec
150 μm	1.520	1.568	10.000	0.048	
106 μm	4.930	5.002	10.000	0.072	
75 μm	10.080	10.136	10.000	0.056	
53 μm	11.180	11.378	10.000	0.198	
38 μm	15.220	15.957	10.000	0.737	
PAN	78.670	77.385	10.000	-1.285	

150

Assays of size fractions for SOF2

Au g/t	Meas.	Calc.	Std. Dev.	Adjustment	%Rec
150 μm	7.760	7.784	10.000	0.024	
106 μm	12.980	12.989	10.000	0.009	
75 μm	11.800	11.800	10.000	-0.000	
53 μm	17.760	17.691	10.000	-0.069	
38 μm	25.430	25.493	10.000	0.063	
PAN	28.110	26.704	10.000	-1.406	

Assays of size fractions for PCF1

Au g/t	Meas.	Calc.	Std. Dev.	Adjustment	%Rec
150 μm	5.100	4.982	20.000	-0.118	
106 μm	20.050	17.229	20.000	-2.821	
75 μm	15.570	18.203	20.000	2.633	
53 μm	37.560	38.309	20.000	0.749	
38 μm	93.000	82.352	20.000	-10.648	
PAN	39.020	41.656	20.000	2.636	

Assays of size fractions for PCF2

Au g/t	Meas.	Calc.	Std. Dev.	Adjustment	%Rec
150 μm	23.950	22.848	20.000	-1.102	
106 μm	10.400	20.539	20.000	10.139	
75 μm	14.670	21.864	20.000	7.194	
53 μm	17.000	31.326	20.000	14.326	
38 μm	36.130	49.745	20.000	13.615	
PAN	13.080	27.262	20.000	14.182	

Assays of size fractions for PUF1

Au g/t	Meas.	Calc.	Std. Dev.	Adjustment	%Rec
150 μm	5.530	6.673	20.000	1.143	
106 μm	31.890	25.262	20.000	-6.628	
75 μm	20.420	15.285	20.000	-5.135	
53 μm	44.600	36.193	20.000	-8.407	
38 μm	167.590	160.866	20.000	-6.724	
PAN	75.450	73.943	20.000	-1.507	

Assays of size fractions for PUF2

Au g/t	Meas.	Calc.	Std. Dev.	Adjustment	%Rec
150 μm	20.540	21.932	20.000	1.392	
106 μm	23.090	15.561	20.000	-7.529	
75 μm	33.580	30.130	20.000	-3.450	
53 μm	54.260	48.642	20.000	-5.618	
38 μm	65.110	54.939	20.000	-10.171	
PAN	54.700	53.110	20.000	-1.590	

Assays of size fractions for PCOF

Au g/t	Meas.	Calc.	Std. Dev.	Adjustment	%Rec
150 μm	9.900	9.938	20.000	0.038	
106 μm	13.410	11.249	20.000	-2.161	
75 μm	14.800	12.811	20.000	-1.989	
53 μm	23.600	18.662	20.000	-4.938	
38 μm	34.880	21.658	20.000	-13.222	
PAN	22.600	17.614	20.000	-4.986	

Assays of size fractions for SCUF

Au g/t	Meas.	Calc.	Std. Dev.	Adjustment	%Rec
150 μm	82.110	118.723	50.000	36.613	
106 μm	85.670	104.376	50.000	18.706	
75 μm	98.760	116.474	50.000	17.714	
53 μm	160.790	167.855	50.000	7.065	
38 μm	246.960	249.339	50.000	2.379	
PAN	518.910	447.067	50.000	-71.843*	

Assays of size fractions for RMDS

Au g/t	Meas.	Calc.	Std. Dev.	Adjustment	%Rec
·150 μm	193.970	170.013	50.000	-23.957	
106 μm	126.620	109.132	50.000	-17.488	
75 μm	132.350	114.553	50.000	-17.797	
53 μm	160.590	152.857	50.000	-7.733	
38 μm	208.400	205.504	50.000	-2.896	
PAN	174.830	290.647	50.000	115.817*	

Appendix III: Ballmill Simulation Results

Ball Mill Simulation Results

Tau Plug Flow= 0.10   Tau Small= 0.10   Tau Large= 0.70

1) Gold

Breakage Function

```
0.75
0.08  0.75
0.04  0.08  0.75
0.04  0.04  0.08  0.75
0.03  0.04  0.04  0.08  0.75
0.02  0.03  0.04  0.04  0.08  0.75
0.01  0.02  0.03  0.04  0.04  0.08  0.75
```

Size μm	Feed (%)	Measured Product (%)	Calculated Product (%)	Selection Function
505	3.05	2.98	2.98	0.0233
357	1.77	1.68	1.68	0.0837
252	2.71	2.66	2.66	0.0608
178	7.53	7.51	7.51	0.0208
126	14.48	14.14	14.14	0.0336
89	23.95	23.90	23.90	0.0182
63	22.87	22.80	22.80	0.0198
45	10.95	10.92	10.92	0.0400

Ball Mill Simulation Results

Tau Plug Flow = 0.10   Tau Small = 0.10   Tau Large = 0.70

2) Ore

Breakage Function

0.60
0.13 0.60
0.07 0.13 0.60
0.05 0.07 0.13 0.60
0.04 0.05 0.07 0.13 0.60
0.04 0.04 0.05 0.07 0.13 0.60
0.03 0.04 0.04 0.05 0.07 0.13 0.60

Size μm	Feed (%)	Measured Product (%)	Calculated Product (%)	Selection Function
505	2.26	0.37	0.37	2.703
357	2.13	0.80	0.80	2.219
252	3.97	2.54	2.54	1.084
178	10.48	8.75	8.75	0.4439
126	19.49	18.22	18.22	0.2375
89	28.99	28.93	28.93	0.1269
63	19.18	20.90	20.90	0.0833
45	6.13	7.55	7.55	0.1255

Appendix IV: Preliminary Falcon Test Work at AELR

Test number: 1   Date: 07/21/91

Sample Name: Flotation Concentrate

1) Plant Conditions and Comments

Both lines of the grinding circuit were operating.
Regrind mill used to regrind scavenger concentrate.

Experimental procedure slightly modified. The slurry distribution system was not used.
Because of the large masses involved with the following tests, the Falcon was put directly
on-line by means of a by-pass valve connected to the concentrate thickener feed pipe.
Flows were measured with a stopwatch and a bucket.
Flowrate was not as stable as when the slurry distribution system was used.

2) Experimental Conditions

Flow of slurry: 20 l/min
Percent Solids: 20
Solids Density: 3.10
Slurry Density: 1.16
    Sample Mass: 9.28 Kg
        Test time: 2 min

3) Subsample Masses

a) Concentrate: 647.9 g
        Assays: 548.60 g/t   (repeat: 548.45 g/t)

b) Tails:

Tail	Time(min)	Sample Mass(g)	Assays g/t		Percent Solids
1	0.5	673.13	80.43	81.05	18.46
2	1.5	602.89	40.43	42.24	16.45
3	2.5	582.05	44.47	42.10	17.43
4	4.0	654.13	257.39	261.67	17.23

Test number: 2   Date: 07/21/91

Sample Name: Flotation Concentrate

1) Plant Conditions Comments

2) Experimental Conditions

Flow of slurry: 20 l/min
Percent Solids: 20
Solids Density: 3.1
Slurry Density: 1.16
   Sample Mass: 19.00 Kg
     Test time: 5 min

3) Subsample Masses

a) Concentrate: 1128.3 g
            Assays: 980.37 g/t   (repeat: 966.90 g/t)

b) Tails:

Tail	Time(min)	Sample Mass(g)	Assays g/t		Percent Solids
1	1.0	954.98	85.44	83.55	21.60
2	2.0	713.85	60.51	60.65	16.02
3	3.0	991.41	131.21	133.06	19.70
4	4.0	1103.26	231.91	236.16	22.78

Test number: 3   Date: 07/21/91

Sample Name: Flotation Concentrate

1) Plant Conditions and Comments

2) Experimental Conditions

Flow of slurry: 20 l/min
Percent Solids: 20
Solids Density: 3.1
Slurry Density: 1.16
  Sample Mass: 37.12 Kg
    Test time: 8.0 min

3) Subsample Masses

a) Concentrate: 847.8 g
          Assays: 1724.24 g/t

b) Tails:

Tail	Time(min)	Sample Mass(g)	Assays g/t		Percent Solids
1	1.0	987.42	189.84	187.20	20.25
2	3.0	947.43	224.23	226.97	18.18
3	5.0	1249.08	140.16	144.00	22.34
4	7.0	798.41	129.64	132.82	17.81
5	8.0	1133.55	185.76	184.56	21.23

Test number: 4   Date: 07/21/91

Sample Name: Flotation Concentrate

1) Plant Conditions and Comments

2) Experimental Conditions

Flow of slurry: 20 l/min
Percent Solids: 20
Solids Density: 3.1
Slurry Density: 1.16
   Sample Mass: 55.68 Kg
      Test time: 12 min

3) Subsample Masses

a) Concentrate: 806.30 g
         Assays: 2098.44 g/t   (repeat:2125.32 g/t)

b) Tails:

Tail	Time(min)	Sample Mass(g)	Assay g/t		Percent Solids
1	1.0	1197.10	105.46	100.80	16.76
2	3.0	1272.43	125.08	. 126.31	21.67
3	5.0	1123.53	176.92	172.25	22.05
4	7.0	1125.64	195.45	. 198.45	21.06
5	9.0	1190.82	146.06	146.74	21.24
6	11.50	1011.65	88.32	89.59	18.56

Test number: 5   Date: 07/21/91

Sample Name: Flotation Concentrate

1) Plant Conditions and Comments

2) Experimental Conditions

Flow of slurry: 20 l/min
Percent Solids: 20
Solids Density: 3.13
Slurry Density: 1.16
   Sample Mass: 92.80 Kg
   Test time: 20 min

3) Subsample Masses

a) Concentrate: 881.00 g
         Assays:1561.93 g/t   (repeat:1570.51 g/t)

b) Tails:

Tail	Time(min)	Sample Mass(g)	Assay g/t		Percent Solids
1	1.0	1369.29	136.60	135.50	21.38
2	3.0	1136.03	120.96	123.57	20.24
3	5.0	1126.41	179.18	179.52	19.54
4	7.0	1116.21	100.08	102.21	18.78
5	9.0	1284.83	54.82	54.45	20.90
6	11.0	945.85	77.38	78.72	18.91
7	13.0	1143.36	61.58	64.46	19.00
8	15.0	1351.24	83.79	82.97	20.72
9	17.0	1240.37	109.72	117.33	22.54
10	19.5	1291.58	85.30	86.13	19.67

Test number: 6   Date: 07/17/91

Sample Name: Primary Cyclone Overflow (PCOF)

1) Plant Conditions and Comments

Only half the grinding circuit was functioning.
Regrind circuit was not operational.
Grinding mill feed was at 37 tonnes/hour

2) Experimental Conditions

Flow of slurry: 10 l/min
Percent Solids: 20
Solids Density: 3.13
Slurry Density: 1.16
  Sample Mass: 15.00 Kg
   Test time: 7.5 min

3) Subsample Masses and Assays

a) Concentrate: 475.73 g
      Assays: 14.71 g/t

b) Tails:

Tail	Time (min)	Solids Mass(g)	Assay g/t		Percent Solids
1	1.0	295.10	2.36	2.88	9.98
2	3.0	310.43	2.10	2.54	20.00
3	5.0	297.22	2.35	1.91	20.20
4	7.0	297.71	4.40	4.82	19.90

Test number: 7   Date: 07/17/91

Sample Name:PCOF

1) Plant Conditions and Comments

2) Experimental Conditions

Flow of slurry: 15 l/min
Percent Solids: 20
Solids Density: 3.13
Slurry Density: 1.16
   Sample Mass: 15.00 Kg
   Test time: 5.00 min

3) Subsample Masses

a)Concentrate: 471.98 g
      Assays: 15.70 g/t

b) Tails:

Tail	Time(min)	Solids Mass(g)	Assays g/t		Percent Solids
1	1.0	284.42	2.46	1.92	12.10
2	2.0	283.74	2.01	1.10	16.06
3	3.0	310.52	2.56	2.61	18.90
4	4.0	272.55	4.99	5.90	19.20

Test number: 8   Date: 07/17/91

Sample Name: PCOF

1) Plant Conditions and Comments

2) Experimental Conditions

Flow of slurry: 20 l/min
Percent Solids: 20
Solids Density: 3.13
Slurry Density: 1.16
  Sample Mass: 15.00 Kg
   Test time: 3.75 min

3) Subsample Masses

a) Concentrate: 402.08 g
        Assays: 15.14 g/t   (repeat: 14.90 g/t)

b) Tails:

Tail	Time (min)	Sample Mass(g)	Assays g/t		Percent Solids
1	0.5	396.31	2.67	2.95	10.40
2	1.0	402.06	2.34	2.19	19.34
3	2.0	400.53	1.98	2.19	20.03
4	3.0	410.40	2.67	2.25	19.49

Test number: 9   Date: 07/17/91

Sample Name: PCOF

1) Plant Conditions and Comments

2) Experimental Conditions

Flow of slurry: 30 l/min
Percent Solids: 20
Solids Density: 3.13
Slurry Density: 1.16
   Sample Mass: 15.00 Kg
     Test time: 3.75 min

3) Subsample Masses

a) Concentrate: 354.80 g
        Assays: 11.66 g/t   (repeat: 12.18 g/t)

b) Tails:

Tail	Time (min)	Solids Mass(g)	Assays g/t		Percent Solids
1	0.5	291.32	1.99	1.78	13.21
2	1.5	281.91	1.54	1.58	16.50
3	2.5	298.10	3.15	2.95	17.40
4	3.5	283.90	2.67	3.50	17.13

Test number: 10 Date: 07/25/91

Sample Name: Secondary Cyclone Overflow (SCOF)

1) Plant Conditions and Comments
The slurry distribution system was used.
Because of the low percent solids of this stream (15%) and the fineness of the particles, flocculant was added to the bucket samples to increase the settling rate. The water was then decanted from the bucket. This proved to be a most efficient method to deal with the fine material.

2) Experimental Conditions

Flow of slurry: 20 l/min
Percent Solids: 20
Solids Density: 3.1
Slurry Density: 1.16
  Sample Mass: 20 Kg
   Test time: 6 min

3) Subsample Masses

a) Concentrate: 351.00 g
     Assays: 546.68 g/t (repeat: 546.13 g/t)

b) Tails:

Tail	Time (min)	Sample Mass(g)	Assay g/t		Percent Solids
1	0.5	1596.23	64.46	61.51	15.04
2	1.5	1551.48	63.63	62.13	15.02
3	2.5	1602.71	52.80	59.25	14.94
4	3.5	1616.16	56.85	52.87	14.54
5	4.5	1549.50	59.93	60.55	13.24
6	5.5	1602.24	61.30	58.29	14.48

Test number: 11   Date: 08/02/91

Sample Name: Regrind Mill Discharge (RMDS)

1) Plant Conditions and Comments

The percent solids in the mill discharge was very low (15%).
Again, flocculant was added to increase settling rate.

2) Experimental Conditions

Flow of slurry: 20 l/min
Percent Solids: 15
Solids Density: 3.1
Slurry Density: 1.11
   Sample Mass: 20 Kg
      Test time: 6 min

3) Subsample Masses

a) Concentrate: 430.94 g
      Assays: 665.42 g/t   (repeat: 658.18 g/t)

b) Tails:

Tail	Time(min)	Sample Mass(g)	Assay g/t		Percent Solids
1	0.5	982.17	125.49	132.82	13.72
2	1.5	1025.32	110.26	110.95	14.54
3	2.5	995.05	198.52	201.81	13.29
4	3.5	958.89	107.66	107.80	13.76
5	5.5	1013.08	139.13	140.92	14.56

Test number: 12   Date: 08/03/91

Sample Name: Primary Ball Mill Discharge (BMD)

1) Plant Conditions and Comments

This stream is probably not a good location for gravity recovery with the Falcon.
The material is rather coarse and would have to be screened to remove the pebbles.
The gold is not well liberated.
Because of the material's large size and high pyrite content, it settles very rapidly.
Roughly 4 kg of material settled at the bottom of the tank and was not processed.

2) Experimental Conditions

Flow of slurry: 20 l/min
Percent Solids: 20
Solids Density: 3.1
Slurry Density: 1.16
   Sample Mass: 20 Kg
     Test time: 6 min

3) Subsample Masses

a) Concentrate: 364.86 g
         Assays: 21.71 g/t   (repeat: 21.72 g/t)

b) Tails:

Tail	Time(min)	Sample Mass(g)	Assays g/t		Percent Solids
1	0.5	472.20	27.03	30.86	8.68
2	1.5	322.17	8.85	8.78	6.32
3	2.5	349.00	32.09	30.10	6.36
4	3.5	177.87	28.39	29.83	3.91
5	5.0	161.23	10.42	11.38	2.93

Sample	Tail Mass(g)	Assays	(g/t)	Mean Assay	S.D.	D.F.
1) FLOT	673.13	80.43	81.05	106.22	96.11	7
CONC	602.89	40.43	42.24			
	582.05	44.47	42.10			
	1064.44	257.39	261.67			
2) FLOT	954.98	85.44	83.55	127.81	71.12	7
CONC	713.85	60.51	60.65			
	991.41	131.21	133.06			
	1103.26	231.91	236.16			
3) FLOT	987.42	189.84	187.20	174.52	36.07	9
CONC	947.43	224.23	226.97			
	1249.08	140.16	144.00			
	798.41	129.64	132.82			
	1133.55	185.76	184.56			
4) FLOT	1197.10	105.46	100.80	139.29	39.68	11
CONC	1272.43	125.08	126.31			
	1123.53	176.92	172.25			
	1125.64	195.45	198.45			
	1190.82	146.06	146.74			
	1011.65	88.32	89.59			
5) FLOT	1369.29	136.60	135.50	101.71	36.50	19
CONC	1136.03	120.96	123.57			
	1126.41	179.18	179.52			
	1116.21	100.08	102.21			
	1284.83	54.82	54.45			
	945.85	77.38	78.72			
	1143.36	61.58	64.46			
	1351.24	83.79	82.97			
	1240.37	109.72	117.33			
	1291.58	85.30	86.13			

Sample	Tail Mass(g)	Assays	(g/t)	Mean Assay	S.D.	D.F.
6) PCOF	295.10	2.36	2.88	2.92	1.09	7
	310.43	2.10	2.54			
	297.22	2.35	1.91			
	297.71	4.40	4.82			
7) PCOF	284.42	2.46	1.92	2.94	1.64	7
	283.74	2.01	1.10			
	310.52	2.56	2.61			
	272.55	4.99	5.90			
8) PCOF	396.31	2.67	2.95	2.41	0.32	7
	402.06	2.34	2.19			
	400.53	1.98	2.19			
	410.40	2.67	2.25			
9) PCOF	291.32	1.99	1.78	2.40	0.77	7
	281.91	1.54	1.58			
	298.10	3.15	2.95			
	283.90	2.67	3.50			
10) SCOF	1596.23	64.46	61.51	59.46	3.75	11
	1551.58	63.63	62.13			
	1602.71	52.80	59.25			
	1616.16	56.85	52.87			
	1549.50	59.93	60.55			
	1602.24	61.30	58.29			
11) RMDS	982.17	125.49	132.82	137.54	35.37	9
	1025.32	110.26	110.95			
	995.05	198.52	201.81			
	958.89	107.66	107.80			
	1013.08	139.13	140.92			
12) BMD	472.20	27.03	30.86	21.77	10.37	9
	322.17	8.85	8.78			
	349.00	32.09	30.10			
	177.87	28.39	29.83			
	161.23	10.42	11.38			

Tables IVa and IVb: Tail Masses and Assays for the Various Tests

Appendix V: Results for Tests to Study the Effect of Flowrate

Appendix V.1: Mass Balance Results for Section 3.5.3: Studying the Effect of Mass Processed with Samples of Flotation Concentrate (Tests 1 to 5)

	Stream	Absolute Solids Flowrate	Pulp Mass Flowrate Meas	Calc	S.D.	Adjust
1	Global Feed	223.13	218.1	223.1	30.0	5.0
2	Feed 1	9.21	9.3	9.2	1.0	-0.1
3	Feed 2	22.95	23.2	22.9	5.0	-0.3
4	Feed 3	38.30	37.1	38.3	10.0	1.2
5	Feed 4	56.68	55.7	56.7	10.0	1.0
6	Feed 5	96.00	92.8	96.0	20.0	3.2
7	Conc 1	0.55	0.5	0.5	0.0	-0.0
8	Conc 2	0.97	1.0	1.0	0.0	-0.0
9	Conc 3	1.72	1.7	1.7	0.0	0.0
10	Conc 4	2.11	2.1	2.1	0.0	0.0
11	Conc 5	1.57	1.6	1.6	0.0	0.0
12	Tail 1	8.66	8.6	8.7	1.0	0.0
13	Tail 2	21.97	22.1	22.0	5.0	-0.1
14	Tail 3	36.57	35.4	36.6	10.0	1.2
15	Tail 4	54.57	53.6	54.6	10.0	1.0
16	Tail 5	94.43	91.2	94.4	20.0	3.2

	Stream	Relative Solids Flowrate
1	Global Feed	100.00
2	Feed 1	4.13
3	Feed 2	10.28
4	Feed 3	17.16
5	Feed 4	25.40
6	Feed 5	43.02
7	Conc 1	0.25
8	Conc 2	0.44
9	Conc 3	0.77
10	Conc 4	0.95
11	Conc 5	0.70
12	Tail 1	3.88
13	Tail 2	9.85
14	Tail 3	16.39
15	Tail 4	24.46
16	Tail 5	42.32

<u>Assay Data</u>

Gold g/t	Meas.	Calc.	Std. Dev.	Adjust.	% Rec
Global Feed	149.740	152.686	7.497	2.946	100
Feed 1	137.100	135.019	20.000	-2.081	4
Feed 2	168.940	165.784	20.000	-3.156	11
Feed 3	205.810	215.829	20.000	10.019	• 24
Feed 4	164.590	176.379	20.000	11.789	29
Feed 5	114.860	112.072	20.000	-2.788	32
Conc 1	548.530	548.667	27.437	0.136	1
Conc 2	973.640	973.892	48.692	0.252	3
Conc 3	1724.240	1712.846	86.222	-11.394	9
Conc 4	2111.880	2094.114	105.604	-17.766	13
Conc 5	1566.220	1564.657	78.321	-1.563	7
Tail 1	106.220	108.793	30.000	2.573	3
Tail 2	127.810	129.964	30.000	2.154	8
Tail 3	174.520	145.259	30.000	-29.261	16
Tail 4	139.290	102.216	30.000	-37.074*	16
Tail 5	101.710	87.917	30.000	-13.793	24

Appendix V.2: Mass Balance Results for Section 3.6.3: Studying the Effect of Flowrate with Samples of PCOF (Tests 6 to 9)

	Stream	Absolute Solids Flowrate	Pulp Mass Flowrate			
			Meas	Calc	S.D.	Adjust
1	Global Feed	60.00	60.0	60.0	2.0	0.0
2	Feed 1	15.00	15.0	15.0	1.0	0.0
3	Feed 2	15.00	15.0	15.0	1.0	0.0
4	Feed 3	15.00	15.0	15.0	1.0	0.0
5	Feed 4	15.00	15.0	15.0	1.0	0.0
6	Conc 1	0.48	0.5	0.5	0.0	0.0
7	Conc 2	0.47	0.5	0.5	0.0	0.0
8	Conc 3	0.40	0.4	0.4	0.0	0.0
9	Conc 4	0.35	0.4	0.4	0.0	0.0
10	Tail 1	14.52	14.5	14.5	1.0	0.0
11	Tail 2	14.53	14.5	14.5	1.0	-0.0
12	Tail 3	14.60	14.1	14.6	1.0	0.5
13	Tail 4	14.65	14.6	14.6	1.0	-0.0

	Stream	Relative Solids Flowrate
1	Global Feed	100.00
2	Feed 1	25.00
3	Feed 2	25.00
4	Feed 3	25.00
5	Feed 4	25.00
6	Conc 1	0.79
7	Conc 2	0.79
8	Conc 3	0.67
9	Conc 4	0.59
10	Tail 1	24.21
11	Tail 2	24.21
12	Tail 3	24.33
13	Tail 4	24.41

Assay Data

Gold g/t	Meas.	Calc.	Std. Dev.	Adjust.	% Rec
Global Feed	3.020	3.020	0.161	-0.000	100
Feed 1	3.290	3.293	2.000	0.003	27
Feed 2	3.340	3.343	2.000	0.003	28
Feed 3	2.800	2.802	2.000	0.002	23
Feed 4	2.640	2.643	2.000	0.003	22
Conc 1	14.710	14.710	0.500	0.000	4
Conc 2	15.700	15.700	0.500	0.000	4
Conc 3	14.660	14.660	0.500	0.000	3
Conc 4	12.690	12.690	0.500	0.000	2
Tail 1	2.920	2.919	20.000	-0.001	23
Tail 2	2.940	2.941	20.000	0.001	24
Tail 3	2.410	2.475	20.000	0.065	20
Tail 4	2.400	2.399	20.000	-0.001	19

Appendix VI: Results for 3^3+2 Design with the Flotation Concentrate

Test #	Flowrate	Density	Tail Mass	Tail Assay	Conc Mass	Conc Assay	Feed Grade	Gold Recovery
1	10	10	677.48	79.41	659.11	533.30	98.05	18.20
			645.46	83.21				
			639.36	86.54				
		Weighted	Average	82.98				
2	10	20	360.37	85.00	723.05	620.90	123.15	18.81
			1263.63	87.91				
			1203.58	126.07				
		Weighted	Average	103.78				
3	10	30	758.80	124.67	678.90	987.60	150.69	22.82
			929.20	115.30				
			489.10	123.90				
		Weighted	Average	120.50				
4	20	10	607.08	127.86	675.23	876.50	162.83	18.64
			874.67	144.34				
			663.07	136.46				
		Weighted	Average	137.24				
5	20	20	990.60	69.47	564.72	854.68	118.72	20.85
			1604.95	101.83				
			1118.20	113.70				
		Weighted	Average	96.77				
6	20	30	1011.50	98.45	757.80	666.84	120.22	21.56
			998.20	95.24				
			1213.20	100.21				
		Weighted	Average	98.12				
7	30	10	895.25	83.76	576.11	955.20	117.59	24.00
			1089.59	87.80				
			812.33	107.01				
		Weighted	Average	92.09				
8	30	20	905.34	136.50	800.00	1048.11	180.08	23.88
			1011.20	141.40				
			956.80	150.70				
		Weighted	Average	142.95				
9	30	30	890.52	142.95	896.43	900.50	179.33	23.08
			973.19	146.30				
			900.10	144.32				
		Weighted	Average	144.58				
10	10	20		84.08	480.60	765.32	100.87	18.70
11	20	20		105.70	630.00	689.12	124.55	17.88
12	30	20		272.41	738.00	764.30	291.03	9.94

Table VI: Optimization Test Results for AELR

Sample:Flotation Concentrate
Sample Mass: 21 kg

Appendix VII: Results for Meston Resources Test Work

Flowrate (L/min)	Percent Solids	Bowl Type	Feed Mass (g)	Tail Mass (g)	Conc Mass (g)	Feed Grade (g/t)	Corrected Assays (g/t) f	c	t	Corrected Recovery
10	10	8	8500	7876	624.10	0.64	0.77	2.62	0.62	25.08
20	20	8	8487	7490	997.40	0.80	0.80	3.43	0.45	50.26
20	10	8	8475	7714	760.60	0.87	0.82	4.49	0.46	49.15
20	20	8	8462	7553	909.40	0.78	0.80	3.53	0.47	47.63
20	30	8	8449	7448	1001	0.66	0.77	2.31	0.56	35.57
10	30	8	8437	7594	842.80	0.87	0.82	4.72	0.39	57.56
10	10	8	8424	7477	946.90	0.77	0.80	3.09	0.51	43.66
20	20	8	8411	7488	923.50	0.76	0.79	3.60	0.45	49.88
10	20	8	8399	7630	768.23					
20	10	10	8386	7687	711.20	0.96	0.84	6.16	0.35	62.18
10	20	10	8373	7474	912.10	0.69	0.78	2.99	0.51	41.96
20	20	10	8361	7393	980.20	1.03	0.86	5.39	0.25	73.75
10	30	10	8348	7459	901.80	0.73	0.79	3.33	0.48	45.84
20	30	10	8335	7429	919.50	1.15	0.89	6.82	0.15	84.88
10	10	10	8323	7520	802.70	0.72	0.78	2.99	0.55	36.76
20	20	10	8310	7346	964.50		0.80			
10	10	14	8084	7767	317.04					
10	20	14	7754	7366	387.74	0.57	0.75	3.54	0.61	23.54
20	20	14	5924	5529	394.90	0.85	0.81	6.00	0.44	49.15

Table VII.1: Raw Data for Meston Test Work (Gold)

Flowrate (L/min)	Percent Solids	Bowl Type	Feed Mass (g)	Tail Mass (g)	Conc Mass (g)	Feed Grade (%)	Corrected Assays f	t	c	Corrected Recovery
10	10	8	8500	7876	624.10	1.07	0.87	0.83	1.36	11.5
20	20	8	8487	7490	997.40	0.68	0.78	0.68	1.57	23.6
20	10	8	8475	7714	760.60	0.73	0.79	0.65	2.25	25.4
20	20	8	8462	7553	909.40	0.78	0.81	0.70	1.68	22.5
20	30	8	8449	7448	1001	0.64	0.77	0.69	1.42	21.8
10	30	8	8437	7594	842.80	0.62	0.77	0.72	1.16	15.1
10	10	8	8424	7477	946.90	0.79	0.81	0.58	2.63	36.6
20	20	8	8411	7488	923.50	0.78	0.80	0.59	2.52	34.5
10	20	8	8399	7630	768.23	0.85	0.82	0.78	1.22	13.6
20	10	10	8386	7687	711.20	1.00	0.86	0.77	1.76	17.4
10	20	10	8373	7474	912.10	0.97	0.85	0.79	1.37	17.5
20	20	10	8361	7393	980.20	0.69	0.78	0.66	1.68	25.1
10	30	10	8348	7459	901.80	0.93	0.84	0.78	1.35	17.4
20	30	10	8335	7429	919.50	1.00	0.86	0.83	1.04	13.4
10	10	10	8323	7520	802.70	1.02	0.86	0.84	1.07	12.0
20	20	10	8310	7346	964.50	0.54	0.75	0.69	1.16	18.0
10	10	14	8084	7767	317.04	0.83	0.82	0.77	1.94	9.3
10	20	14	7754	7366	387.74	0.80	0.81	0.75	1.90	11.7
20	20	14	5924	5529	394.90	0.74	0.80	0.73	1.68	14.1

Table VII.2:Raw Data for Meston Test Work (Pyrite)

176

Appendix VIII: Size Distribution of Silica used in Fundamental Work

Size (μm)	425 μm	212 μm	75 μm
840	99.98		
600	98.40		
420	85.52	99.64	
300	52.20	96.42	
212	18.43	75.18	
150	5.86	47.58	
105	1.70	27.16	
75	0.63	9.73	99.99
53	0.00	3.82	99.74
38		0.00	99.06
25			93.86
15			80.59

Table VIII.1: Size Distribution of Silica used in Fundamental Test Work

Appendix IX: Results for Systematic Variable Testing Program

Test #	Percent Solids	Flowrate (L/min)	Gangue P80 (um)	Ore Mass Conc	Mass of Tail	Magnetite (g) Conc	Tail	Mags. Recovery	Grade (%) Conc	Tail	Feed
1	10	20	425	1786	7094	56.95	189.1	23.15	3.19	2.66	2.77
2	30	20		2057	6531	69.50	191.5	26.63	3.38	2.93	3.04
3	10	10		1666	7043	82.52	171.5	32.49	4.95	2.43	2.92
4	30	10		1889	7324	85.43	151.6	36.05	4.52	2.07	2.57
5	30	20	212								
6	10	10		1745	6432	97.91	166.1	37.09	5.61	2.58	3.23
7	30	10		1978	5986	101.15	136.9	42.50	5.11	2.29	2.99
8	10	20		1549	6546	107.86	161.1	40.10	6.97	2.46	3.32
9	10	10	45	820.5	8489	197.97	56.0	77.94	24.13	0.66	2.73
10	30	10		856.8	8412	134.62	121.4	52.59	15.71	1.44	2.76
11	30	20		834.2	8231	202.13	54.9	78.65	24.23	0.67	2.84
12	10	20		780.9	8219	189.45	100.3	65.39	24.26	1.22	3.22

Test #	Percent Solids	Flowrate (L/min)	Gangue P80 (um)	Particle Size (um) 600	425	300	212	150	106	75	53
1	10	20	425	44.40	38.65	29.95	15.78	11.31	10.81	19.66	30.58
2	30	20		50.08	63.67	35.33	10.45	9.46	11.00	21.67	74.10
3	10	10		42.03	74.40	56.73	27.61	18.42	15.75	15.76	33.78
4	30	10		53.20	59.80	35.30	19.20	25.50	25.90	35.80	46.60
5	30	20	212								
6	10	10		82.80	89.65	65.35	19.43	13.42	13.29	23.58	86.30
7	30	10		68.44	87.07	62.61	28.35	22.42	25.82	27.33	45.64
8	10	20		89.56	80.37	76.61	27.07	19.90	16.79	26.45	72.34
9	10	10	45	39.20	94.29	95.95	58.36	55.41	55.84	75.13	99.73
10	30	10		17.55	48.89	56.42	34.55	40.45	40.42	50.62	89.61
11	30	20		54.62	93.50	94.60	63.28	60.34	65.41	80.23	89.65
12	10	20		35.17	54.48	92.12	60.53	59.21	56.11	75.60	86.80

Table IX1: Silica-Magnetite Test Results for 8 Degree Bowl

Test #	Percent Solids	Flowrate (L/min)	Gangue P80 (um)	Ore Mass Conc	Mass of Feed	Magnetite (g) Conc	Tail	Mags. Recovery	Grade (%) Conc	Tail	Feed
13	10	20	425	1658	241.00	44.54	196.46	18.48	2.69	2.87	3.91
14	30	20		1306	241.00	55.95	185.05	23.22	4.28	2.57	3.91
15	10	10		1765	241.00	74.73	166.27	31.01	4.23	2.47	3.91
16	30	10		1398	241.00	79.51	161.49	32.99	5.69	2.27	3.91
17	30	20	212								
18	10	10		1204	241.00	85.55	155.45	35.50	7.11	2.13	3.91
19	30	10		1784	241.00	93.38	147.62	38.75	5.23	2.20	3.91
20	10	20		1155	241.00	99.97	141.03	41.48	8.66	1.92	3.91
21	10	10	45	745.6	241.00	123.5	117.55	51.22	16.56	1.52	3.91
22	30	10		699.2	241.00	124.6	116.44	51.68	17.81	1.49	3.91
23	30	20		800.8	241.00	176.5	64.50	73.24	22.04	0.84	3.91
24	10	20		761.5	241.00	180.2	60.80	74.77	23.67	0.79	3.91

Test #	Percent Solids	Flowrate (L/min)	Gangue P80 (um)	Particle Size (um) 600	425	300	212	150	106	75	53
13	10	20	425	39.78	36.56	21.31	13.21	10.43	9.99	16.45	25.45
14	30	20		45.32	59.59	33.84	12.67	10.11	9.96	17.12	51.34
15	10	10		45.37	73.25	49.86	28.10	22.19	14.35	15.27	28.53
16	30	10		54.21	56.37	30.60	26.32	33.77	32.14	36.01	53.57
17	30	20	212								
18	10	10		76.66	82.13	65.50	26.55	21.69	19.53	23.79	43.46
19	30	10		60.43	85.45	61.46	35.47	30.69	32.06	27.54	52.61
20	10	20		84.59	78.47	63.11	34.19	28.17	23.03	26.66	79.31
21	10	10	45	40.24	92.19	81.27	65.48	63.68	62.08	75.34	83.58
22	30	10		18.63	47.13	50.15	41.67	48.72	46.66	50.83	64.31
23	30	20		51.82	65.26	78.28	70.40	68.61	71.65	80.44	85.96
24	10	20		24.54	54.48	86.45	67.65	67.48	62.35	75.81	78.15

Table IX2: Silica-Magnetite Test Results for 10 Degree Bowl

Test #	Percent Solids	Flowrate (L/min)	Gangue P80 (um)	Ore Mass Conc	Mass of Tail	Magnetite (g) Conc	Tail	Mags. Recovery	Grade (%) Conc	Tail	Feed
33	10	10	425	608.3	7758	23.50	234.6	9.10	3.86	3.02	3.08
34	30	10		653.2	8543	44.03	197.0	18.27	6.74	2.31	2.62
35	30	20		703.1	8246	46.81	193.0	19.52	6.66	2.34	2.68
36	10	20		614.5	7956	33.91	225.6	13.07	5.52	2.84	3.03
29	30	20	212	768.3	7890	55.71	200.2	21.77	7.25	2.54	2.96
30	10	10		631.7	7492	39.29	218.9	15.22	6.22	2.92	3.18
31	30	10		774.1	7112	44.84	206.2	17.86	5.79	2.90	3.18
32	10	20		652.0	7396	41.96	215.2	16.32	6.44	2.91	3.20
25	10	20	45	399.2	8765	88.76	156.8	36.15	22.23	1.79	2.68
26	30	20		411.2	8667	164.2	188.8	46.51	39.92	2.18	3.89
27	10	10		394.0	9245	56.21	196.8	22.22	14.27	2.13	2.62
28	30	10		413.2	8496	76.27	165.6	31.53	18.46	1.95	2.71

Test #	Percent Solids	Flowrate (L/min)	Gangue P80 (um)	Particle Size (um) 600	425	300	212	150	106	75	53
33	10	10	425	18.40	48.60	15.30	8.30	5.20	4.90	6.40	12.80
34	30	10		20.50	21.85	18.95	7.70	6.88	9.86	18.37	43.54
35	30	20		37.36	43.92	28.16	9.87	10.58	8.46	9.70	22.47
36	10	20		37.49	43.18	24.68	6.92	4.14	3.93	5.07	14.02
29	30	20	212	17.62	22.16	22.52	10.68	10.22	11.50	20.82	54.97
30	10	10		38.82	13.66	10.26	4.72	5.24	7.82	14.42	47.19
31	30	10		32.85	22.18	21.69	10.00	8.64	9.08	12.88	34.68
32	10	20		31.36	14.21	15.15	6.99	6.00	7.16	14.48	47.40
25	10	20	45	75.83	74.16	32.81	23.34	21.52	23.39	29.18	53.65
26	30	20		58.47	93.13	90.24	48.51	49.26	42.45	46.17	79.48
27	10	10		59.90	62.10	17.60	16.30	12.90	13.10	18.50	35.80
28	30	10		69.10	68.90	25.40	20.13	17.11	17.83	22.50	41.20

Table IX3: Silica-Magnetite Test Results for 14 Degree Bowl

Appendix X: Results for Effect of Particle Size Tests

Effect of Particle Size

X.1 Summary of Experimental Conditions

Flowrate: 20 1/min

% Solids: 20

Sample Mass: Approximately 12 kg

X.2 P_{80} of Silica in Bed and Feed, Respectively

Test 1: 212 μm 212 μm

Test 2: 212 μm 425 μm

Test 3: 425 μm 212 μm

X.3 Samples Masses

Test #	Sample	Sample Mass (g)	Subsample Mass (g)	Subsample Magnetite (g)	Sample Magnetite(g)
1	Unprocessed	1894			53.2
	Concentrate	1743			32.8
	Tail	8709	1099	21.8	172.4
2	Unprocessed	1752			48.2
	Concentrate	1827			20.8
	Tail	8345	1102	23.0	173.9
3	Unprocessed	2060	1001	38.7	102.8
	Concentrate	2500	1005	20.2	50.3
	Tail	7680	1002	16.2	124.4

X.4 Size-by-Size Magnetite Recovery

Size (μm)	Mass of Magnetite		Mag Rec'y	Mass of Magnetite		Mag Rec'y	Mass of Magnetite		Mag Rec'
	Conc	Tail		Conc	Tail		Conc	Tail	
600	1.2	2.0	37.2	0.7	0.6	52.8	1.1	1.1	49.3
425	3.3	11.9	21.3	1.8	8.4	21.3	2.7	12.4	18.0
300	3.5	43.7	7.3	8.8	43.2	16.9	2.5	46.5	5.2
212	2.0	37.5	5.0	7.7	37.6	17.0	1.2	38.8	3.0
150	2.2	29.9	6.7	11.9	23.1	34.0	1.0	30.9	3.1
106	2.6	21.5	10.7	6.9	9.1	43.0	1.0	21.3	4.6
75	3.6	15.7	18.5	4.9	1.8	73.0	1.8	14.6	11.2
53	4.9	6.7	42.5	4.2	0.3	93.0	3.1	6.4	32.8
38	4.0	1.8	68.5	2.1	0.2	86.0	2.4	1.3	64.8
30	2.9	1.0	82.1	0.1	0.0	100	2.1	0.5	82.3
-30	2.7	0.2	92.2	1.4	0.0	100	1.7	0.2	92.0
Total	32.9	172	16.0	50.3	124	28.8	20.8	174	10.7

Appendix XI: Results of Overload Tests

Results of First Overload Test with Silica/Magnetite Feed

Measured Sample Mass: 32.5 kg
% Solids and Flowrate: 20

1) Mass of Head Samples and Subsamples (g)

Absolute Time (min)	Sample	Total Mass Sample	Subsample	Mass of Magnetite Subsample	Sample (A)
	Conc	1645	1004	170.0	278.6
0:45	T1	740.0	740.0	0.61	0.61
1:45	T2	2882	1020	21.5	60.74
2:45	T3	3149	1120	65.07	182.9
3:45	T4	3420	1009	27.81	94.26
4:45	T5	3691	1008	34.34	125.7
5:45	T6	3827	954.8	37.34	141.8
6:45	T7	3771	1001	49.71	187.3
7:45	T8	3663	1010	31.99	122.4
8:45	T9	2766	1030	42.32	113.2
9:30	T10	2096	1071	47.83	93.59
End	T11	353.0	353.0	72.12	72.12
Total		31991	11321	600.7	1473

*(A) Calculated Mass of Magnetite in Original Sample

2) Mass Distribution of Magnetite for Subsamples (g)

Tail Sample Size (um)	T1	T2	T3	T4	T5	T6	T7	T8	T9	T10	T11	Concentrate	Calculated Feed
420	0.02	0.06	0.05	0.03	0.06	0.05	0.05	0.00	0.02	0.04	0.02	0.28	0.68
300	0.05	0.13	0.21	0.10	0.07	0.07	0.09	0.05	0.05	0.06	0.03	1.19	2.1
210	0.09	0.49	0.94	0.32	0.15	0.12	0.10	0.05	0.07	0.09	0.13	1.21	3.76
150	0.10	0.50	1.25	0.44	0.12	0.11	0.11	0.04	0.05	0.08	0.12	0.97	3.89
105	0.07	0.28	0.91	0.31	0.12	0.12	0.11	0.04	0.06	0.11	0.11	0.63	2.87
75	0.13	2.74	5.44	3.08	3.44	3.39	3.98	3.92	3.53	5.16	7.57	8.06	50.44
53	0.10	6.30	24.28	10.84	9.68	9.64	12.22	11.02	9.84	15.67	28.00	28.26	165.9
37	0.05	6.62	13.29	6.14	11.44	11.65	15.80	11.34	13.06	16.19	24.48	48.46	178.5
30	0.00	2.65	10.38	3.88	5.00	5.94	8.25	3.77	7.41	5.94	7.14	35.48	95.84
20	0.00	1.73	8.32	2.67	4.26	6.25	9.00	1.76	8.23	4.49	4.52	45.50	96.73
Total	0.61	21.5	65.07	27.81	34.34	37.34	49.71	31.99	42.32	47.83	72.12	170.0	600.7

3) Calculated Mass Distribution of Magnetite for Original Samples (g)

Tail Sample Size (um)	T1	T2	T3	T4	T5	T6	T7	T8	T9	T10	T11	Concentrate
420	0.02	0.17	0.14	0.10	0.22	0.19	0.19	0.00	0.05	0.08	0.02	0.46
300	0.05	0.37	0.59	0.34	0.26	0.27	0.34	0.19	0.13	0.12	0.03	1.95
210	0.09	1.38	2.64	1.08	0.55	0.46	0.38	0.19	0.19	0.18	0.13	1.98
150	0.10	1.41	3.51	1.49	0.44	0.42	0.41	0.15	0.13	0.16	0.12	1.59
105	0.07	0.79	2.56	1.05	0.44	0.46	0.41	0.15	0.16	0.22	0.11	1.03
75	0.13	7.74	15.29	10.44	12.59	12.88	14.99	14.99	9.44	10.10	7.57	13.21
53	0.10	17.80	68.26	36.74	35.44	36.62	46.04	42.15	26.32	30.66	28.00	46.30
37	0.05	18.70	37.36	20.81	41.89	44.25	59.52	43.38	34.93	31.68	24.48	79.40
30	0.00	7.49	29.18	13.15	18.31	22.56	31.08	14.42	19.82	11.62	7.14	58.13
20	0.00	4.89	23.39	9.05	15.60	23.74	33.91	6.73	22.01	8.79	4.52	74.55
Total	0.61	60.74	182.9	94.26	125.7	141.8	187.3	122.4	113.2	93.59	72.12	278.6

187

Results of Second Overload Test with Silica/Magnetite Feed

Sample Mass: 32 kg
% Solids and Flowrate: 30

1) Mass of Head Samples and Subsamples (g)

Absolute Time (min)	Sample	Total Mass Sample	Subsample	Mass of Magnetite Subsample	Sample
	Conc	1641	1004	203.5	332.7
0:20	T1	1343	1000	3.79	5.09
0:40	T2	2219	1000	43.92	97.44
0:57	T3	2210	1000	46.55	102.9
1:15	T4	2095	1000	35.70	74.80
1:30	T5	2060	1000	31.29	64.46
2:05	T6	5120	1000	42.11	215.6
2:40	T7	2095	1000	90.13	187.9
3:15	T8	4814	1000	48.02	231.1
3:45	T9	1855	1000	108.2	200.8
4:15	T10	3581	1000	60.21	215.6
4:45	T11	1340	1000	92.92	124.5
End	T12	1487	1000	32.71	48.64
Total		31950	13004	839.1	1902

2) Mass Distribution of Magnetite for Subsamples (g)

Tail Sample Size (um)	T1	T2	T3	T4	T5	T6	T7	T8	T9	T10	T11	T12	Concentrate
420	0.00	0.03	0.05	0.05	0.02	0.06	0.11	0.05	0.10	0.05	0.05	0.00	0.06
300	0.02	0.08	0.15	0.09	0.08	0.15	0.33	0.18	0.37	0.19	0.27	0.08	0.25
210	0.04	0.11	0.31	0.20	0.22	0.36	0.77	0.41	0.81	0.40	0.66	0.26	0.68
150	0.05	0.10	0.32	0.20	0.18	0.37	0.80	0.43	0.79	0.36	0.63	0.27	0.84
105	0.04	0.14	0.30	0.20	0.14	0.28	0.59	0.31	0.59	0.28	0.52	0.24	0.73
75	1.33	3.94	4.31	3.59	3.50	3.97	7.85	3.88	7.82	3.94	8.04	4.10	10.76
53	1.78	17.84	19.01	13.30	14.01	16.88	33.21	16.33	35.78	19.45	34.69	15.24	64.79
37	0.21	9.55	10.05	7.36	6.75	8.80	18.70	9.90	21.86	11.96	19.04	7.08	39.36
30	0.13	6.48	6.74	5.33	3.73	5.86	13.20	7.34	18.13	10.79	14.27	3.48	37.93
20	0.19	5.65	5.31	5.38	2.66	5.38	14.57	9.19	21.98	12.79	14.75	1.96	48.09
Total	3.79	43.92	46.55	35.7	31.29	42.11	90.13	48.02	108.23	60.21	92.92	32.71	203.51

3) Calculated Mass Distribution of Magnetite for Original Samples (g)

Tail Sample Size (um)	T1	T2	T3	T4	T5	T6	T7	T8	T9	T10	T11	T12	Concentrate
420	0.00	0.07	0.11	0.10	0.04	0.31	0.23	0.24	0.19	0.18	0.07	0.00	0.10
300	0.03	0.18	0.33	0.19	0.16	0.77	0.69	0.87	0.69	0.68	0.36	0.12	0.41
210	0.05	0.24	0.69	0.42	0.45	1.84	1.61	1.97	1.50	1.43	0.88	0.39	1.11
150	0.07	0.22	0.71	0.42	0.37	1.89	1.67	2.07	1.47	1.29	0.84	0.40	1.37
105	0.05	0.31	0.66	0.42	0.29	1.43	1.23	1.49	1.09	1.00	0.70	0.36	1.19
75	1.79	8.74	9.53	7.52	7.21	20.33	16.37	18.68	14.51	14.11	10.78	6.10	17.59
53	2.39	39.58	42.02	27.87	28.86	86.43	69.25	78.60	66.37	69.66	46.49	22.66	105.93
37	0.28	21.19	22.21	15.42	13.90	45.06	38.99	47.65	40.55	42.83	25.52	10.53	64.36
30	0.17	14.36	14.90	11.17	7.68	30.00	27.52	35.33	33.63	38.64	19.12	5.18	62.01
20	0.26	12.53	11.74	11.27	5.48	27.55	30.38	44.24	40.77	45.81	19.77	2.91	78.62
Total	5.09	97.44	102.89	74.80	64.46	215.60	187.94	231.15	200.75	215.63	124.53	48.64	332.73

Appendix XII: Results for Multi-Pass Separation Test

Appendix XII: Results of Three-Stage Falcon Test

Cycle 3

Size (um)	Concentrate		Tails		Feed		Recovery
	Act.	Corr.	Act.	Corr.	Tot.	Dist.	(%)
105	0.45	0.83	0.35	2.98	3.81	2.32	21.88
75	5.85	10.85	0.98	8.34	19.19	11.68	56.53
53	31.77	58.90	1.66	14.13	73.03	44.47	80.65
37	19.41	35.99	0.43	3.66	39.65	24.14	90.77
30	7.89	14.63	0.11	0.94	15.56	9.48	93.99
(in fact -30 um) 20	6.45	11.96	0.12	1.02	12.98	7.90	92.13
Tot.	71.82	133.16	3.65	31.07	164.23	1.58	81.08
Total	1003.30	1860.20	1002.80	8535.00	10395.20		

Cycle 2

Size (um)	Concentrate		Tails		Feed		Recovery
	Act.	Corr.	Act.	Corr.	Tot.	Dist.	(%)
105	0.64	0.91	0.37	4.43	5.34	1.43	17.02
75	8.19	14.82	1.88	22.51	37.33	10.01	39.70
53	37.56	70.23	7.17	85.85	156.08	41.86	45.00
37	39.22	45.47	3.89	46.58	92.05	24.69	49.40
30	16.82	23.00	1.53	18.32	41.32	11.08	55.67
(in fact -30 um) 20	17.35	25.51	1.27	15.21	40.72	10.92	62.65
Tot.	119.78	179.94	16.11	192.89	372.83	2.70	48.26
Total	1020.00	1567.50	1020.50	12219.00	13786.50		

Cycle 1

Size (um)	Concentrate		Tails		Feed		Recovery
	Act.	Corr.	Act.	Corr.	Tot.	Dist.	(%)
105	1.14	3.16	0.40	5.75	8.91	1.24	35.46
75	4.62	12.81	2.76	39.69	52.50	7.32	24.40
53	29.19	80.93	11.53	165.80	246.73	34.42	32.80
37	29.12	80.74	6.80	97.78	178.52	24.91	45.23
30	21.94	60.83	3.05	43.86	104.69	14.61	58.11
(in fact -30 um) 20	29.62	82.12	3.01	43.28	125.41	17.50	65.49
Tot.	115.63	320.59	27.55	396.16	716.76		
Total	500.40	1387.40	1018.10	14640.00	16027.4		

Bibliography

Bibliography

1) Bacon, W.G., Hawthorn, G.W., Poling, G.W., "Gold Analyses- Myths, Frauds and Truths", CIM Bulletin, Nov., 1989

2) Bagnold, R.A., " An Appproach to the Sediment Transport Problem from General Physics", Geol. Survey Professional Paper 422-I, U.S. Gov't Printing Office, Washington, 1966

3) Bagnold, R.A., "The Physics of Blown Sand and Desert Dunes", Chapman and HAll, London, 1973

4) Bagnold, R.A., "An Approach to the Sediment Trnasport Problem from General Physics", Geological Survey Professional Paper 422-I, US Government Printing Office, Washington (1966)

5) Bagnold, R.A., "Experiments in Gravity Free Dispersion of Large Solid Spheres in a Newtonian Fluid under Shear", Proc. Royal Soc. of London, 1954

6) Banisi, S., "An An Investigation of the Behavior of Gold in Grinding Circuits", M.Eng. Thesis, Department of Mining and Metallurgical Engineering, McGill University, Dec., 1990

7) Burt, R.O., "Slime Recovery by Gravity Concentration- A Viable Alternative?", Fine Particle Processing, Ch. 29, ed. P. Somasundaran, vol. 2, published by AIME, 1980

8) Burt, R.O., "Gravity Concentration Technology", Pergamon Press, Ch. 17, 1984

9) Burt, R.O., Ottley, D.J., "Developments in Fine Gravity Concentration using the Bartles-Mozley Concentrator", Min. Mag., no. 41, 1979

10) Carrier, C., Houdouin, D., Courchesne, M., "Dynamic Simulation of the CIP Gold Recovery Process", unpublished

11) Chaston, I.R.M., "Gravity Concentration of Fine Cassiterite", Trans. Inst. Min. and Met., no. 71, 1962

12) Cook, N.J., "Mineralogical Examination of Gold-Bearing Samples", CIM Bulletin, Dec., 1990

13) Douglas, J.K.E., Moir, A.T., " A Review of South African Gold Recovery Practice", Trans. 7th Commonwealth Min. and Met. Congress, Johannesburg, Vol. III, 1961

14) Douglas, J.K.E., Bailey, D.L.R., *"Performance of a Shaken Helicoid as a Gravity Concentrator"*, Trans. Inst. Min. and Met., no. 70, 1960

15) Ferrara, G., *"A Process of Centrifugal Separation using a Rotating Tube"*, Proc. 5th Int. Cong., Inst. Min. and Met., London, 1960

16) Finch, J.A., Matwijenko, O., *"Individual Mineral Behavior in a Closed Grinding Circuit"*, CIM Bulletin, Sept, 1977

17) Hallbauer, D.K., Joughin, N.C., *"The Size Distribution and Morphology of Gold Particles in Witwatersrand Reefs and their Crushed Products"*, Journal of SAIMM, June, 1973

18) Herbst, J.A., Fuerstenau, D.W., *"The Zero Order Production of Fine Sizes in Comminution and its Implications in Simulation"*, Trans. AIME, vol. 241, 1968

19) Holtham, P.N., *"Particle Transport in Gravity Concentrators and the Bagnold Effect"*, Min. Eng., Vol. 5, no. 2, 1992

20) Kelly and Spotiswood, *"An Introduction to Mineral Processing"*, John Wiley and Sons", Chapters 4,5, 1982

21) Knelson, B.V., *"Centrifugal Concentration and Separation of Precious Metals"*, 2 nd Int. Conf. on Gold Mining, Vancouver, Nov., 1988

22) Laohapanit, R., *"Flotation Column Test Work at Les Mines Camchib Inc."*, M.Eng. Thesis, M.Eng. Thesis, Department of Mining and Metallurgical Engineering, McGill University, March, 1991

23) Laplante, A.R., *"The Use of Gravity Concentration for Gold Recovery, Part I- Economic Rationale and Basic Principles"*, paper presented at the Professional Development Seminar on Small-Scale Gold Projects; Mining, Processing, Economics, and Policy Framework", McGill University, 1988

24) Laplante, A.R., Course Notes on *"Modelling of Mineral Processing Systems"*, McGill University, Sept., 1989

25) Laplante, A.R., Course Notes on *"Mathematical Applications in the Mineral Processing Industry"*, McGill University, Jan., 1991

26) Laplante, A.R., Shu, Y., *"The Use of a Laboratory Centrifugal Separator to Study Gravity Recovery in Industrial Circuits"*, paper presented at 24th Annual General Meeting, CIM, Montreal, paper 12, 1992

27) Liu, L., "An Investigation of Gold Recovery in the Grinding and Gravity Circuit of Les Mines Camchib", M.Eng. Thesis, Department of Mining and Metallurgical Engineering, McGill University, Nov., 1989

28) McAlister, S., "Case Studies in the use of the Falcon Concentrators (Beach Sand Applications)", paper presented at the 24th Annual General Meeting, CIM, Montreal, paper 11, 1992

29) McAlister, S., "Fine Gold Recovery using Falcon Concentrators", paper presented at Northwest Mining Association, 95th Annual Convention, Short Course and Trade Show, Dec., 1989

30) Mills, C., Burt, R.O., "Thin Film Concentrating Devices and the Bartles-Mozley Concentrator", Min. Mag., no. 41, 1979

31) Morley, C., "Cassiterite Recovery with a Falcon Concentrator", Memorandum to B. Lewis, Rio Kemptville Tin Company, Jan., 1992

32) Nicol, M.J., Fleming, C.A., Cromberg, G., "The Adsorption of Gold Cyanide onto Activated Carbon, Part II- Application of the Kinetic Model to Multistage Adsorption Circuits, Journal of SAIMM, vol. 84, no. 3, March, 1984

33) Ounpuu, M., "Gravity Concentration of Gold from Base Metal Flotation Mills", paper presented at 24th Annual General Meeting, CIM, Montreal, paper 10, 1992

34) Pitard, F., "Pierre Gy's Sampling Theory and Practice", Ed. CRC Press, 1989

35) Plitt, L., "A Mathematical Model of the Hydrocyclone Classifier", CIM Bulletin, Dec., 1976

36) Sivamohan, R., Forssberg, E., "Recovery of Heavy Minerals from Slimes", Int. J. of Min. Proc., 15, 1985

37) Splaine, M., Browner, J.J., Dohm, C.E., "The Effect of Head Grade on Recovery Efficiency in a Gold-Reduction Plant, Journal of SAIMM, May, 1982

38) Spring, R., "Norbal2", Research Report # N-8325-RR85-1, Centre de Recherche Noranda, Pointe Claire, Q.C., 1985

39) Svarovsky, L., "Solid-Liquid Separation", Butterworth and Co. Ltd., Chapter 23, 1990

40) Robitaille, J., Private Communication, 1991

41) Williams, D.F., Glasser, D., "The Modelling and Simulation of Processes for the Adsortion of Gold by Activated Charcoal", Journal of SAIMM, vol. 85, no. 8, Aug., 1985

42) Wyslouzil, H.E., "Evaluation of the Kelsey Centrifugal Jig at Rio Kemptville Tin", paper presented at 22nd Annual General Meeting, CIM, Montreal, paper 23, 1990